Effect of Molecular Chirality on the Morphology of Biomimetic Langmuir Monolayers

Nilashis Nandi

Chemistry Department, Birla Institute of Technology and Science, Pilani, Rajasthan 333031, India

Dieter Vollhardt*

Max Planck Institute of Colloids and Interfaces, Potsdam D-14424, Germany

Received June 10, 2002

Contents

1. Introduction 4033
2. Experimental Results Obtained from Surface Pressure−Area Isotherm Measurements in Chiral Monolayers 4035
   2.1. Amphiphiles Containing an Amino Acid Headgroup with a Single Chiral Center 4036
   2.2. Amphiphiles Containing an Acidic Headgroup with a Single Chiral Center 4037
   2.3. Amphiphiles Containing a Glycerolic Headgroup with a Single Chiral Center 4037
   2.4. Amphiphiles Containing a Phospholipid Headgroup with a Single Chiral Center 4038
   2.5. Amphiphiles Containing Multiple Chiral Centers 4038
3. Experimental Results Obtained from Optical Methods (Brewster Angle Microscopy and Fluorescence Studies) in Chiral Monolayers 4040
   3.1. Amphiphiles Containing an Acid Amide Headgroup with a Single Chiral Center 4041
   3.2. Amphiphiles Containing an Amino Acid Headgroup with a Single Chiral Center 4041
   3.3. Amphiphiles Containing a Glycerolic Headgroup with a Single Chiral Center 4043
   3.4. Amphiphiles Containing a Phospholipid Headgroup with a Single Chiral Center 4046
4. Experimental Results Obtained from Grazing Incidence X-ray Diffraction (GIXD) Measurements in Chiral Monolayers 4051
   4.1. Amphiphiles Containing Amino Acid or Acid Amide Headgroups, Each with a Single Chiral Center 4052
   4.2. Amphiphiles Containing a Glycerolic Headgroup with a Single Chiral Center 4054
   4.3. Amphiphiles Containing a Phospholipid Headgroup with a Single Chiral Center 4056
   4.4. Mixture of Amphiphiles Containing Acid and Amine Headgroups, Each with a Single Chiral Center 4056
5. Continuum Theories of Chiral Monolayers 4057
6. Molecular Theories of Chiral Monolayers 4058
7. Chiral Discrimination Effects in Chiral Monolayers 4065
8. Concluding Remarks 4071
9. Symbols and Abbreviations 4072
10. Acknowledgments 4073
11. References 4073

* Author to whom correspondence should be addressed (fax 49 331 567 9202; e-mail vollh@mpikg-golm.mpg.de).

1. Introduction

Chirality (originated from the Greek word "*cheir*", meaning "hand") is an expression of nature, which is observed in its various forms. Traditionally, a lack of symmetry is considered to be the signature of chirality. In nature, diverse macroscopic objects such as hands, animal organs, biological organisms, and macromolecules, as well as microscopic objects such as molecules, are chiral. From a molecular point of view, molecules with equal atomic composition (same molecular formula) could be superimposable (homomeric; identical) or non-superimposable (isomeric; structural isomers). Of these two categories, the isomers could be of the same constitution (stereoisomeric) or of different constitutions (constitutionally isomeric). All stereoisomers have the same constitution, but they could be either non-superimposable mirror images (enantiomers) or not related by mirror image relationship (diastereoisomers). The enantiomers are chiral objects. A chiral molecule is non-superimposable on its mirror image. Thus, a molecular structure having no reflection symmetry is considered to be chiral or dissymmetric[1]. Such a molecule lacks a σ plane (a mirror plane, through which the reflection of all atoms makes a three-dimensional arrangement, indistinguishable from the original). A chiral molecule could be asymmetric when it additionally lacks n-fold axes of symmetry (C_n; $n > 1$). An asymmetric molecule belongs to point group C_1. A common example of such a point group is a carbon atom to which four different groups are attached. A detailed account of chiral elements is available in the standard literature.[1] Topological concepts are also applied to understand the chirality of molecules.[2] However, the topic of chirality is as broad as its abundance in nature, and we refer to the literature for various aspects of molecular chirality.[1,2] In the present review we will confine ourselves to the chirality expressed by (one or more) asymmetric carbon atoms as commonly observed in natu-

10.1021/cr0006674 CCC: $44.00
Published on Web 08/29/2003

Nilashis Nandi received his Ph.D. from Visva Bharati University at Santiniketan. He was a postdoctoral fellow at the Indian Institute of Science, India (1993–1997), a J.S.P.S. postdoctoral fellow at the Nagoya University, Japan (1997–1999) and an Alexander von Humboldt postdoctoral fellow at the Max Planck Institute of Colloids and Interfaces, Germany (1999–2000). He joined the chemistry group of Birla Institute of Technology and Science, India, at the beginning of 2001. His research interests include the morphology and dynamics of biomimetic and biomolecular systems.

Dieter Vollhardt, senior scientist at the Max Planck Institute of Colloids and Interfaces, has been Professor of Physical Chemistry at Potsdam University since 1999. His thesis at the Humboldt University, Berlin, was about desorption kinetics of surfactants. Currently, his main areas of research are molecular recognition systems, supramolecular organization in monolayers and biomimetic systems, and auto-oscillation of surface tension.

ral and synthetic amphiphiles as well as its manifestation in mesoscopic aggregates of such molecules.

Molecules containing asymmetric carbon centers can rotate the plane of polarized light. These molecules are referred to as optically active.[3] It was pointed out by van't Hoff [4,5] and Le Bel[6] that the rotation of plane-polarized light by a solution of chiral molecules is due to the presence of an asymmetric carbon atom. Pasteur discovered that chiral molecules exhibit optical isomerism.[7] However, few dissymmetric molecules do not show detectable optical activity, so the term "optical isomer" is a misnomer. A century later J. M. Bijvoet determined the first absolute configuration (the actual arrangement of atoms in space) of a chiral molecule using X-ray analysis. Understanding the absolute configuration seems to be essential for enantiomeric drug technology.[8−11] Due to the continued interest in chiral chemistry, the crystal structures and physical properties of several enantiomeric molecules as well as the racemates have been studied in great detail.[12]

Although it is easy to observe that chiral objects are abundant in nature, a closer look into the details of organization present in their structures reveals an interesting correlation. Chirality is operative in many biological systems at both microscopic and macroscopic levels. Common examples are proteins and their constituent amino acids and nucleic acids and their constituent sugars as well as membranes and their constituent lipids and membrane proteins. In each case, both the basic building block and the architecture formed by such blocks are chiral. However, most important to note is that these biological units lose functionality when their chiral structures are altered. In most cases, only one enantiomer is biologically active. Why nature prefers only one enantiomer remained a puzzle. The small energy difference between the two enantiomeric forms poses a further challenge to understand this famous *problem of homochiral evolution*.[13−17]

Understanding the reason for chiral preference shown by nature has also practical applications. Single enantiomeric drugs constitute >30% of the total therapeutic drugs used in recent years.[8−11] Enantiomeric drugs constitute >50% of total sales in particular classes such as cardiovascular, antibiotics and antifungals, hormones, and cancer- and hematology-related drugs. Consequently, an understanding of the orientation and distance-dependent interaction due to the chiral structure of the molecules in the biomimetic and biomolecular systems is expected to be helpful in designing drugs in a more effective way. The growing use of enantiomeric drugs draws our attention to another fact. The structure−function relationship in nature is so powerful that when a functional disorder manifests in the form of a disease, it can be handled in many cases only by using a molecule of a specific chiral structure. Consequently, the importance of understanding the role of chirality can hardly be ignored. As mentioned before, various biomolecular and biomimetic systems are chiral. Chirality in proteins is observed to originate from geometrical as well as topological features.[18] Geometrical (Eucledian) chiral features observed in proteins are the asymmetric tetrahedral α carbon atom of L-amino acids, twisted peptide chains, helices, cylindrical packing of helices, etc. The topological properties of an object are related to its invariant features with respect to particular types of general transformations such as continuous deformation (object cannot be torn and rejoined during the transformation). Suggested chiral objects, which may be found in proteins, are links, loops, knots, and graphs. Although it is easy to find the correlation between the geometrical chiral features at the lower level of structural hierarchy (such as L-stereochemistry of the individual amino acids) and at the higher level (such as right-handed twist in extended polypeptide chains), it is less clear-cut to follow such a correlation in the case of topological chirality. We refer to the literature for further details.[18] In the case of nucleic acids, the molecular chirality of the sugar units may be related to the origin of the specific handedness of A-, B-, and Z-DNA strands. Bilayers composed of cholesterols develop chiral helical struc-

tures, which gradually change into gallstones under disordered physiological conditions. Understanding the origin of such chirality effects are of fundamental importance. However, all of these biological systems are inherently complex. Biomimetic systems could be used as simple model systems in which such chiral effects are well-known but can be studied much more easily compared to their biological counterparts.

Monolayers are simpler systems (they are two-dimensional systems, and one degree of freedom is reduced, compared to the corresponding three-dimensional systems), and the understanding of the effect of chirality is expected to be relatively simpler in these systems than in the corresponding three-dimensional systems. Due to the fundamental importance of understanding the chirality-dependent interactions in biomolecular assemblies, monolayers are used as biomimetic systems to study the structures and properties of several chiral surfactants in recent years and past. Even in simpler systems such as monolayers, chirality manifests itself in several ways. It is now well-known that mesoscopic domains are formed in monolayers in the condensed phase as detected by various optical techniques[19,20] and such domain shapes could be chiral (anisotropic). The underlying lattice structure in these monolayers could also be anisotropic (for example, oblique) and hence chiral. Further chiral effects can be observed in the discriminating behavior of enantiomeric or diastereomeric pairs in the $\pi-A$ isotherms.[21,22] Preference of interaction between enantiomeric pairs of the same type or between the opposite enantiomers is also observed. In some cases, such preference of molecular interaction is strong enough to lead to the segregation of separate domains composed of only one type of enantiomeric molecule. Detailed understanding of such diverse chirality effects in monolayers is emerging only recently.

Due to the fundamental importance and ongoing intense activity in this area, several excellent reviews have appeared on the various morphological features of monolayers at the air/water interface of amphiphilic assemblies. Many of the amphiphiles studied are chiral. Möhwald reviewed the phospholipid and phospholipid−protein monolayers at the air/water interface.[19] Knobler reviewed the experimental and theoretical aspects of the monolayers of fatty acids and phospholipids.[20] The review by Arnett, Harvey, and Rose covered the early studies of the chiral recognition in monolayer systems.[21] McConnell reviewed the structure, shape, and phase transitions in lipid monolayers at the air/water interface.[23] Vollhardt reviewed the morphological features of chiral and achiral amphiphiles probed by recent optical techniques.[24a,b] Vollhardt recently discussed the morphology of monolayers at the air/water interface.[24b] Kaganer, Möhwald, and Dutta reviewed the results obtained from recent experimental techniques as well as theoretical methods.[25] Recently, the Lahav and Leiserowitz groups reviewed the results of X-ray crystallographic studies in various monolayers including chiral systems.[26] Harris, Kamien, and Lubensky recently reviewed the fundamental physical aspects of chirality with reference to liquid crystal systems.[27] However, no review was devoted so far to the topic of the present review, namely, the effect of molecular chirality on biomimetic Langmuir monolayers.

In the present review we discuss the various experimental and theoretical results concerning the monolayers composed of chiral molecules as well as their microscopic interpretations. With this end in view, we have organized the review as follows. In the beginning we discuss various experimental studies such as pressure−area isotherm measurements, optical studies (Brewster angle microscopic studies and fluorescence studies), and grazing uncidence X-ray diffraction studies in different chiral monolayers in sections 2, 3, and 4, respectively. In these sections we focus on the experimental results, which demonstrate interesting chirality effects. In sections 5 and 6 we discuss the continuum theories and molecular theories of chiral monolayers. Various chiral discrimination effects are observed in chiral monolayers, and these topics are discussed in section 7. Finally, we conclude in section 8.

2. Experimental Results Obtained from Surface Pressure−Area Isotherm Measurements in Chiral Monolayers

Thermodynamic conclusions on the phase behavior of amphiphilic monolayers can be drawn considering the surface pressure−area ($\pi-A$) isotherms at different temperatures. The $\pi-A$ isotherms are usually recorded using a computer-interfaced film balance with a Wilhelmy-type pressure measuring system. Neglecting details, three general single-phase states can be distinguished, namely, the *fluid* [gaseous, liquid-expanded (LE)], *condensed* [liquid-condensed (LC)], and *solid* (S) phases. Three characteristic shapes of generalized $\pi-A$ isotherms representative of respective temperatures or alkyl chain length can be measured.[24a,b] The most interesting type of $\pi-A$ isotherm shows a nonhorizontal plateau region after a kink point in the isotherm characteristic for a first-order phase transition from the fluid to the condensed phase. The plateau represents a two-phase coexistence between the fluid and the condensed phase. The lower the temperature, the lower is the surface pressure of the plateau, but the more extended is the area covered by the plateau. The transition to the solid monolayer phase is usually indicated by a kink in the steep part of the isotherm. At temperatures low enough and long-chain amphiphiles, the two-phase coexistence region exists already at a surface pressure $\pi \sim 0$; that is, this is the second general type of isotherm. In this case, the $\pi-A$ isotherm does not allow the exact determination of the first-order phase transition point. Oppositely, at temperatures high enough, a continuous increase of the surface pressure with decreasing area per molecule suggests that over the whole area range no phase transition to the condensed or solid phase occurs. This third type of isotherm is not of interest for studies of the monolayer characteristics.

The stereochemical effects on the monolayer phase behavior are small when the intermolecular separa-

tion is large.[21] Consequently, the effects due to the chirality of the molecule are expected to be dominant in the condensed phase compared to the fluid (gaseous or liquid expanded) phase. With increasing temperature or decreasing surface pressure, the rotational disorder of the molecules increases rapidly. They rotate more freely about their long axis. As a result, the intermolecular interaction gradually becomes insensitive to any asymmetry present about their short axis of the respective molecule and the molecule becomes effectively symmetric to the neighboring molecules. In such a case, orientation-dependent interaction due to the chiral structure of the molecules is relatively unimportant. It is expected that the chiral discrimination will gradually disappear as the system approaches the free rotating limit ($V_{ij} \ll k_B T$, where V_{ij} is the van der Waals interaction between the enantiomeric components *i* and *j*). Thus, orientation- and distance-dependent interaction due to the chiral structure of the molecules is more dominant at lower temperature or higher surface pressure when spatial or orientational correlations between the molecules are present, as recently pointed out.[27] Lundquist performed the first pioneering studies of chiral discrimination observed in the $\pi-A$ isotherms.[28] We further discuss the discrimination effects in section 7. In the following we discuss chirality effects as observed on the basis of $\pi-A$ isotherm measurements of chiral amphiphilic molecules containing various headgroups such as amino acids, amides, glycerol derivatives, and phospholipids.

2.1. Amphiphiles Containing an Amino Acid Headgroup with a Single Chiral Center

Amphiphiles containing amino acid residues are extensively investigated due to the importance of understanding the orientation- and distance-dependent interaction due to the chiral structure of the molecules in the amino acids themselves. Note that the chiral structure dependent interaction in amino acids is intriguing due to the unsolved problem of homochiral evolution of amino acids in nature. Therefore, Arnett et al. studied the $\pi-A$ isotherms of a series of stearoylamino acid methyl esters and dilaurylamino acid dimethyl esters with amino acid residues such as serine, cysteine, threonine, and *allo*-threonine monolayers.[21,22] They found discriminating features between the pure enantiomers and the racemic mixtures in the condensed phase region of the $\pi-A$ isotherms and introduced the idea of stereoselective interaction. It was observed that the enantiomeric monolayer of stearoylserine methyl ester (SSME) is in a more condensed state than the racemic monolayers at the same molecular area, suggesting homochiral preference. We discuss in detail the discrimination effects observed in section 7.

The $\pi-A$ isotherms of the D and L enantiomers of *N*-SSME are found to be equivalent, but the time-dependent surface pressure relaxation of the racemic monolayer is faster compared to that of the enantiomeric monolayer.[29] It was observed that the transition pressure of the enantiomeric *N*-docosyl-leucine monolayer is markedly lower than that of the racemic monolayer, which is suggestive of chiral discrimination.[30] Stine et al. studied the monolayers of numerous chiral amino acid amphiphiles.[29,31−33] The isotherm of L-*N*-stearoylvaline at 18 °C on a pH 2 HCl subphase shows that the monolayer is more compressed than the corresponding racemic monolayer, clearly indicating homochirality.[31] Similarly, the monolayer of enantiomeric *N*-palmitoylvaline at 10 °C on a pH 2 HCl subphase was found to be more compressed than the corresponding racemic monolayer.[31] Similar chiral discrimination effects were obtained with *N*-stearoyltyrosine monolayers.[32] At 33 °C the racemic monolayer shows a phase transition similar to that in the enantiomeric monolayer at lower temperatures. However, at 22 °C on a subphase adjusted to pH 7.0, the $\pi-A$ isotherm shows that the enantiomeric and racemic monolayers are both expanded and are virtually identical. The effect of the increased subphase pH indicates that, obviously the polarity of the headgroup is increased by dissociation of the carboxylic group. This was supported by a comparison with results of the corresponding methyl ester, as the ester group is nondissociable and, thus, the polarity is decreased. The compression isotherms of the enantiomeric and racemic monolayers are nonidentical. The $\pi-A$ isotherm of the enantiomeric monolayer was more compressed than that of the racemic monolayer, what indicates homochirality. A homochiral preference in the $\pi-A$ isotherms of *N*-hexadecanoylalanine monolayer was observed on acidic (pH 2) aqueous subphase within the temperature range of 20−35 °C.[33] It is observed that the phase transition point of the racemic monolayer shifts to smaller values of area per molecule with increasing temperature, whereas the isotherm features of the enantiomeric monolayer remain almost unaltered over the measured temperature.

Homochiral preference is also observed in the $\pi-A$ isotherms of enantiomeric and racemic *N*-stearoylglutamic acid monolayers at 20 °C on aqueous subphase at pH 2 and also in the presence of $CdCl_2$.[34] The $\pi-A$ isotherm of the L-enantiomer exhibits features of a more condensed state than the racemic monolayers at areas/molecule of ≤ 40 Å^2 for an aqueous subphase in acidified water and in the aqueous $CdCl_2$ subphase. The hysteresis effects of the $\pi-A$ isotherms of *N*-octadecanoyl-L-alanine monolayers are discussed in the literature.[35−37]

The identical shapes of $\pi-A$ isotherms of enantiomeric and racemic myristoyl alanine in the LE phase measured on pH 2 water at 19 °C indicate that chiral discrimination cannot be observed in the fluid monolayer state.[38] The transition pressure for LE−LC transition is higher for the racemic amphiphile compared to those of the enantiomeric amphiphile, but the racemic monolayer relaxes with time to lower pressures. The estimation of closely packed area indicates that the alanine headgroup determines the packing. This indicates the influence of the chiral amino acid headgroups on the packing properties.

Recent theoretical studies on amino acid headgroup containing monolayers suggested that both the orientation- and distance-dependent interaction due to

the chiral structure of the molecules and the hydrogen bonding interaction might play important roles in the monolayer morphology of these systems.[39,40] Like other intermolecular forces, the fundamental origin of hydrogen bonding is electrostatic. Interactions related to moderate to weak hydrogen bonds, which are dominant types in biological and biomimetic systems, are primarily of Coulombic type and attenuate with the distance (r) as r^{-1}. The dispersion force attenuates as r^{-6}, and the former is of longer range than the latter. The properties of the hydrogen bonds are group properties, depending not only on the atoms directly involved in bonding but also on the sequence of the total pattern in which it exists.[41]

The orientation dependence of the hydrogen bond also makes the properties of the hydrogen bond more dependent on the whole pattern. Due to polarizability of the whole pattern, the binding energy of a hydrogen-bonded structural pattern is greater than the sum of the binding energy of the individual bonds. This is the signature of the cooperative nature of the hydrogen bond network. It is thus better to study a particular hydrogen bond within the context of the whole pattern in which it exists rather than treating it as an isolated atomic (or group) pair. Thus, it is justified to use the pair potential approximation in the case of van der Waals interaction (being relatively shorter ranged); such an approximation is quantitatively incorrect for hydrogen bonding. It is possible that the optimum geometry and energetics of an individual hydrogen bond are controlled by the requirement of the energy and geometry optimization of the whole pattern. It is indicated that the hydrogen bond imposes a precise geometric pattern (with increasing lattice symmetry), which disfavors compactness.[12] For a pair of enantiomeric molecules, their chiral structure prefers compactness and, thus, favors less symmetry in lattices. It is suggested that chirality-dependent interactions may lead to an orientationally anisotropic molecular arrangement at the domain boundary (favoring compactness), which competes with the hydroge-bonding interaction (increasing symmetry and disfavoring compactness). Further detailed studies are necessary to understand the role of hydrogen bonding in these systems.

2.2. Amphiphiles Containing an Acidic Headgroup with a Single Chiral Center

There are also examples without any chiral discrimination effect in the $\pi-A$ isotherms. For example, the isotherms of the enantiomeric and the racemic *N*-tetradecyl-γ,δ-dihydroxypentanoic acid (TDHPA) are identical within the range of experimental error.[42a,b] However, the images from Brewster angle microscopic studies (BAM) indicate that the single condensed phase domains develop with dendritic shapes and the direction of the main growth axes bears the mirror image relationship for enantiomers. These shapes are developed at the beginning of the two-phase coexistence region. Details of the BAM observation will be discussed in section 3.

2.3. Amphiphiles Containing a Glycerolic Headgroup with a Single Chiral Center

Monolayers of monoglycerol amphiphiles such as *rac*-1-monostearoylglycerol or *rac*-1-monopalmitoylglycerol are good candidates for systematic studies of chiral discrimination effects.[43] The morphological features of the condensed phase domains are investigated by BAM and are described in section 3. Figure 1 shows a set of $\pi-A$ isotherms of 1-monopalmitoyl-

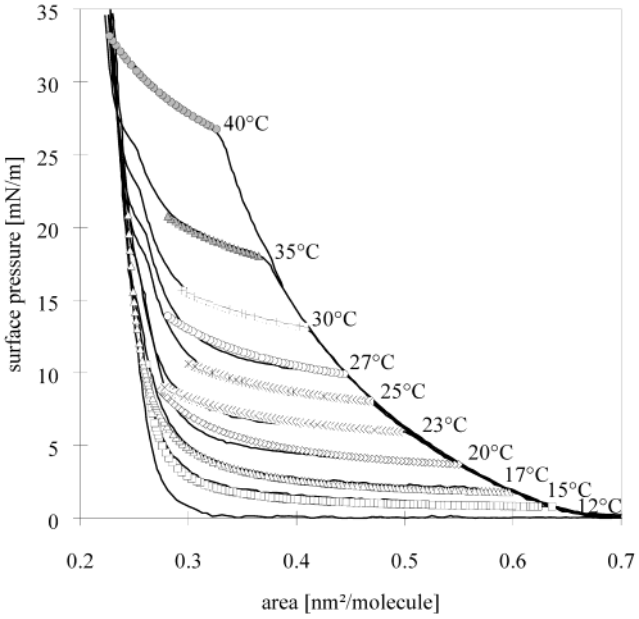

Figure 1. Temperature dependence of the $\pi-A$ isotherms of 1-monopalmitoyl-*rac*-glycerol monolayers. Experimental results are presented by curves; symbols correspond to the calculations using eq 26 in ref 44.

rac-glycerol monolayers in the temperature interval between 12 and 40 °C.[44]

Beyond the two-phase coexistence region, indicated by the nonhorizontal "plateau" in the $\pi-A$ isotherms, a steep increase in the surface pressure takes place. The nonequilibrium structures of 1-monopalmitoyl-*rac*-glycerol monolayers are completely different.[45,46]

The molecular formulas of the 1-*O*-hexadecyl-*rac*-glycerol and 1-monopalmitoyl-*rac*-glycerol are closely similar. The change from an ether linkage to an ester linkage does not affect the $\pi-A$ isotherm significantly, so the $\pi-A$ isotherms of the two compounds are closely similar[45] (Figure 2).

However, BAM studies reveal that the mesoscopic domain shapes in the condensed phase of the two compounds are drastically different. The features are discussed in detail in the next section. The fact that the $\pi-A$ isotherms of 1-*O*-hexadecyl-*rac*-glycerol and 1-monopalmitoyl-*rac*-glycerol are similar but the underlying phases behavior are different (as shown by BAM investigation) clearly indicates the important fact that the common assumption that monolayers of amphiphiles with similar isotherm features have similar phase behaviors is not always sufficient. Thus, $\pi-A$ isotherm studies must be used in conjunction with other techniques such as optical methods (for example, BAM and fluorescence microscopy

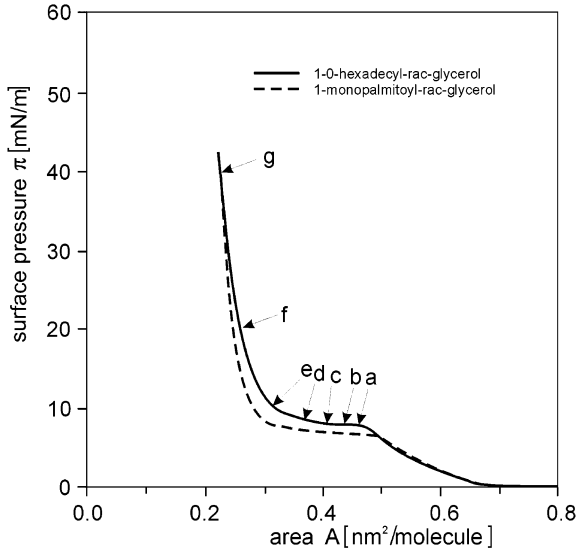

Figure 2. $\pi-A$ isotherms of 1-monopalmitoyl-*rac*-glycerol and 1-*O*-hexadecyl-*rac*-glycerol monolayers measured simultaneously to BAM imaging at 23 °C. See also section 3.

study) or grazing incidence X-ray diffraction (GIXD) in order to have a correct understanding about the microscopic features and ordering of the monolayer.

The thermodynamic behaviors of the two enantiomeric forms as well as the racemic 1-stearylaminoglycerol monolayers are also identical.[47] However, fluorescence microscopic studies revealed that chiral discrimination is manifested in the morphological features of the condensed phase domains. These features are described in the next section.

2.4. Amphiphiles Containing a Phospholipid Headgroup with a Single Chiral Center

Phospholipid amphiphiles constitute an important class of chiral compounds due to their biological significance. As a result, monolayers of homologous dialkanoylphosphatidylcholine (DMPC, DPPC), dialkanoylphosphatidic acid (DMPA, DPPA), dialkanoylphosphatidylethanolamine (DMPE), etc., are investigated in detail by several techniques. The usual phospholipids have two alkyl tails and the chiral carbon atom is in close proximity to the headgroup. The temperature at which the characteristic features of the phase diagram of phospholipids appear is dependent on the alkyl chain length and the headgroup.[20] This suggests that the characteristic features of the phase diagram are dependent on the chirality of the phospholipid molecules, because the variation in the alkyl chain length and the nature of the headgroup change the stereochemical arrangement of the groups about the chiral center. However, no detailed study is available yet to quantify this correlation.

Monolayers of phospholipids with more than two chains have also been studied.[48−52] The isotherm of a triple-chain phosphatidylcholine is investigated in order to address the important issue of estimation of the relative importance of the interactions arising from the head and those arising from the tail regions of the amphiphile.[48]

2.5. Amphiphiles Containing Multiple Chiral Centers

The chirality-driven features of amphiphiles containing multiple chiral centers are significant. The presence of more than one chiral center might enhance the chirality effects compared to that in amphiphilic systems with a single chiral center. It is expected that the multiple chiral centers of neighboring molecules would give rise to complex interactions between them. The study of *N*-alkylaldonamide monolayers is interesting because these compounds form three-dimensional aggregates of different structures in aqueous solutions and gels. The aggregate morphology of these aggregates depends on the polyolic headgroup.[53−55]

The $\pi-A$ isotherms of enantiomeric and racemic *N*-dodecylgluconamide are studied.[56] The shape of the isotherms (Figure 3) is strongly dependent on the

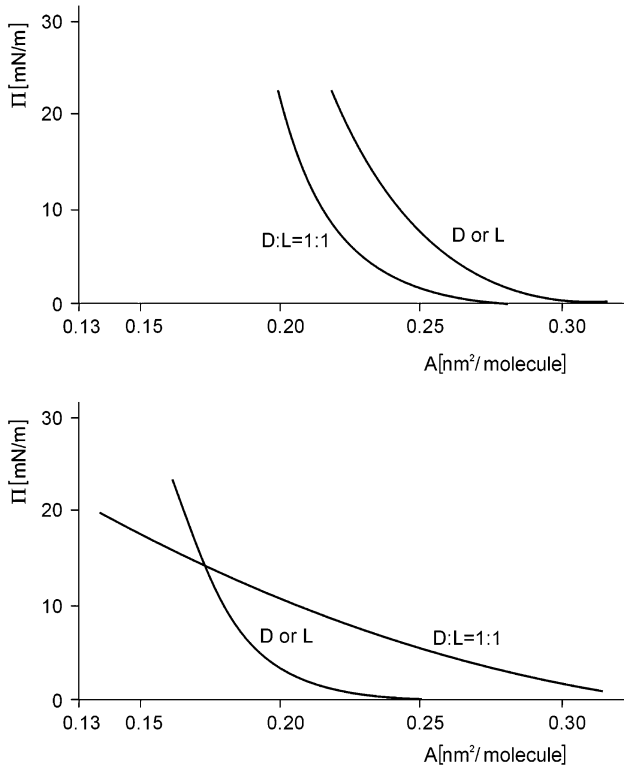

Figure 3. $\pi-A$ isotherms for the enantiomeric *N*-dodecyl-D- or -L-gluconamide and the racemic mixture (D:L = 1:1) at 10 °C (top) and 25 °C (bottom).

compression rate at temperatures between 10 and 40 °C. This event is complicated by the relaxation phenomenon in the monolayer. It is observed that the surface pressure rapidly decreases when the barrier is stopped at a certain value and the isotherm is shifted to lower molecular areas upon compression. This relaxation effect is diminished at higher compression rates of the monolayer. The isotherms are strongly temperature dependent. When the temperature is increased from 10 to 25 °C, the molecular area shifts to lower values for a certain surface pressure. The shape of the $\pi-A$ isotherm corresponding to the racemic monolayer is strongly affected by temperature, and the slope of the isotherm is rapidly decreased.

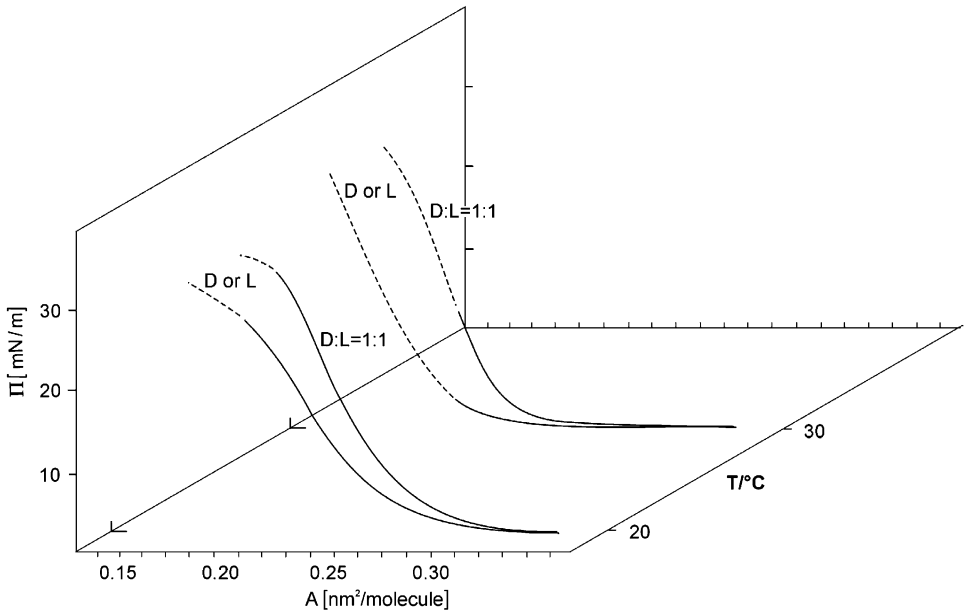

Figure 4. $\pi-A$ isotherms of the enantiomeric and racemic monolayers of *N*-dodecylmannonamide at 20 and 30 °C. Homochiral discrimination is indicated for both temperatures.

The thermodynamic features of the monolayers of another diastereomeric *N*-alkylaldonamide, namely, of dodecylmannonamide are completely different.[57] The isotherms and relaxation of mannonamide headgroup monolayers are shown in Figures 4 and 5.

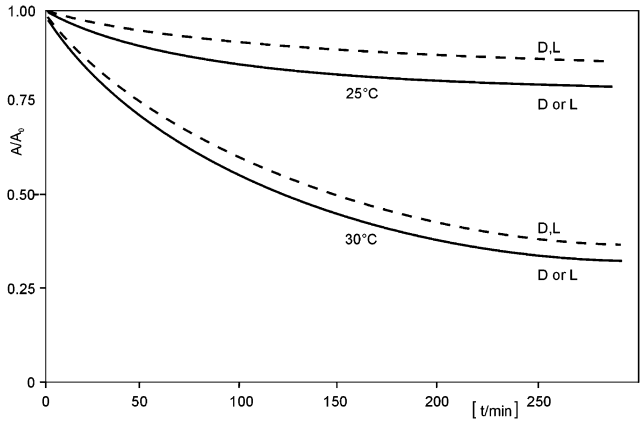

Figure 5. Constant surface pressure relaxation at $\pi = 10$ mN/m of the enantiomeric and racemic monolayers of *N*-dodecylmannonamide at 25 and 30 °C. The difference in the relaxation curves between the enantiomeric and the racemic monolayers is opposite that of the diastereomeric *N*-dodecylgluconamide.

The $\pi-A$ curves of the racemic mixtures show temperature dependences similar to those of pure enantiomers. However, the enantiomeric amphiphiles are more densely packed than the racemic monolayers (Figure 4). The surface pressure relaxation curves of the enantiomeric forms agree with each other, and that of the racemic form is not drastically different (Figure 5). However, the relaxation of enantiomeric forms is more rapid in this case compared to the diastereomeric *N*-dodecylgluconamide. The relaxation increases with temperature. Consequently, the surface pressure studies clearly indicate that the chiral monolayer properties of the two diastereomers *N*-dodecylmannonamide and *N*-dodecylgluconamide are very different. Oppositely to the heterochiral preference of *N*-dodecylgluconamide monolayers, *N*-dodecylmannonamide monolayers show homochiral discrimination.

The $\pi-A$ isotherm of monolayers of synthesized achiral and chiral imidazole amphiphiles at the air−water interface are also studied.[58] These systems have metal-binding capabilities. The chirality is introduced in the molecule by substituting the methyl group at the α position of the amine group. The compression isotherm of the chiral compound is similar to that of the achiral compound except that the collapse pressure values are lower for the former than the corresponding values in the latter. The molecular area observed for the chiral monolayer in the LE state is lower than the corresponding area observed in the LE state of the achiral monolayer.

Chiral features of compounds containing multiple chiral centers are interesting due to the complicated nature of orientation- and distance-dependent interaction due to the chiral structure of the molecules. Hexadecylthiophospho-2-phenylglycinol (HTPPG) is a nice candidate for such an amphiphile as it contains besides chiral carbon also chiral phosphorus. The $\pi-A$ isotherms of four stereoisomers (*RR*, *SS*, *RS*, and *SR*) of HTPPG monolayers were studied.[59] The isotherm measurements of R_pS and S_pR (the subscript p denotes the chiral phosphorus) diastereomers give identical isotherms in the fluid (LE) phase and displayed no chiral discrimination at room temperature. Chiral discrimination was found for the R_pR and S_pS diastereomeric pairs. A phase transition was observed in the case of racemic monolayers but was not observed in the pure enantiomeric films. Such discrimination effects occurred on the aqueous H_2SO_4 subphase.

On the basis of measurements of the $\pi-A$ isotherm, the nature of the chiral structure dependent interaction and the chiral preference can be concluded from

a comparison of the isotherm shape. However, isotherm measurement gives only thermodynamic information and, hence, the interpretation of the interaction at the molecular level must be concluded very carefully. Very different molecular events could give rise to closely similar results in the thermodynamic limit. Furthermore, the chiral structure dependent interaction is clearly visible in the results of optical measurements but unobserved in isotherm measurements in many cases as will be discussed in the next section. Consequently, the results of the isotherm studies must be interpreted very carefully and other experimental techniques should be applied to the same system whenever possible. The thermodynamic features of the monolayers of enantiomeric and racemic amphiphile are fundamental to the understanding of the chiral preference and could be helpful in the understanding of the underlying molecular arrangement.

3. Experimental Results Obtained from Optical Methods (Brewster Angle Microscopy and Fluorescence Studies) in Chiral Monolayers

In this section we shall review studies based on two optical methods, which are most extensively used in the Langmuir monolayer. They are BAM and fluorescence microscopic technique. Reflection spectroscopy is an extremely useful technique for studying the organized molecular assembly at interfaces.[60−63] This technique allows the researcher to draw inference about the molecular orientation by direct visualization of the monolayer (Figure 6). When *p*-polarized light is used and incidence takes place at the Brewster angle, no light is reflected from the pure air−water interface.[64−67] However, changes in the molecular density and/or refractive index by the condensed phase of a monolayer on the aqueous subphase lead to a measurable change in the reflectivity and allow one to visualize and record the monolayer morphology.

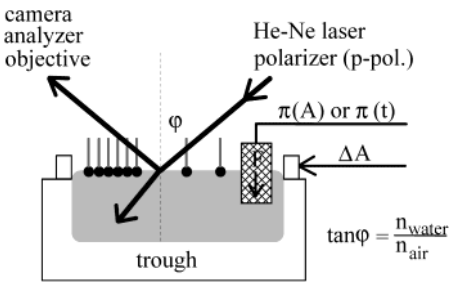

Figure 6. Principle of Brewster angle microscopy (BAM).

In a typical experimental setup (Figure 7), a Brewster angle microscope (BAM) is mounted to a computer-interfaced film balance.[24a] The light source of the BAM is a He−Ne laser. The spatial resolution of the microscope is in the range of a few micrometers. BAM images were taken with a CCD camera, and images are formed in a video unit and can be stored there. The distortion caused due to incidence at the Brewster angle is corrected by digital image processing software. If the BAM image were recorded as a mirror image, then the sense of the curvature of the corresponding domain in the enantiomeric monolayers would be opposite that of the BAM image. The correct sense of the domain can be obtained by using a corresponding image processing software.

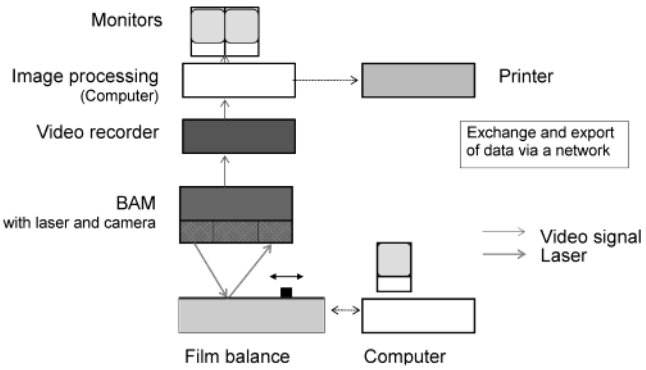

Figure 7. Schematic diagram of the experimental setup for combined surface pressure and BAM measurements.

BAM studies of monolayers revealed an enormous variety of domains in the condensed phase. The structures of the corresponding molecules have profound influence in driving these domain shapes as well as the molecular orientation within a particular domain. Many of the molecules are chiral, and in many cases the chirality has a major influence on the morphology, which is clearly detected by BAM. As pointed out earlier, the effect of chiral discrimination is unobserved in $\pi-A$ isotherm measurements of enantiomeric and racemic amphiphiles, but clear discrimination is revealed from the direct visualization of the domain shape and inner texture by BAM in several chiral monolayers. The texture gives a direct indication about the orientation of the average molecular orientation in the monolayer. However, characterization of the orientational order in a condensed phase requires that the observed textures occur under well-defined conditions. BAM can also distinguish between the jumps of orientations and a continuous change in orientation. Careful observation must be made whether the lines that separate the dark and bright areas remain at a fixed position or are shifted, respectively, when the analyzer is rotated. Observing the sequence of images using a video camera rather than observing single images can achieve this. It may be noted that no external probe is used in the BAM technique. Thus, careful investigation using BAM can reveal many microscopic details of the monolayer without any external perturbation. BAM is advantageous compared to the fluorescence technique, which requires dye molecules as probes to investigate the monolayer morphology.

In the fluorescence microscopic studies, a fluorescent probe (a dye molecule) is added to the monolayer, which is excited using a high-pressure mercury lamp. Then the monolayer state is observed with a microscope mounted with a camera.[19,20,23] A variety of probes have been used. A few commonly used probes are, for example, 4-(hexadecylamino)-7-nitrobenzoxa-1,3-diazole, L-α-phosphatidylcholin-*β*-(NBD-aminohexyl)-*γ*-palmitoyl, *sn*-1,2-dipalmitoyl-3-glycerophosphatidylethanolamine (DPPE), sulforhodamine, dipalmitoylnitrobenzooxadiazolphosphati-

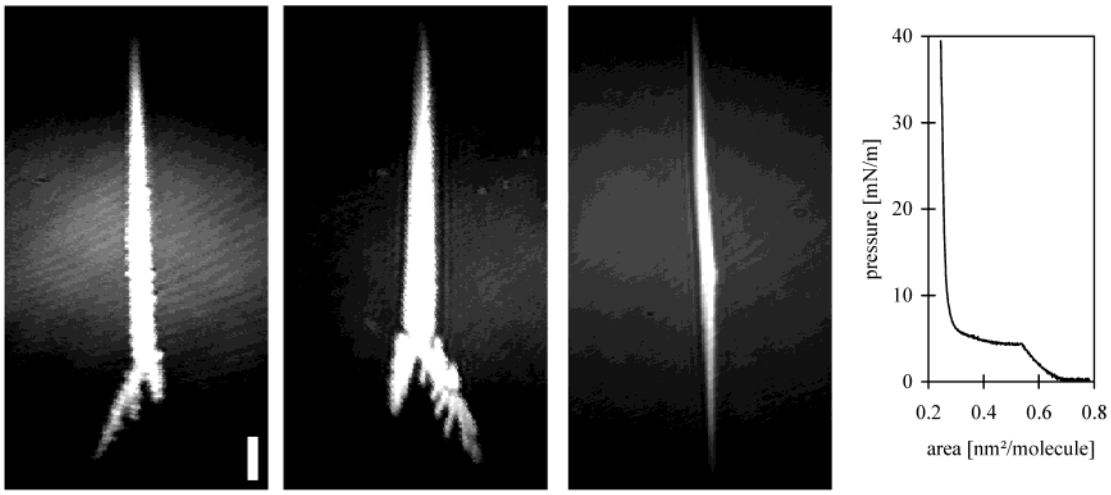

R-TDPAA

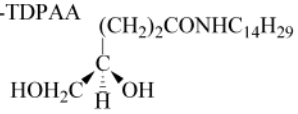

Figure 8. Chiral discrimination of the condensed phase textures of *N*-tetradecyl-γ,δ-dihydroxypentanoic acid amide monolayers observed by BAM.

dylethanolamine (DP-NBD-PE), and 1-palmitoyl-2-{2-[(7-nitro-2-1,3-benzoxadiazol-4-yl)amino]dodecanoyl}phosphatidylcholine (NBD-PC). Due to the presence of dye molecules the effect of trace components on the monolayer properties cannot be ignored in fluorescence studies.

3.1. Amphiphiles Containing an Acid Amide Headgroup with a Single Chiral Center

Representative examples can demonstrate that BAM and fluorescence microscopy are effective and sensitive methods in visualizing chiral discrimination effects in the monolayer morphology. In some cases, the thermodynamic differences between enantiomeric and racemic monolayers are too small to be measured by recording the $\pi-A$ isotherms, as mentioned earlier. However, the BAM studies clearly reveal a chiral discrimination effect. For example, the $\pi-A$ isotherms of the enantiomeric and racemic monolayers of TDHPA are nearly identical, whereas the BAM images indicate that single condensed phase domains, developed at the beginning of the two-phase coexistence region, grow with dendritic shapes, and the direction of the main growth axes bears the mirror image relationship for the enantiomers.[42b] The domains of the racemic mixture are quite similar; however, they have no mirror symmetry. The BAM images of enantiomeric and racemic TDHPA are shown in Figure 8.

The growth patterns are symmetric for achiral acid amide amphiphilic systems. *N*-Tetradecyl-β-hydroxypropionic acid amide monolayer[68] and *N*-alkyl-γ-hydroxybutyric acid amide monolayer with various chain lengths (dodecyl and tetradecyl)[69] develop achiral shapes of the domains, which reflect the influence of the underlying achiral molecular structure.

3.2. Amphiphiles Containing an Amino Acid Headgroup with a Single Chiral Center

The isotherm studies of amphiphiles containing amino acid headgroups such as *N*-alkanoylamino acid derivatives revealed chiral discrimination effects. This is discussed in the previous section. These amphiphiles are studied extensively by optical techniques. Chiral domain shapes are observed in *N*-acylalanine and *N*-acylvaline monolayers using fluorescence studies.[31] "Wishbone"-shaped domains with right-handed or left-handed curvatures are observed in a racemic monolayer of *N*-palmitoylvaline and *N*-stearoylvaline monolayers at low temperatures in the range of 5−22° C. The domain arm breaks when it touches another arm, which indicates solid-like or highly ordered states of the monolayer. In contrast to the *N*-acylvaline derivatives, the monolayers of *N*-palmitoylalanine measured at 30 °C show development of domains with irregular side branching. The systems may be far from equilibrium as the chiral preference is not yet developed.

Fluorescence microscopic studies of enantiomeric myristoylalanine monolayer show dendritic condensed phase domains.[38,70] The size of the dendrites could be in the range from a few micrometers to 1 cm. The main branch width is in the range of 10−20 μm. Several branches grow from the sides, making 60−90° angles, depending on the internal orientation of the main branch. Distances of a few tens of micrometers separate them from each other.[70] The domains are solid-like, and they break rather than bend when they are stressed on each other.[38,70] The domains of racemic monolayer are isotropic and circular. Their shapes change to elliptical by shear flow. The tip shape of the dendritic growth is related with the line tension anisotropy.[71] It is proved theoretically as well as experimentally that the surface tension anisotropy is a prerequisite for the

dendritic growth in three-dimensional systems.[71−76] Theoretical studies have also indicated that the line tension anisotropy is related with the chirality of the molecules composing the monolayer.[77] However, it is undecided whether the dendritic domain shape is manifested by the underlying chirality in these amphiphilic systems via the anisotropic line tension.

In the domains of enantiomeric myristoylalanine monolayer, when the compression was stopped, dark and irregular rings were observed at the peripheral regions after 1 min and gradually curved needles were seen within the domain after a longer time (1 h). It is suggested that the appearance of the dark ring and the curved spines is due to the formation of organized regions with enantiomeric richness (chiral segregation).[38] However, recent combined GIXD and surface pressure studies of racemic myristoylalanine monolayers have shown that there is no indication for such long-time segregation, but rather instantaneous chiral segregation takes place after transition to the condensed state.[78]

Fluorescence microscopic studies demonstrated the growth of an elongated condensed phase domain in monolayers of *N*-stearoyltyrosine at a subphase adjusted to pH 7.0 using a phosphate buffer.[32] In many instances, the domain shapes seem to be broken. In contrast, the domains composed of racemic molecules are compact in shape. The fluorescence microscopy studies of *N*-stearoyltyrosine methyl ester at the same subphase show condensed phase patterns of the racemic monolayers with both clockwise and counterclockwise curvatures. This suggests homochiral preference.

Recent comprehensive studies of the condensed phase domains of various amino acid amphiphiles such as *N*-palmitoylaspartic acid, *N*-palmitoyl- or *N*-stearoylserine methyl ester, *N*-palmitoylthreonine and its diastereomer *N*-palmitoyl-*allo*-threonine, and their methyl esters, *N*-palmitoyl- or *N*-myristoylalanine reveal a large morphological variety depending also on the system conditions, particularly on the compression rate and temperature.[39,40,79] Many fascinating domain shapes have been found, but in all cases the curvature of the two enantiomeric forms are directed in an opposite sense. The domain shape of the 1:1 racemic mixtures is usually different, but very often oppositely curved texture elements can be observed within a single domain, which indicate homochiral preference and, correspondingly, chiral segregation. This can be demonstrated by some characteristic examples as follows.

Figure 9 shows typical domain shapes of *N*-stearoylserine methyl ester monolayers. The spiral-shaped domains of the two enantiomeric forms are curved in opposite directions. The 1:1 racemic monolayer tends to form compact domains in equilibrium, but both of the opposite curvatures within a domain in the form of hooks at the domain periphery or opposite growth diections in newly formed domains can be observed during the growth kinetics.

Now we consider the chiral discrimination in the domain morphology of an amino acid amphiphile with a very different chemical structure.[79]

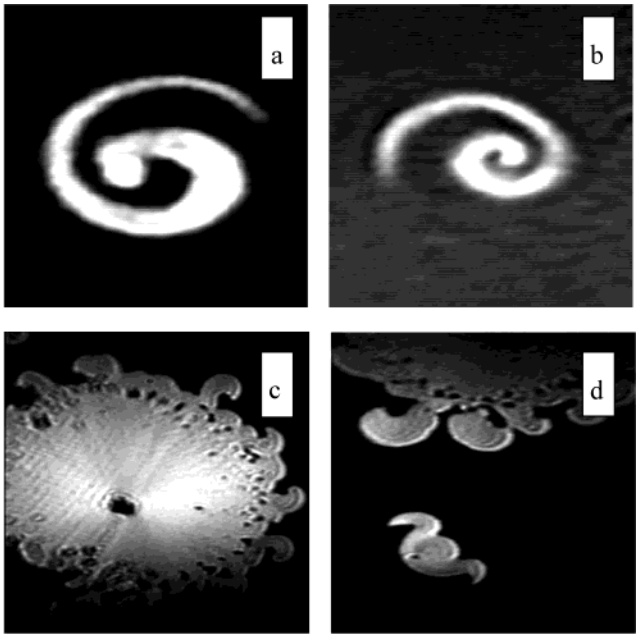

Figure 9. BAM images of the chiral discrimination of the condensed phase domains of *N*-stearoylserine methyl ester monolayers spread on pH 3 water: (a) D-enantiomer; (b) L-enantiomer; (c and d) 1:1 DL-racemate. Image size 80 × 80 μm. (Figure is reproduced here at 67% of its original size.)

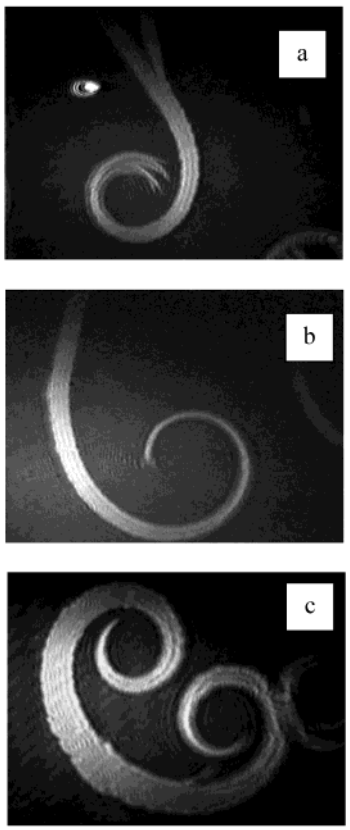

Figure 10. Chiral discrimination in the domain texture of *N*-α-palmitoylthreonine monolayers observed by BAM: (a) D-enantiomer; (b) L-enantiomer; (c) 1:1 DL-racemate. Image size 350 × 350 μm. (Figure is reproduced here at 67% of its original size.)

Figure 10 allows the comparison of the condensed phase domains formed by enantiomeric and racemic

N-α-palmitoylthreonine monolayers. In this case, the domains of the two enantiomeric monolayers are spirally curved at one end of the domain in the sense of the respective chiral form, again in opposite directions to each other. The racemic monolayers grow (Figure 11) from a center in opposite direction

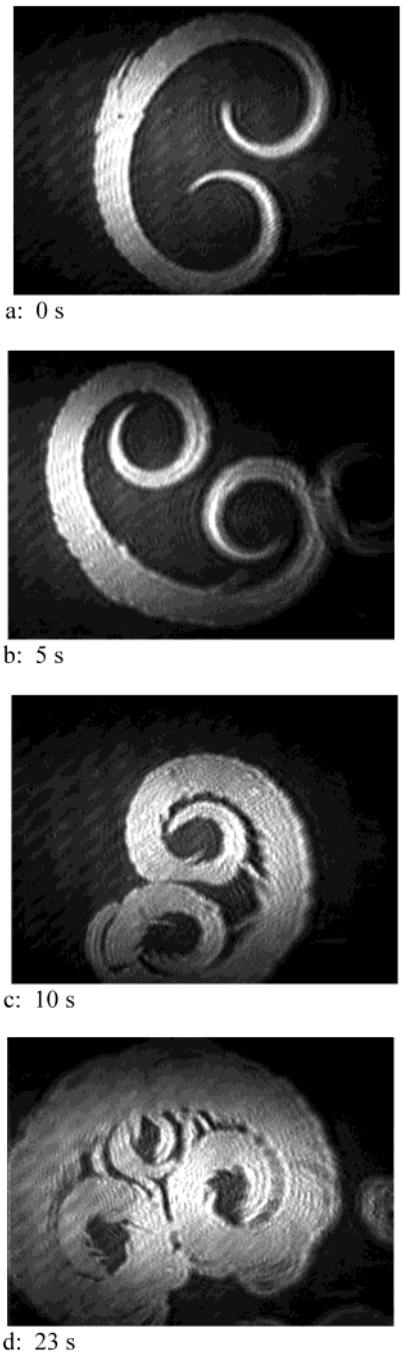

Figure 11. Growth kinetics of *N*-palmitoyl-DL-threonine domains in the two-phase coexistence region at 2 °C at compression from 0.50 to 0.37 nm/molecule: (a−d) development of the domain within 23 s. Symmetric domain structures with opposite curvatures grow from the center of the nucleus and suggest chiral segregation.

and with opposite curvature indicating chiral segregation within a domain in accordance to the homochirality which can be concluded from the $\pi-A$ isotherm measurements.

It is interesting to note that domains formed by the amino acid amphiphiles, so far studied, have no inner anisotropy, as revealed by BAM. Therefore, it can be concluded that the azimuthal projection of the tails of neighboring molecules should be parallel to each other within a domain. Note that this in contrast with the concept that the presence of mutual orientation of a pair of chiral molecules leads to a spontaneous curvature,[55] which can lead to domain curvature.[39,40,77] The absence of mutual intermolecular orientation in amino acid amphiphiles and the concomitant curvature of the domain composed of the enantiomeric amphiphile are suggested to be due to competing with hydrogen-bonding interaction.[39,40] However, this proposition is yet to be experimentally verified and is discussed in section 6.

3.3. Amphiphiles Containing a Glycerolic Headgroup with a Single Chiral Center

Domain textures and chiral discrimination effects are studied in various monoglycerol monolayers using optical microscopy. Interesting inner structural elements are observed in these monolayers. BAM studies of these systems also show that the apparent similarity of the $\pi-A$ isotherms of any two amphiphiles cannot be taken as evidence that the underlying morphologies or the phase behaviors are the same for them. This will be discussed below.

It is observed that subtle molecular structural changes can lead to changes in domain morphology. For example, the replacement of the ether linkage by the ester linkage has a significant effect on the monolayer structure.[46] It is suggested that the greater configurational freedom for the ether linkage compared to the ester group leads to the more complex phase behavior of 1-*O*-hexadecyl-*rac*-glycerol. The C═O dipoles in the ester group might cause a fixed configuration of chain and headgroup.[46] This implies that the molecular structural factors play an important role in the monolayer morphology. BAM studies of 1-*O*-hexadecyl-*rac*-glycerol and 1-monopalmitoyl-*rac*-glycerol monolayers clearly establish the important fact that the apparent similarity of the $\pi-A$ isotherms of the two amphiphiles cannot be taken as evidence that the underlying morphologies or the phase behaviors are the same for them.[46,69] BAM images of the amphiphiles at different surface pressures are shown in Figures 12 and 13.

The images of Figure 12 correspond to the surface pressures of the two-phase coexistence region of the 1-*O*-hexadecyl-*rac*-glycerol monolayer described in Figure 2. The condensed phase domains of 1-*O*-hexadecyl-*rac*-glycerol (Figure 12) are subdivided into segments reflecting differently and meeting at a point on the edge of a domain. This indicates that the molecular director is oriented in different directions in the several segments. The boundaries between the different segments are straight lines in this case. All domains have a characteristic notch in the circumference, and the notch in the domain shape is preserved independent of the shape changes. Three-armed structures are formed when the area/molecule is compressed to 40 Å^2/molecule, and each arm is divided into two segments of different orientations.

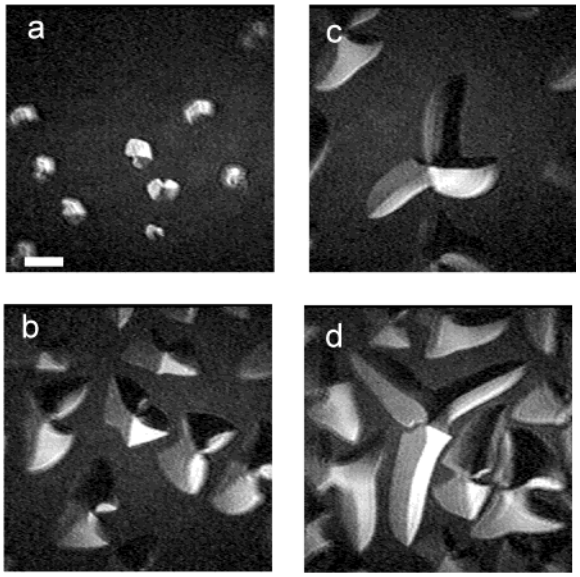

Figure 12. Domain development in the two-phase coexistence region of 1-*O*-hexadecyl-*rac*-glycerol monolayers at 23 °C

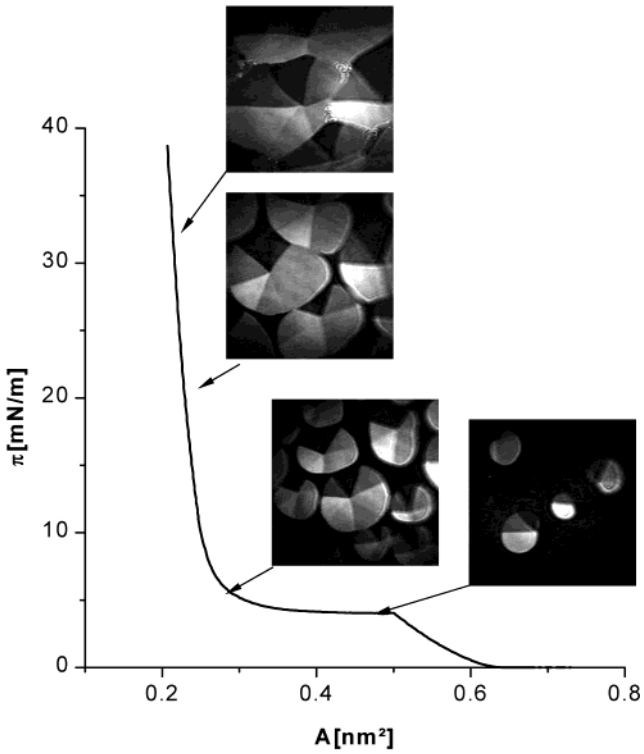

Figure 13. Domain growth along the compression isotherm of a 1-monopalmitoyl-*rac*-glycerol monolayer at 23 °C.

Continuous changes in molecular orientation within both regions of arms are observed. The marked change in the orientational order of the condensed phase within the two-phase coexistence region is an interesting phenomenon. At the end of the plateau region starts a complicated change in the domain structure. The three- or multi-arm structures decay in the course of this transformation process with numerous spiral substructures (Figure 14).[80]

Only clockwise-curved spirals are formed in the *S*-enantiomeric monolayer of 1-*O*-hexadecyl-*rac*-glycerol, whereas in the 1:1 racemic mixture the spirals are wound both clockwise and counterclockwise. It was sugggested that the opposite curvatures of these spiral structures reflect obviously segregation of the two enantiomeric forms into substructures, but these first results should be corroborated by additional experiments. Finally, at 20 mN/m the contrast vanishes, which could be due to either a vertical orientation of the alkyl chains or the change of long-range order of the tilt azimuth to short-range order so that the regions of uniform chain orientation are smaller than the spatial resolution of the microscope.

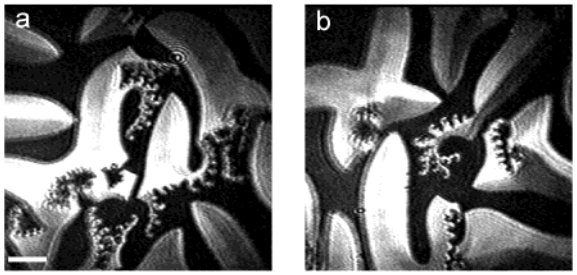

Figure 14. Chiral discrimination in 1-*O*-hexadecylglycerol domains, $T = 23$ °C, $A \approx 0.3$ nm/molecule: (a) racemic mixture with curvatures of the spirals in two opposite directions; (b) *S*-enantiomer having only clockwise curved spirals.

In contrast to the sharp-edged shapes of condensed phase domains of 1-*O*-hexadecyl-*rac*-glycerol, the domain shapes of 1-monopalmitoyl-*rac*-glycerol have a disklike shape (Figures 13 and 15). The representative domains of 1-monopalmitoyl-*rac*-glycerol are subdivided into seven segments of different molecular orientations meeting at the domain center (Figure 15a). In some cases, the intersection point of the domain boundaries is located at the edge of the domain and the number of segments is less than

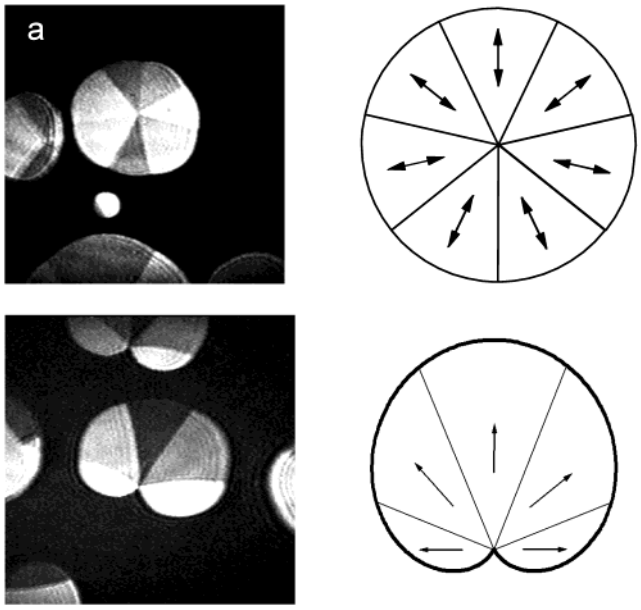

Figure 15. BAM images of a round and cardioid domain of 1-monopalmitoyl-*rac*-glycerol monolayers and schematic presentation of the tilt direction of the alkyl chains in both domain forms.

seven (see, e.g., five segments in Figure 15b). The inner structure of the domains can be regarded as multiple twins. When the surface pressure is increased, the domains gradually deform and fill the gap occupied by the fluid phase. At high pressures >25 mN/m, the general domain shape with tilted molecules is preserved and all gaps are filled (Figure 13). If at high surface pressure the monolayer is kept for ~30 min, a transition to 6-fold domains can be observed, which remains stable also after a following decompression (Figure 16b). The presence of small

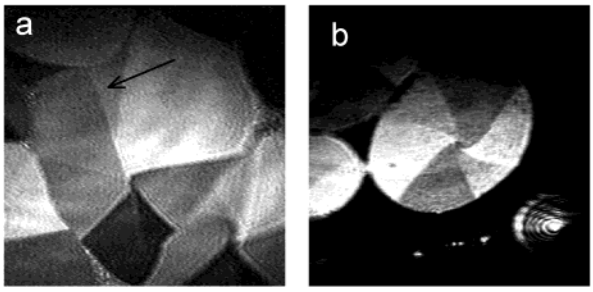

Figure 16. Transition to 6-fold domains in 1-monopalmitoyl-*rac*-glycerol monolayers at high surface pressures (π > 25 mN/m), T = 23 °C: (a) transition state with a small segment (arrow); (b) 6-fold domain formed after compression to 45 mN/m and maintained after decompression to 10 mN/m.

segments and zigzag lines within some intermediate domains indicates reorientation of the molecules (Figure 16a). The transition back to a 7-fold structure is probably kinetically hindered.

The domain structure of the homologous 1-monostearoyl-*rac*-glycerol monolayers resembles that observed in 1-monopalmitoyl-*rac*-glycerol monolayers in the temperature range from 23 to 45 °C.[43] The ratio of the condensed phase to the homogeneous fluid phase increases with increasing molecular density between the main phase transition point and the kink in the steep part of the $\pi-A$ isotherm (for example, observed at 24 mN/m at 35 °C). The condensed phase domains of 1-monopalmitoyl-*rac*-glycerol are first observed after the sharp break of the slope in the $\pi-A$ isotherm at the beginning of the plateau region (Figure 13).[81] The initially formed domains grow to a size of ~0.25 mm in diameter. The disklike domains are subdivided into seven segments of different reflectivities separated by sharp boundaries and meeting in a center. Each segment is homogeneously reflecting and, thus, has a constant chain tilt.

When a set of domains is observed by rotating the analyzer of BAM, it is observed that the segments change their reflectivity in the same way (Figure 17). The optical anisotropy of the domains is due to the different molecular orientations in different parts of the domain. Analysis of the optical anisotropy resulted in the conclusion that the chains of all segments have the same polar tilt but the azimuthal tilt jumps at the segment boundaries by a constant value of (360°/7) angle. Explicitly, the azimuthal angle is changed at each segment boundary, whereas the tilt angle with respect to the normal possesses a definite value. The alkyl chains of the molecules within the

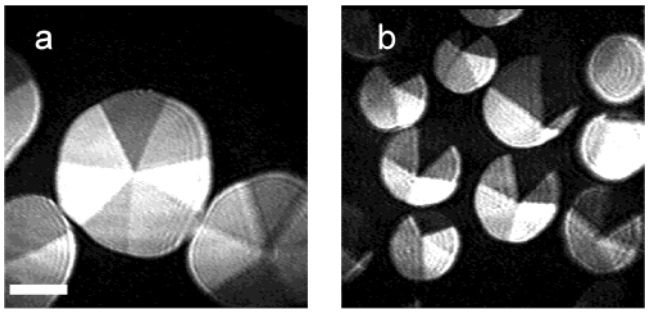

Figure 17. BAM images of domains of 1-monopalmitoyl-*rac*-glycerol monolayer: (a) representative round domain with seven segments; (b) several domains with the same reflectivity of the corresponding segments.

7-fold domains of 1-monoglycerides are tilted in a radial direction. This is demonstrated in Figure 15.

Upon compression, the domains impinge on each other and start to deform. A characteristic point of the monolayer is observed at ~24 mN/m at 35 °C when the domains coalesce into a homogeneous phase without any gap (Figure 13).

In some cases, cardioid-shaped domains are formed when the segment contact occurs at the edges of the domain (Figure 15, bottom). The outer segment shapes are distorted, which is suggested to be due to anisotropic line tension. The line energy for a domain is the line tension integrated over the whole domain boundary. Minimum line energy can be realized for a domain shape for which the boundary area is not the minimum at the constant domain area when the line tension is anisotropic. The boundary length of a cardioid-shaped domain is only 4% larger than that of the circular domain of the same area. It is known that the minimum line tension is realized when the domain boundary is perpendicular to the tilt azimuth of the alkyl tails.[68] Thus, the part of the domain boundary where the tilt azimuth of alkyl tails are nearly perpendicular is shorter in circular domain compared to that in cardioid-shaped domains, if the contact point of segments is situated at the domain boundary. Consequently, the domain shape becomes cardioid-shaped if the contact point of the segments is situated at the domain boundary.[81] When the segment boundaries meet at a center, the molecules are observed to be tilted nearly perpendicular to the boundary in the whole domain (Figure 15, top). The centered domains have lower total line energy than the cardioid-shaped domains, but the total length of segment boundaries is higher. However, neither the molecular origin of the anisotropic line tension nor the origin of the wide spread of the position of the segment center is understood. Possibly the position of the segment center is determined by the directional dependence of the growth rate of the domains.

A geometric concept based on considerations of the molecular packing is proposed to describe the inner structure of the condensed phase domains of 1-monopalmitoyl-*rac*-glycerol, which exhibits 7-fold domain substructure.[82] In this concept, different structures arising from multiple twinning in a two-dimensional centered orthorhombic lattice are considered. Twin planes are planes with a high loading density.[83] Therefore, the boundaries between segments of dif-

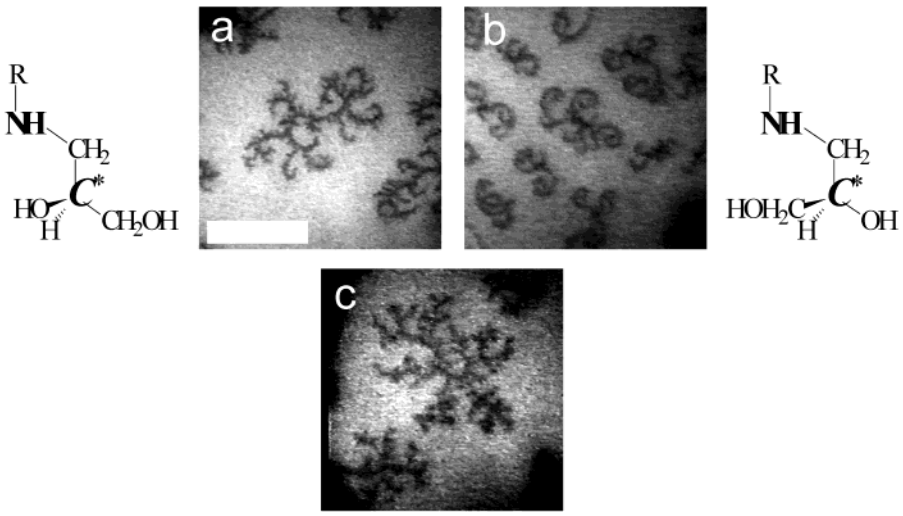

Figure 18. Fluorescence microscopy of the chiral discrimination in 1-stearylamine glycerol monolayers, $T = 35$ °C, $\pi = 5$ mN/m: (a) *S*-enantiomer; (b) *R*-enantiomer; (c) 1:1 racemate. The asterisk marks the chiral C atom. The bar length is 100 μm.

ferent molecular orientations are thought of as dense lattice rows so that a well-defined change in molecular orientation occurs at the boundary between two segments. The segment boundaries are considered to be mirror lines as well as contact lines of segments rotated by 360°/*n* around the meeting point of the segments (*n* is the segment number). Experimental evidence for this assumption was provided by a later AFM study.[84] The intersection angle δ of the lattice directions which form the segment boundaries is related to the segment number *n* by $n = 360°/\delta$; that is, for a seven-segment domain ($n = 7$), δ should be ~51.4°. The geometrical analysis has shown that seven segments can occur only if (i) the segment boundaries are along the densest lattice rows and the chains are tilted toward next nearest neighbors or (ii) the segment boundaries are along the second densest lattice rows and the chains are tilted toward nearest neighbors. The second case is realized in the 7-fold domain structure under the studied experimental conditions. As the study does not explicitly include the molecular structure of the amphiphiles, a future study, which combines the molecular interaction and the concomitant preferred orientational arrangements in a lattice, is expected to provide additional information.

The enantiomeric domains of 1-stearylaminoglycerol monolayers show an interesting chiral discrimination effect in the fluorescence microscopic studies, which is not detected in the $\pi-A$ isotherm measurements.[47] Filigree-like domains are found, which are curved in a clockwise direction for the *R*(+)-enantiomer and in a counterclockwise direction for the *S*(−)-enantiomer (Figure 18a,b). The racemic mixture evolves fractal-like domains without any specific sense of direction (Figure 18c). Note that chiral discrimination of a different kind but having the same sense of curvature has been found in the domain morphology of the monoglycerol ethers.[45,80] As shown above, spiral shapes grow from initially compact domains at the end of the plateau region of the $\pi-A$ isotherm. The sense or the handedness of the curvature is dependent on the enantiomeric forms. The spirals developed in the racemic monolayers are curved with both handednesses.

Polygonal shapes are observed in the fluorescence microscopic studies of enantiomeric and racemic monolayers of 4-hexadecyloxybutane-1,2-diol (HOBD) above the transition pressure.[85] The branches of *S*-HOBD turn in only a clockwise direction, whereas the racemic mixture and mixtures containing other proportions of enantiomers develop branches in other directions. The numbers of left- and right-handed arms depend on mixing ratio.

3.4. Amphiphiles Containing a Phospholipid Headgroup with a Single Chiral Center

Most of the initial studies about the effect of chirality on the morphology of biomimetic monolayers were focused on the model phospholipids DPPC and DMPE. Before some results of phospholipid monolayers are discussed in detail, a short summary will be given of how basically chirality is apparent in the domain morphology of phospholipids (Figure 19−23). In equilibrium, phospholipid monolayers form compact domains of different shapes and inner textures (Figure 19). As the relaxation time for reaching equilibrium is rather high, nonequlibrium structures in the form of dendritic or fractal-like structures are observed under the corresponding experimental conditions (Figure 20). The chirality of the enantiomeric forms of the compact domains can be apparent in clockwise or counterclockwise curvatures of the defect lines, domain arms, for example, triskelions, or regions of the same azimuthal orientation (Figure 23). The curved defect lines can meet within the domain or at their edge. In all cases, the two enantiomers show curvatures of opposite senses.

The corresponding nonequilibrium structures with dendritic growth develop curvatures of the same sense. In the fractal-like structures the effect of chirality cannot be observed, because at the beginning the patterns are obviously nonordered (Figure 20). In the corresponding racemic mixtures of different phospholipids, curvatures are not formed, but

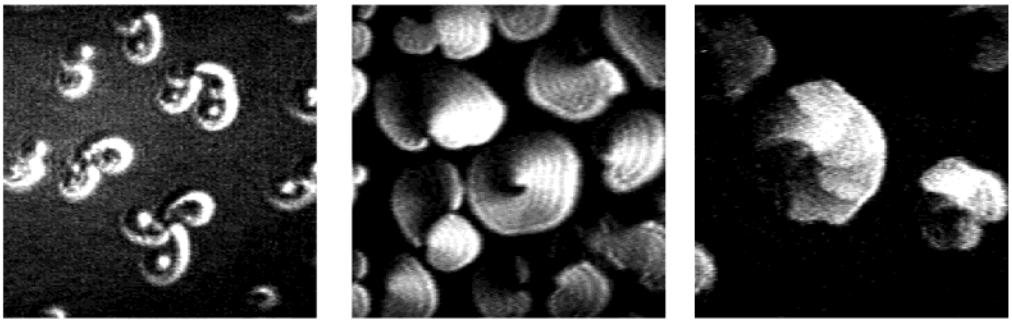

Figure 19. Representative equilibrium domains of phospholipids: (left) D-DPPC monolayers with curved domain arms; (middle) D-DPP(Me)$_2$E monolayers with curvature in the brightness change within the domains; (right) L-DPPE monolayers with curved defect lines.

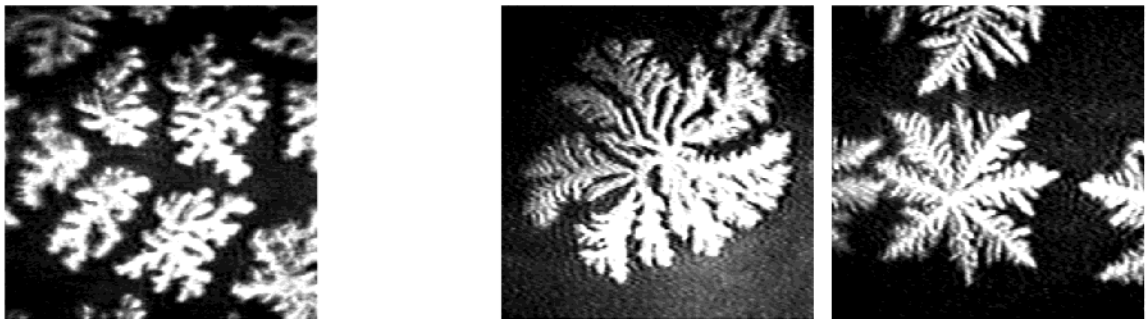

Figure 20. Representative nonequilibrium domains of phospholipids: (left) L-DPPC monolayer far from equilibrium with fractal-like (disordered) growth without chiral influence; (right) L- and DL-DPPE monolayer not so far from equilibrium with dendritic (ordered) growth with chiral influence [curved axes and arms for enantiomeric monolayers (L-DPPE); straight axes and arms for racemic monolayers (DL-DPPE)].

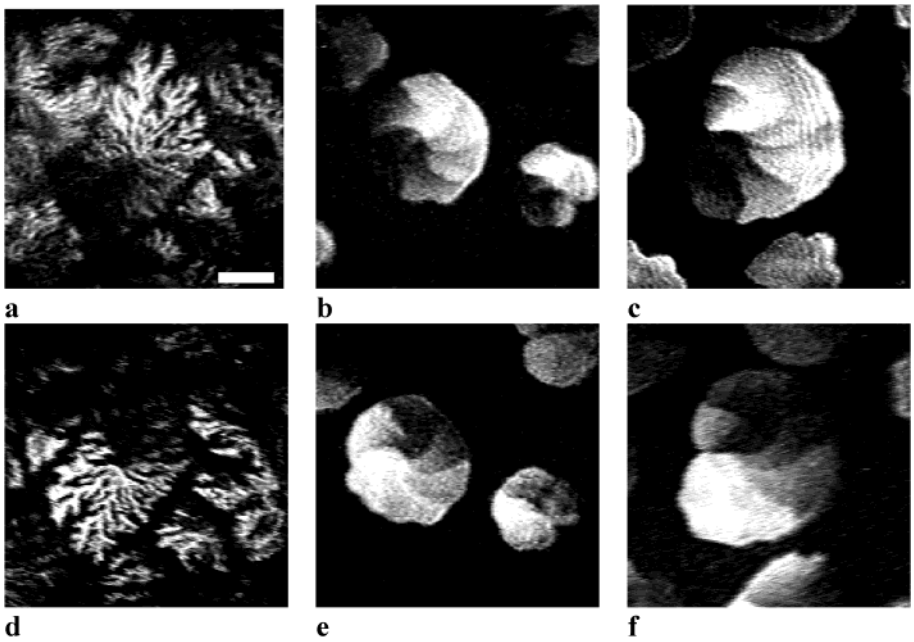

Figure 21. Domain structures of L-DMPE monolayers. The molecule orientation in the compact domains (b, c) is generally the same as in the branched domains (a). The centered (b) and noncentered (c) domains show the same arrangement. The domains are presented for two opposite positions of the analyzer [analyzer angle α (above) and $-\alpha$ (below); $\alpha \approx 50°$]. The bar length is 100 μm.

rather straight dendrite arms or uncurved compact domains are formed.

If the formation of the condensed phase domain occurs far from equilibrium, the growth kinetics can be so rapid that the stable phase does not have time to reach its lowest energy state on the microscopic level. A metastable microstructure results, and the growth patterns formed under these nonequilibrium conditions are mainly affected by the complicated interplay between the microscopic interfacial dynamics, such as surface kinetics, surface tension, and crystalline anisotropy, and external driving forces, such as supersaturation and undercooling.[24a] In highly supersaturated monolayers, the macroscopic dynamics is determined by the diffusion field, which tends to drive to the formation of fractal-like objects.

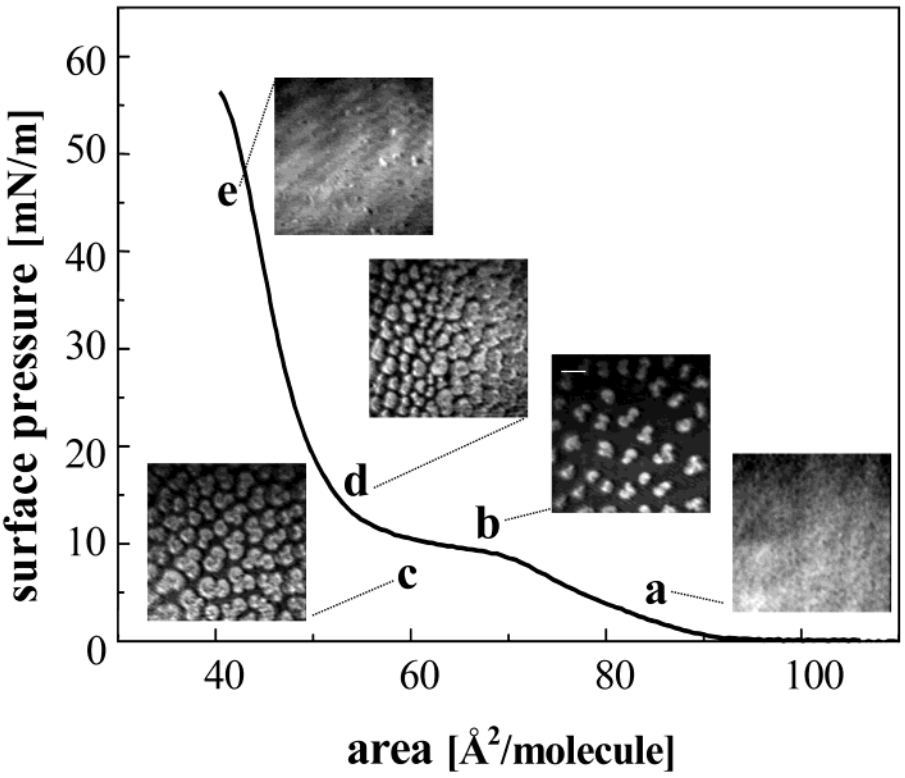

Figure 22. $\pi-A$ isotherm of a DPPC monolayer on water and corresponding BAM images at $T = 23$ °C: (a) fluid (gaseous) state; (b−d) domain growth in the two-phase coexistence (plateau) region; (e) fully condensed phase. The bar represents 80 μm. All images have the same scale of 500 × 500 μm. (Figure is reproduced here at 62% of its original size.)

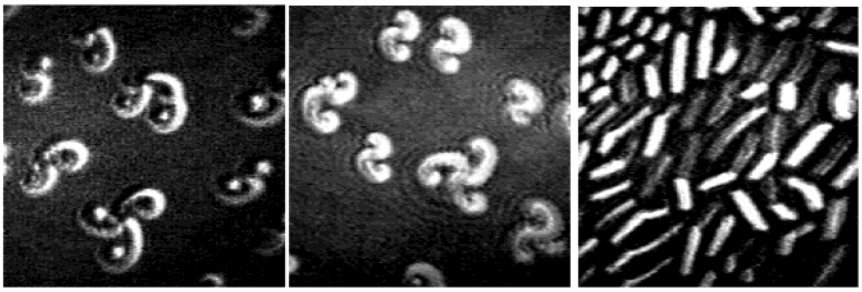

Figure 23. Chiral discrimination in DPPC monolayers. The two enantiomeric triskelions are curved in opposite direction, clockwise for D-DPPC (left) and counterclockwise for L-DPPC (middle). The arms of the racemic DL-DPPC are straight. Image size 500 × 500 μm. (Figure is reproduced here at 50% of its original size.)

Consequently, the growth shapes of the condensed phase domains can substantially depend on the compression rate of the monolayer. For example, the shapes of the DMPE domains are fractal-like at high compression rates as expected for diffusion-limited aggregation, whereas only at very low compression rates are compact domains evolved.[24a,86] It would be very interesting to study the effect of the molecular chirality on the growth kinetics or the relaxation of the condensed phase structure, if any.

Comparison of the BAM images of the enantiomeric phospholipids L-DMPE and L-DPPC monolayers reveals very different domain textures. In equilibrium L-DMPE monolayers form compact domains with different numbers of segments (five to eight) separated by chirally curved lines where the molecular orientation jumps. The lines join together in a center located inside the domain (the shape of the domain is circular) or in its edge (the shape of the domain is bean-shaped). The molecule orientation in the branched domains formed at high compression rates under nonequilibrium is similar to that in the compact domains.

A compression isotherm of enantiomeric DPPC and corresponding BAM images are shown in Figure 22. Point a in Figure 22 represents the fluid (gaseous) state. The next images (b−d) are taken from successive stages of the two-phase coexistence region and show formation, growth, and compression of the characteristic triskelions. Point e corresponds to the fully condensed state. The texture of the condensed phase domains of DPPC monolayers is strongly affected by the compression rates. At very low compression rates, equilibrium shapes are evolved in the form of triskelions curved oppositely for the two enantiomeric forms and noncurved arms for the racemic mixture (Figure 23). The lines running through the arms of the enantiomeric domains mark a strong continuous change in the orientation. In the enantiomeric DPPC domains, the orientation changes

gradually within each arm of the triskelions.[86−88] This difference in the outer shape of the domain and their inner structure is striking. The difference in molecular structure and the corresponding differences in the chiral features of the two molecules are responsible for the observed differences. Epifluorescence microscopic studies of DPPC established that the handedness of the highly ordered domains is directly related to the absolute configuration of the enantiomer.[89] It is observed that the condensed phase domains of the monolayers composed of 75% *R*-DPPC and 25% *S*-DPPC are triskelion-shaped and the arms of the domains are oriented in an anticlockwise (left-handed) fashion. The domains composed of 75% *S*-DPPC and 25% *R*-DPPC are also triskelion-shaped, with their arms oriented in a clockwise (right-handed) fashion. The domains of racemic DPPC (equimolar mixture of *R*-DPPC and *S*-DPPC) show development of arms without curvature. The arms of the domains are oriented in specific directions, which is a chiral object in a mesoscopic length scale. Clearly this mesoscopic chirality is triggered by the microscopic chirality present at molecular level. Theoretical studies on the effect of molecular chirality and the curvature of the enantiomeric domains of DPPC are discussed in section 7.

An interesting comparative study of the morphological features of phospholipid monolayers with very similar chemical structures is carried out using BAM.[88] Four phospholipids of the same chain length are different only with respect to the number of methyl groups at the nitrogen of the headgroup (Figure 24). The morphological features of dipalmi-

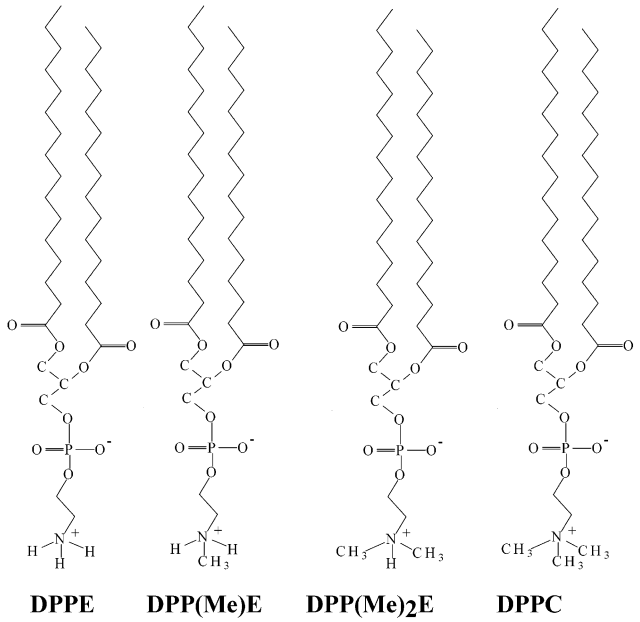

Figure 24. Systematic headgroup variation in phospholipids: DPPE, dipalmitoylphosphatidylethanolamine; DPP-(Me)E, dipalmitoylphosphatidyl-*N*-monomethylethanolamine; DPP(Me)E, dipalmitoylphosphatidyl-*N*,*N*-dimethylethanolamine; DPPC, dipalmitoylphosphatidylcholine.

toylphosphatidyl-*N*-monomethylethanolamine [DPP-(Me)E] and dipalmitoylphosphatidyl-*N*-dimethylethanolamine [DPP(Me)$_2$E] are studied and compared with those of monolayers of dipalmitoylphosphatidylethanolamine (DPPE), dimyristoylphosphatidylethanolamine (DMPE), and dipalmitoylphosphatidylcholine (DPPC).

The BAM images of Figure 25 demonstrate how the chirality affects the domain texture in equilibri-

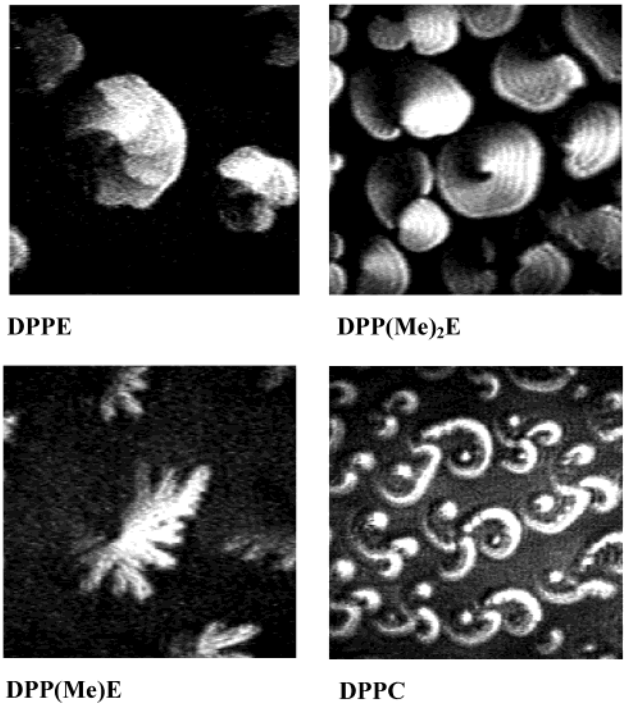

Figure 25. Effect of the headgroup variation of chiral phospholipids on the texture of the equilibrium domains.

um. The properties of the condensed phase domains of DPP(Me$_2$)E and DPP(Me)E are between those of DPPC and DPPE or DMPE. In nonequilibrium, fractal-like or dendritic domains are formed depending on the compression rate. The fractal-like domains of DPP(Me)$_2$E or DPPC do not reflect chirality as they are grown obviously too far from the equilibrium, whereas the dendritic domains of DPP(Me)E and DPPE are specifically curved, indicating the influence of chirality. However, in the racemic mixtures of phospholipids, for example, in DL-DPPE monolayers, straight dendritic arms are observed. The absence of a curvature in the dendritic arms of racemates points out that the curvature is an effect of the chirality and not a characteristic of the observed texture.

Compact phospholipid domains can be obtained at very low compression rates or as a result of a long-time shape relaxation after the monolayer compression has been stopped. Under these conditions close to the equilibrium, chirality affects the domain texture in a different way, but always curvatures corresponding to the enantiomeric forms are observed in the domain texture. Enantiomeric DPPC domains form triskelions with curved arms and a remarkable continuous change in the orientation within the arms. It is interesting to note that domain shapes with noncurved arms are formed in monolayers of the racemic DL-DPPC mixture.[24b] Compact domains subdivided into segments by curved lines at which the orientation jumps are observed in enantiomeric L-DMPE monolayers. In the compact L-DPP(Me$_2$)E

domains the orientation changes by 360° around a point inside or at the edge of the domain, and no jump in the orientation is observed.

Growth of chiral domains in DMPA monolayers containing 1 mol % cholesterol is observed.[91] The shape is spiral. The domain shape is dependent on pH. Ionic strength and pH are controlled by the addition of NaCl and NaOH, respectively. The lipid spirals are observed at a narrow range of pH ~11. At lower pH (~10.5) the spirals convert into coffee bean shapes. These effects are suggested to be related with the increase or decrease in the electrostatic forces, which lead to a change in the boundary/area ratio. It is argued that the lipids have an excess charge or a dipole moment normal to the surface and the surface electrostatic repulsion is driving the thin, elongated shape. The line tension competes to reduce the boundary line, and the effect of cholesterol is to decrease the line tension, thereby favoring the elongated shape. Clearly, the formation of spiral shapes is additionally driven by the chirality of the molecules.

The role of the headgroup size and the concomitant symmetry in crystalline domains responsible for a given domain shape inDMPA monolayers containing 1 mol % cholesterol is also studied.[90] DMPA at high pH has a double-charged headgroup, which expected to occupy a large area. In condensed monolayer phases the alkyl chains are tilted. In this respect the arrangement of the molecules is similar to that of DPPC monolayers. It is suggested that the symmetry is reduced from hexagonal symmetry as observed in lipids with small headgroups and the domain shape becomes elongated rather than symmetric.[91] Such elongation is not to be expected when the chain tilt is small or zero. This is the case for the DMPA monolayers with cholesterol at pH 8 and DMPE monolayers with cholesterol. On the basis of this proposition, the formation of the elongated domain shape is essentially driven by the chain tilt, which in turn can be controlled by the presence of ions in the solution. It is also indicated that the effect of chirality is to bend the elongated domain. The possibilities of chiral diffusion or the specific molecular interactions like those between CO and phosphate groups are suggested to be the reasons for such bending. The permanent dipole moment in the headgroup region has an in-plane dipole moment, which slightly deviates from the preferred growth direction of the crystal (presumably the *X* direction) due to the asymmetric arrangement of the headgroups. The asymmetric arrangement of the headgroups should cause the molecular arrangement to change from rectangular to trapezoidal shape. As a result, the neighboring molecular dipoles would be nonparallel and have a nonzero angle between them with respect to the preferred growth direction.

In many experimental studies on the morphology of lipid monolayers, added substances are present, which could have substantial influence on domain morphology. Cholesterol is an important constituent of biological membranes, and studies on lipid monolayer structure and phases are often made including cholesterol as one of the components. One important reason to include cholesterol in such studies is to understand the lipid distribution and interaction in biological membranes. Due to the chirality of the cholesterol molecule, the results of the structural or morphological studies in such two-component systems (containing an amphiphilic component and cholesterol) are difficult to interpret unambiguously. Explicitly, it is difficult to conclude whether any observed morphological feature is arising from the amphiphile or the added substance. The effect of cholesterol on monolayer packing properties of DPPC and 1-palmitoyl-2-oleoylphosphatidylcholine (POPC) was studied.[91] The introduction of cholesterol to these monolayers decreased the average molecular area occupied by the phosphatidylcholine molecules by inducing the order into the acyl chain. The effect is more prominent in DPPC than in POPC monolayers. The closer packing of the alkyl chains in the presence of cholesterol could drive stronger chirality-dependent interaction compared to the monolayer where the cholesterol is not added. It is, however, unclear whether this condensing effect triggers the stronger chiral shapes in the presence of cholesterol or not.

Chiral features of monolayers of amphiphiles containing headgroups other than amino acid, glycerol, and phospholipids are studied using optical techniques. Epifluorescence microscopic studies of the chiral and achiral imidazole containing amphiphlic monolayers have been performed.[58] The achiral compound develops dark dendritic domains in the LC state. On the other hand, the monolayer composed of the enantiomeric compound develops dendritic domains, which are curved in a specific direction. The domains of the *S*-enantiomer are curved in a counterclockwise direction, whereas the domains of the *R*-enantiomer are curved in a clockwise direction. Fractal-like shapes are observed in monolayers of the racemic compounds. The *R*-domains have very fine branches at 20 °C with mostly 6-fold rotation symmetry. The branches become thick and the interface becomes smooth by lowering the temperature to 15 °C. The number of sidearms is reduced, but the effect of chirality is observable. After 12 h, the domains have a circular shape. However, fractal-like domains without any specific curvature are formed in monolayers composed of enantiomeric molecules containing $ZnSO_4$ in the subphase.

Optical studies in the monolayers draw our attention to the fact that in many cases macroscopic methods such as the $\pi-A$ isotherm measurements fail to detect the chirality effects present at mesoscopic or microsopic level. A bewildering variety of inner structure can be observed in domains composed of different classes of molecular structure also clearly revealed by BAM. The outer shape and some inner structural features of the domains observed in condensed phase monolayers in the liquid condensed phase are shown in Table 1 as observed by optical techniques. The inner structural features are indicative of different molecular orientation as discussed in detail in section 3. The handedness of domain curvature is also indicated in the table when such data are available.

Table 1. Outer Shape and Some Inner Structural Features of the Domains Observed in Condensed Phase Monolayers As Observed by Optical Techniques

amphiphile	outer shape of the domain	inner structural features and handedness (if any)[a]
1-monopalmitoyl-*rac*-glycerol	(i) disk shape	(i) mostly 7 segments, no variation of azimuthal projection within a segment
	(ii) cardioid shape	(ii) <7 segments[43]
1-stearylaminoglycerol	filigree texture	clockwise curvature for *R* (+), counterclockwise curvature for *S* (−); racemic has no specific handedness[47]
imidazole surfactants	dendritic domains	clockwise for *R*, counterclockwise for *S*; no specific sense for racemic (fractal--like domains)[58]
dimyristoylphosphatidic acid	strongly curved spirals at higher pH (∼11) and dendritic shape at lower pH (∼8)[89]	
dipalamitoylphosphatidylcholine	triskellions with all arms curved in one specific direction for enantiomers and racemic domains without any curvature	counterclockwise for D- and clockwise for L-enantiomer[24b,146]
dimyristoylphosphatidylethanolamine	5- and 8-fold domains; segment boundaries are bowed in a specific direction	clockwise for L- and counterclockwise for D-enantiomer[24a]
4-hexadecyloxybutane-1,2-diol (HOBD)	polygonal-shaped domains with curved arms	clockwise for *S*-enantiomers[85]

[a] The inner structural features are indicative of different molecular orientations as discussed in detail in section 3. The handedness of domain curvature is also indicated when such data are available.

Several questions based on these observations are raised: (i) How do only small changes in molecular chirality (by inducing small structural change) of the amphiphile cause significant changes in domain shape and inner structure? (ii) How could the outer domain shape be curved in the absence of mutual intermolecular orientation? Although detailed answers to such questions are yet to be provided, the results of BAM clearly point out the decisive role of molecular chirality in determining the molecular orientation and the resultant domain shape.

4. Experimental Results Obtained from Grazing Incidence X-ray Diffraction (GIXD) Measurements in Chiral Monolayers

Both X-ray and neutron beam techniques are employed to study the molecular organization of monolayers at the air−water interface. Extensive literature on various techniques is available.[25,93−96] Specular reflectometry using X-rays or neutron beams probes the electron density or the neutron scattering length density profiles normal to the interface. The GIXD technique probes the molecular order in crystalline surface films (Figure 26).[25,26,97] X-ray beams obtained from synchrotron radiation facilities are employed for this purpose. The beam is incident on the surface at a very small angle (∼0.1°) and, thus, background scattering is avoided. The beam undergoes total reflection, and only a part penetrates into the subphase. The scattered radiation is detected, and the periodicity of molecular arrangements gives rise to the peaks in the scattered intensity.

The diffraction patterns obtained from the GIXD studies are always averaged over all domain orientations in the monolayer plane. As a result, whereas the vertical out-of-plane component, K_z, of the momentum transfer vector **K** is separately measurable, the two in-plane components (perpendicular to K_z), K_x and K_y, are not separately measurable. Only the combination $K_{xy} = (K_x + K_y)^{1/2}$ is measurable. Thus, the orientation of the projection of the molecular segment, giving rise to the chirality with respect to any particular axis, is impossible to obtain from GIXD data. The first-order peaks correspond to the distance between the neighboring molecules and are the most intense reflexes. When only one value of the in-plane component, K_{xy}, is available, it indicates an equal separation between neighboring molecules and corresponds to the hexagonal packing. Two and three distinct values of K_{xy} correspond to the rectangular and oblique unit cells, respectively. Thus, important lattice information about the monolayer system can be obtained from the GIXD studies. It is important to note that only a translation or a glide having a plane perpendicular to the water surface is the symmetry element common for amphiphilic monolayers at the air/water interface.[26]

An oblique structure composed of enantiomeric molecules in a monolayer system is chiral due to the lack of a mirror or glide plane. However, due to a reduction in crystal symmetry, an oblique lattice can incorporate both enantiomeric forms. This reduction is detectable by minor differences between the GIXD patterns of the enantiomeric and racemic packing arrangements. The observation of an oblique structure is thus possible for homochiral racemic mixtures when two enantiomers separate into D and L isomers. This is an event of spontaneous chiral segregation, which we discuss in the next section. Also, achiral molecules can form chiral lattice structures if the tilt or distortion occurs in a direction intermediate between nearest neighbor (NN) and next nearest neighbor (NNN). Thus, both chiral and achiral molecules can pack in crystalline forms that are mirror images of one another. On the other hand, a chiral molecule, which develops chiral domains in a condensed phase (oriented with a specific

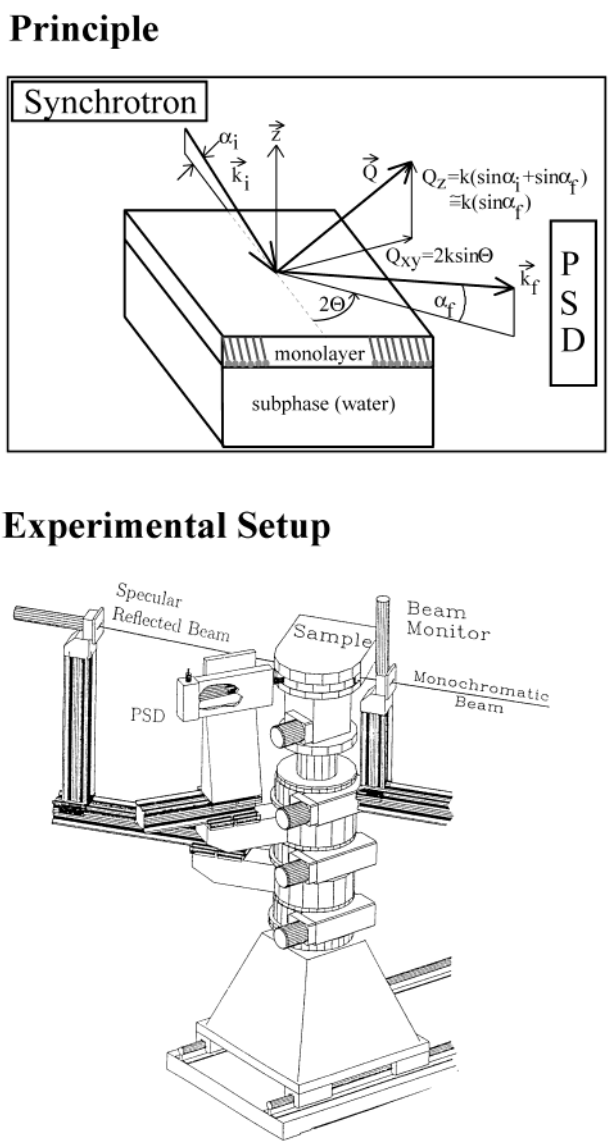

Figure 26. Principle of GIXD measurements (top) and experimental setup (bottom) of the diffractometer at the beamline BW1 (X-ray synchrotron source at Hasylab, Hamburg) for studying of Langmuir monolayers. The diffracted beam is detected with a position sensitive detector (PSD).

handedness), can have a centered rectangular (nonchiral) unit cell.[85,98] It is also to be noted that the local packing determined for a mesophase cannot be straightforwardly extended to the long-range scale because of finite positional correlations in such phases, unlike crystalline phases.[25] Explicitly, the symmetry of the molecule arrangement over a few intermolecular distances may not coincide with the long-range symmetry of the monolayer. Consequently, care must be taken to use the data obtained from the GIXD studies to interpret the long-range correlations present in monolayers. It is also important to note that the specific polar direction (normal to the interface) in the monolayer system couples the molecular chirality and the chain tilt. Thus, the various values of the tilt azimuth observed in monolayers play a role in the formation of mesoscopic domain shapes.[25]

4.1. Amphiphiles Containing Amino Acid or Acid Amide Headgroups, Each with a Single Chiral Center

Interesting GIXD studies were performed with amino acid amphiphiles of the general formula $RHC(NH_3^+)COO^-$ monolayers on water and glycine solution.[26,105] The R groups used are of two types: R = $C_nH_{2n+1}-$, n = 10, 12, or 16, and R = $C_nH_{2n+1}CONH(CH_2)_4-$, n = 11, 17, or 21. GIXD studies were carried out in both enantiomeric and racemic monolayers on water and on glycine solution. According to their chiral nature, the enantiomeric monolayers of both types of amphiphiles form an oblique lattice, whereas different lattice types were observed for the two homologous series. The racemic $C_nH_{2n+1}HC(NH_3^+)COO^-$ monolayers form rectangular lattices, whereas the racemic $C_nH_{2n+1}CONH(CH_2)_4HC(NH_3^+)COO^-$ monolayers have oblique lattices. Generally, there are two possibilities for the monolayers of the racemic mixtures. In the case of homochirality, they can separate spontaneously into islands of the two enantiomeric forms in which the molecules are related only by translation symmetry or in the case of heterochirality they form a racemate in which the molecules are related by glide symmetry. Usually, long aliphatic chains $C_nH_{2n+1}-$ tend to pack in the herringbone motif generated by glide symmetry. Therefore, it was the idea of the authors that the molecule requires an additional functional group that will promote translational packing only. In the case of racemic $C_nH_{2n+1}HC(NH_3^+)COO^-$ monolayers the rectangular unit cell related by glide in a herringbone arrangement of the chains indicates heterochirality. The herringbone arrangement generated by glide symmetry prevents the formation of favorable intermolecular N−H···O═C bonds, which should induce the translation motif. However, in the case of the racemic $C_nH_{2n+1}CONH(CH_2)_4HC(NH_3^+)COO^-$ monolayer a GIXD pattern was obtained indicative of an oblique unit cell with translation symmetry only. Now the N−H···O hydrogen bonding of the amide groups along a 5 Å axis complemented by the N−H···O network of the $^+H_3NCHCOO^-$ moieties induces the spontaneous separation of the racemic mixture into homochiral domains of opposite handedness.

Monolayers of chiral *N*-alkanoylamino acid amphiphiles of the type R−CO−N−CH(R_1)−COOH or R−CO−N−CH(R_1)−$COOCH_3$ [R = $C_{15}H_{31}$; R_1 = $-CH_3$, $-CH_2OH$, $-CH_2COOH$, or $-CH(OH)-CH_3$] are further interesting candidates for systematic studying of chiral effects.

According to the $\pi-A$ isotherms and the domain morphology, most of the monolayers of the *N*-alkanoylamino acid amphiphiles indicate homochirality; that is, interaction between the same enantiomers is preferred in comparison to the interaction between the two different enantiomers. Consequently, chiral segregation may be expected. Therefore, GIXD measurements have been performed for the enantiomers and 1:1 racemic mixtures of monolayers of a series of *N*-alkanoylamino acid amphiphiles. In agreement with foregoing arguments the enantiomeric monolayers show an oblique lattice

Table 2.

A. Lattice Structure Data of Different *N*-Alkanoylamino Acid Amphiphiles[a]

	T (°C)	*a* (Å)	*b* (Å)	*γ* (deg)	A_{xy} (Å^2)	Ψ (deg)	*t* (deg)	A_0 (Å^2)	td
				N-Palmitoylalanine, pH 3					
1 mN/m (D)	20	4.932	5.679	104.35	27.13	87 ± 3	46	18.9	
25 mN/m (D)	20	4.914	5.635	104.55	26.80	87 ± 3	46	18.7	
1 mN/m (DL)	20	4.932	5.679	104.54	27.11	87 ± 3	45	19.1	
25 mN/m (DL)	20	4.922	5.636	104.78	26.83	87 ± 3	45	19.0	
				Palmitoylserine Methyl Ester					
7 mN/m (L)	18	4.899	5.875	104.6	27.9	86	47	19.1	
20 mN/m (L)	18	4.891	5.863	104.5	27.8	86	46	19.1	
18 mN/m (DL)	18	4.903	5.938	104.9	28.2	86	47	19.3	
				Stearoylserine Methyl Ester					
10 mN/m (L)	24	4.894	5.851	104.7	27.71	86	48	18.4	
20 mN/m (L)	24	4.889	5.839	104.8	27.60	86	48	18.4	
10 mN/m (DL)	24	4.908	5.964	105.2	28.23	86	49	18.5	
20 mN/m (DL)	24	4.894	5.851	104.7	27.71	86	48	18.4	
				N-Palmitoylaspartic Acid, pH 3					
27 mN/m (L)	20	4.984	5.235	115.62	23.53	88	31.3	20.1	
27 mN/m (DL)	20	4.982	5.236	115.64	23.52	88	30.4	20.3	
20 mN/m (DL)	5	5.078	10.360		26.3		42	19.4	NNN
30 mN/m (DL)	5		10.258		25.7		41	19.3	NNN

B.1. Data of the Lattice Structure of *S*-(−)-1-Stearylamine Monoglycerol Monolayers at 20 °C[a]

π (mN/m)	*a* (Å)	*b* (Å)	*γ* (deg)	*t* (deg)	A_{xy} (Å^2)	A_0 (Å^2)	td	ψ_a (deg)	*d*
1	5.22	5.57	104.6	46	28.1	19.7		60.2	0.292
10	4.98	5.35	112.7	36	24.5	19.9		74.7	0.162
25	4.93	5.19	117.4	28	22.7	20.0		85.1	0.078
30	4.91	5.05	118.1	24	21.9	20.0		85.0	0.049
35	4.89	5.00	119.2	19	21.3	20.0	NNN	90	0.031

B.2. Data of the Lattice Structure of 1:1 Racemic 1-Stearylamine Monoglycerol Monolayers at 20 °C[a]

π (mN/m)	*a* (Å)	*b* (Å)	*t* (deg)	A_{xy} (Å^2)	A_0 (Å^2)	td	*d*
1	6.36	8.49	43	27.0	19.9	NN	0.256
5	4.83	10.21	36	24.7	19.9	NNN	0.196
10	5.00	10.00	35	25.0	19.9	NNN	0.143
35	4.91	8.58	18	21.0	19.9	NNN	0.0996

[a] *a*, *b*, and *γ* are lattice constants, *t* is polar tilt angle, A_{xy} is molecular area, A_0 is cross-sectional area of alkyl chain, Ψ is the angle between azimuthal tilt direction and *a*-axis, td is tilt direction, *T* is temperature; ψ_a is the angle between azimuthal tilt direction and *a*-axis; and *d* is distortion.

indicated by three reflexes in the contour plots.[25] For the two enantiomeric forms, the same lattice structure must be expected. For the case of instantaneous chiral segregation, also the same lattice structure should be found because the racemic mixture separates spontaneously into two-dimensional islands of the two enantiomers of opposite handedness. In Table 2A the structure data of different monolayers of *N*-alkanoylamino acids or *N*-alkanoylamino acid esters (*N*-palmitoylalanine, *N*-palmitoylserine methyl ester, *N*-stearoylserine methyl ester, and *N*-palmitoylaspartic acid) are listed. These chiral amphiphiles show oblique lattices and agreement between the lattice data of the enantiomeric and racemic monolayers. They demonstrate, thus, spontaneous chiral segregation at room or higher temperatures.

Consequently, as in all other examples, the GIXD patterns of the enantiomeric *N*-palmitoyl-L-aspartic acid and their 1:1 DL-racemic mixture measured at subphase pH 3 and 20 °C are identical (Figure 27, left). However, in the case of palmitoyl-DL-aspartic acid, the situation is changed at low temperatures. According to the GIXD pattern obtained at 5 °C (Figure 27, right), the racemic mixture crystallizes in a rectangular lattice with tilt of the molecule chains toward the NNN direction. There exists obviously weak orientation- and distance-dependent interaction due to the chiral structure of the molecules between the two enantiomeric forms leading to chiral discrimination only at low temperatures. This behavior suggests that increasing thermal movements of the molecule axes prevent the chirality-dependent interaction between the different enantiomers. This is confirmed by the differences in the cross section area A_0 of the alkyl chains of the racemic mixtures at different temperatures. As seen in Table 2A, at $T = 27$ °C and $A_0 = 20.3$ Å^2/molecule for $\pi = 27$ mN/m, whereas at 5 °C $A_0 = 19.3$ Å^2/molecule for a similar pressure of $\pi = 30$ mN/m.

A comparison of the packing arrangements of the three types of amino acid amphiphiles discussed here (Figure 28) demonstrates that the subtle interplay between the relative contributions of the molecule moieties is complicated for determining whether a racemic mixture segregates into two-dimensional islands of the two enantiomers or forms real racemates with preferred interaction between both enantiomers. The problem of spontaneous chiral segregation is further discussed in section 7.

The influence of chirality on the morphology of TDHPA containing an acid amide bonding within the headgroup is studied using GIXD.[42a,b] The results of

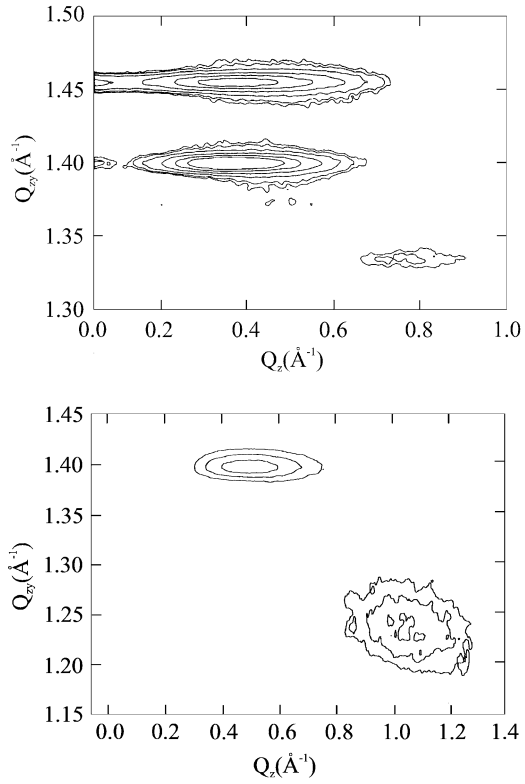

Figure 27. GIXD patterns for *N*-palmitoylaspartic acid monolayers on subphase pH 3 in the form of two-dimensional intensity contour plots: (a, top) identical oblique lattice of the L-enantiomers and the 1:1 racemic mixture at 20 °C; (b, bottom) rectangular lattice of the 1:1 racemic mixture at 5 °C.

the $\pi-A$ isotherms and the BAM results are discussed in sections 2 and 3, respectively, for this system. The GIXD studies at surface pressures in the range of 9−30 mN/m show three typical peaks at almost the same position for the enantiomers and the racemates. Three peaks are indicative of an oblique lattice for both enantiomeric and racemic monolayers with the tilt direction of the alkyl chains very close to the NN direction. It is also observed that with increasing surface pressure the area of the unit cell and the tilt angle of the alkyl chains decrease only weakly, and this could be due to the strong cooperative hydrogen bonding between the amide groups of the molecules, which conserve the crystal structure. The oblique lattice structure, polar tilt angle, and azimuthal projection of the alkyl chain do not depend on the chirality of the molecule concerened. This emphasizes the fact that strong hydrogen bonds can dominate the effects of chirality even in the condensed state (where chirality-dependent interactions are most prominent). This is further supported by the fact that the positional correlation length is anisotropic for both the racemate and the enantiomers. It is also pointed out that the lattice constants and the unit cell area of the racemates are significantly smaller than the corresponding values of the enantiomers. This indicates a denser packing of the racemic monolayer corresponding to weak heterochiral interaction. Note that the chiral discrimination is convincingly observed in BAM studies (section 3).

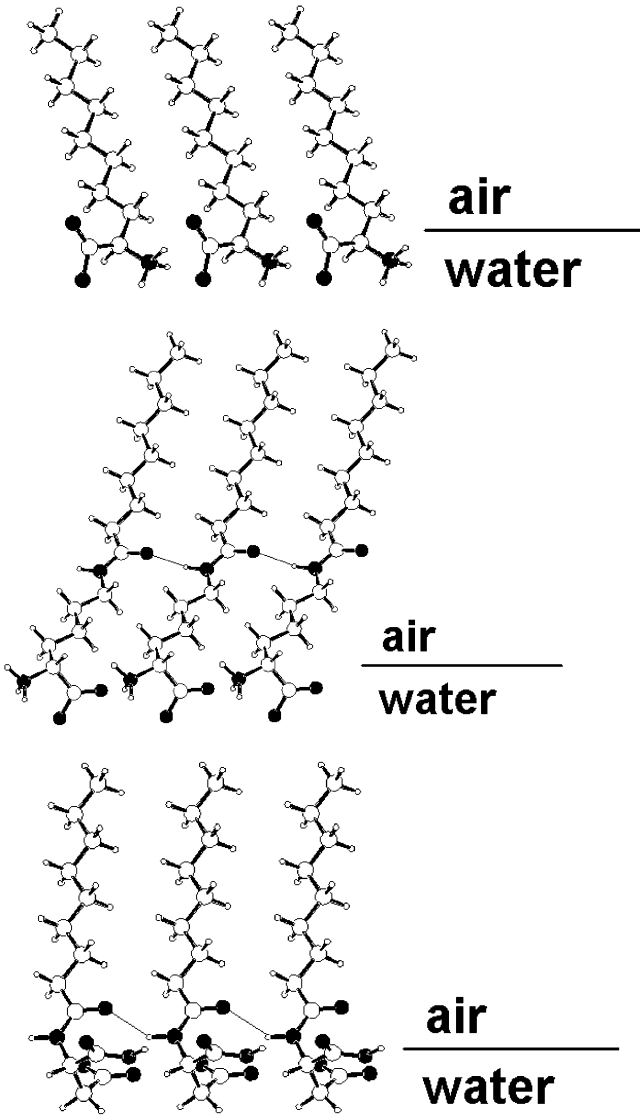

Figure 28. Arrangements of amino acid amphiphiles of the types $^{+}H_3NCH(C_nH_{2n+1})COO^{-}$, $C_nH_{2n+1}CONHC_4H_8CH(NH_3^{+})COO^{-}$, and $C_nH_{2n+1}CONHCH(CH_2COOH)COOH$ at the water−air interface on the basis of molecular structures calculated by force-field methods. The chain tilt and the intermolecular distances correspond to the results from the GIXD measurements. The chain lengths were chosen arbitrarily. N and O atoms are drawn black, and O··H−N−C═O··H hydrogen bonds are indicated by thin lines.

4.2. Amphiphiles Containing a Glycerolic Headgroup with a Single Chiral Center

Lattice structures of 1-monopalmitoyl-*rac*-glycerol monolayers and its L-enantiomer are studied using GIXD.[99] The domains have a 7-fold substructure, which transforms into a 6-fold substructure on compression, as discussed in a previous subsection.[82] The projections of the chains on the surface form a centered rectangular lattice with the tilt azimuth parallel to the *a* axis at 20 °C. It is reasonable to assume that some of the low index directions possess low defect line energy for a jump of the orientation. A low index lattice row possesses a larger number of lattice points per length, so it is expected to be favored for the jump of the molecular orientation, and the segment borders are pointed along these direc-

tions. It is interesting that the diffraction data (as well as BAM images) are identical for enantiomeric and racemic monolayers. Why and under which conditions the headgroup chirality of the enantiomeric monolayer allows a rectangular symmetry is not clear.

Additional combined GIXD and BAM studies on the chiral discrimination in the racemic and enantiomeric monoglyceride monolayers are performed in a later study to obtain first information on the chain length effect.[100] Here monolayers of the homologous monostearoylglycerol with a longer alkyl chain at 20 and 5 °C are studied. Again at 20 °C an influence of chirality was not observed; that is, a rectangular unit cell for both the racemic and the enantiomeric forms is observed. However, at the low temperature (5 °C) chiral discrimination was clearly demonstrated by the GIXD results combined with BAM. At 5 °C, the enantiomeric momolayer has an oblique lattice of the alkyl chains at the investigated surface pressures, which is expected for a chiral lattice structure. On the other hand, the monolayer of the racemic mixture shows at this temperature a phase transition between 6 and 12 mN/m that was identified by GIXD by a transition of a rectangular lattice with NN tilt direction to that with NNN tilt direction and by BAM by visualizing the change in the tilt azimuth. These results suggest that the temperature influences the chiral discrimination of monoglyceride monolayers. The influence of the temperature on the chirality is qualitatively explained by the assumption that at higher temperatures the thermal motion of the headgroups prevents orientation- and distance-dependent interaction due to the chiral structure of the molecules and the lattice can adopt a rectangular structure. This is corroborated by the chain cross section of ~20 Å^2/molecule at 20 °C, characteristic for the free rotator phase of alkanes. When the temperature is decreased, the thermal motion is reduced, so that the chain cross section is reduced to 19.3 Å^2/molecule at 5 °C. The denser packing at lower temperatures allows the more specific chirality-dependent interactions.

To understand in greater detail the reason for the temperature effect observed in this work on the chiral discrimination of monostearoylglycerol monolayers, a systematic comparison of the phase and lattice features of the racemic 1-stearoyl-*rac*-glycerol (R-Gl) and enantiomeric 3-stearoyl-*sn*-glycerol (E-Gl) was performed.[44] The surface pressure−temperature diagrams demonstrate that three phases occur both in the enantiomeric E-Gl (Figure 29) and in the racemic R-Gl monolayers (Figure 30) but with completely different proportions of the single phases and phase transition pressures. Consequently, chiral discrimination can be clearly seen.

The oblique intermediate (I) phase characteristic for a chiral lattice occurs both in the enantiomeric E-Gl and in the racemic R-Gl monolayer with a chain lattice and a chain tilt in a direction between the NN and NNN phases of the rectangular centered lattice. The NN → NNN phase transition splits in two successive NN → I and I → NNN transitions. Whereas the NN → I transition occurs abruptly, the I → NNN

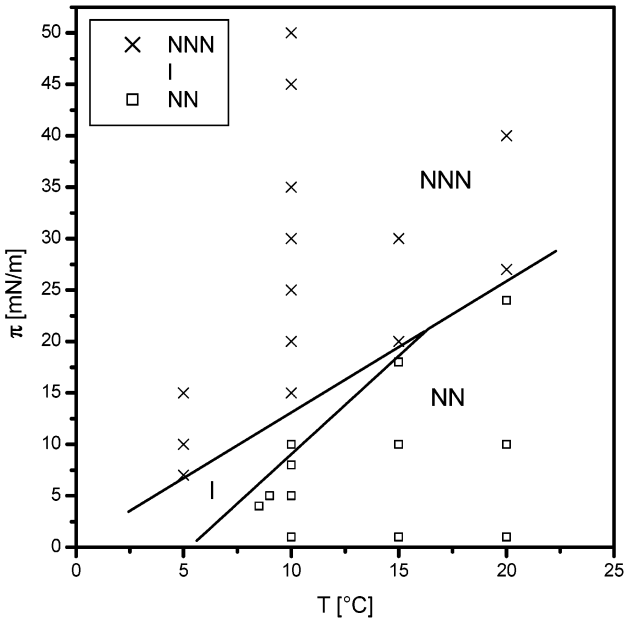

Figure 29. Surface pressure−temperature diagram of the enantiomeric 3-stearoyl-*sn*-glycerol monolayer.

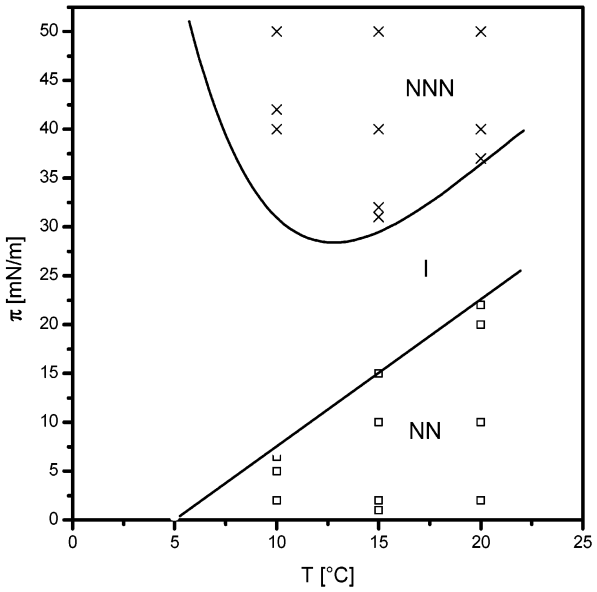

Figure 30. Surface pressure−temperature diagram of the racemic 1-stearoyl-*rac*-glycerol monolayer.

transition takes place continuously. In both the racemic R-Gl and the enantiomeric E-Gl, the NN → I transition begins at 5 °C at zero pressure and changes linearly to higher pressures with increasing temperature but with a stronger slope for R-Gl. The proportions of the I phase are very different for both forms. Symmetry splitting in the racemic R-Gl monolayer occurs only at low temperatures in a small pressure region (Figure 28), so that the I phase was overseen in previous work. At 20 °C already, the I phase disappears in the racemic monolayer and a direct NN → NNN transition takes place. On the other hand, in the enantiomeric E-Gl monolayers the I phase exists over a broad pressure range at all temperatures, but at low temperatures it is so dominant that at 5 °C it was found over the whole accessible pressure range (Figure 29).

The lattice structure of the 1-stearylamine monoglycerol monolayers is also affected by the chirality of the molecules.[47,101] The enantiomeric monolayers have an oblique lattice, in which the tilt direction changes continuously from angles nearly toward the NN direction to angles nearly toward the NNN direction upon compression. In contrast, the condensed phases of the racemic mixtures give rise to rectangular-centered lattices. Here a phase transition occurs that is accompanied by a change in the tilt direction from NN at 1 mN/m to NNN at 5 mN/m. Both the enantiomeric monolayers and their racemic mixtures have highly tilted molecules at low surface pressures. Details of the lattice data of both forms are listed in Table 2B. In agreement with the filigree domain structure observed by fluorescence microscopy, low ordering of the alkyl chains can be concluded from low position correlation. In Table 2B.1 are shown data of the lattice structure of *S*(−)-1-stearylamine monoglycerol monolayers at 20 °C. In Table 2B.2 are shown data of the lattice structure of 1:1 racemic 1-stearylamine monoglycerol monolayers at 20 °C.

Similar chiral discrimination effects on the lattice structure are found in the condensed phases of the monoglycerol ethers that also give rise to oblique lattices in the enantiomeric monolayers and rectangular lattices, having depending on temperature an abrupt NN to NNN transition at medium surface pressure between 15 and 20 mN/m, in the racemic mixtures[102]. Racemic and enantiomeric 1-hexadecylglycerol monolayers are investigated using GIXD at 5 and 20 °C. The lattice of the racemate is centered rectangular at all pressures investigated at both temperatures. With increase in the surface pressure a NN to NNN phase transition takes place at both temperatures. The pure enantiomer, on the other hand, exhibits an oblique lattice at all temperatures.

4.3. Amphiphiles Containing a Phospholipid Headgroup with a Single Chiral Center

An oblique lattice is observed in both enantiomeric and racemic monolayers[103] of DPPC. It was suggested that the oblique lattice structure in DPPC is due to orientational ordering of the glycerol backbone, which links the two chains, at an oblique angle. On the other hand, only the enantiomeric monolayer of DPPE exhibits asymmetric lattice structure.[104] It is assumed that the hydrogen bond network in the headgroup region in enantiomeric DPPE is one-dimensional (along the *b* axis), whereas, in racemic DPPE the network is extended in two dimensions.

Phospholipids with more complicated chemical structures such as triple-chain phospholipid monolayers of enantiomeric and racemic 3-*O*-hexadecyl-2-(2′-hexadecylstearoyl)glycerol-*sn*-1-phosphocholine and racemic 1-*O*-hexadecyl-2-(2′-hexadecylstearoyl)glycerol-3-phosphocholine are investigated by X-ray diffraction in the temperature range of 5−25 °C.[48] The contour plots of the X-ray intensities as a function of in-plane component and out-of-plane component of the scattering vector of the enantiomeric monolayer show that molecular tails are arranged in a nonsymmetric direction, showing a lack of mirror symmetry in the lattice arrangement. Deviation from the rectangular unit cell due to the presence of a chiral carbon atom is completely suppressed at higher lateral pressures, at which a centered rectangular unit cell is found. The tails are tilted in the NN direction for both the enantiomer and the racemate. The chain tilt angle also decreases with increasing pressure. Three chains require more cross-sectional area than that required by the headgroup and determine the packing at higher surface pressures. The spacing between the chiral carbon and the trimethylammonium group is larger than two lattice spacings. Consequently, for parallel orientation of the headgroup to the surface, local interaction between the headgroups is suggested to couple the headgroup with the lattice arrangement of the tail. It is suggested that the long-range interactions between the distributed charges in the headgroups of the chiral molecules gives rise to an interaction which is chiral in nature and may drive the formation of chiral shape. It is also pointed out that short-range orientation- and distance-dependent interaction between the headgroups is possible provided the headgroups are regularly arranged.[25]

4.4. Mixture of Amphiphiles Containing Acid and Amine Headgroups, Each with a Single Chiral Center

The diffraction characteristics of the unit cells of different mixtures of *p*-pentadecylmandelic acid (MA) and *p*-tetradecylphenylethylamine (PEA) such as (*R*-MA, *R*-PEA), (*R*-MA, *S*-PEA), and (*R*,*S*-MA, *R*,*S*-PEA) are investigated.[106,107] In this study, the acid−base interactions involving two different chiral molecules are used to induce chiral segregation. The unit cell area contains two long-chain molecular units corresponding to one acid and one amine molecule, and they are symmetry independent. The integrated intensities and positions of the Bragg peaks and the shapes of the corresponding Bragg rods are different for the *R*,*R*′ and *R*,*S*′ mixtures (here, *R* and *S* correspond to the absolute configurations of MA and *R*′ and *S*′ correspond to the absolute configurations of PEA). Those characteristics of *R*,*S*,*R*′,*S*′ are almost identical with the same characteristics of *R*,*R*′. Considering the highly crystalline state of the monolayer, it is possible that the *R*,*S*,*R*′,*S*′ mixture separates into domains of *R*,*R*′- and *S*,*S*′-enantiomers. The details of the chiral discrimination effects of these systems are discussed in section 7. Different compositions such as (*R*,0.5*R*′,0.5*S*′) and (0.5*R*,0.5*S*,*R*′) are also investigated. The diffraction pattern of (0.5*R*,0.5*S*,*R*′) is similar to that of (*R*,*R*′). There is only one crystalline phase, and it is concluded that (0.5*R*,0.5*S*,*R*′) is isomorphous with (*R*,*R*′) but half of the *R* sites are occupied by its mirror image isomer. The diffraction pattern of (*R*,0.5*R*′,0.5*S*′) combined two overlapping GIXD patterns characteristics of *R*,*R*′ and *S*,*S*′ phases. This indicates that enantiomorphous domains are of the composition ([(1 − *x*)-*R*,*xS*],*R*′) and ([(1 − *x*)*S*,*xR*],*S*′), where *x* is the fraction of MA within *R*,*R*′ and *S*,*S*′ domains. Further support of chiral disorder is obtained from the corresponding three-dimensional crystal analysis.

GIXD studies of heneicosanoic acid (C_{21}) acid monolayer at near zero surface pressure and at 9° C showed that within the pH range from 7 to 9, the lattice structure is chiral (oblique) in the presence of cadmium ions.[108a] Chiral structure is not observed below or above this pH range and in the absence of cadmium ions. The chiral structure is destroyed at higher temperatures. The authors suggest that a layer of a larger ionic complex is formed only in this pH window in the presence of cadmium ions. However, conclusive evidence of the formation of such a layer of complex is yet to be confirmed.

Lattice structures of enantiomeric and racemic monolayers of HOBD are investigated using GIXD.[85] The racemates exhibit a rectangular unit cell in contrast to the oblique structure of the pure enantiomer or a nonracemic mixture. This indicates the strong influence of the chiral center above the transition pressure. The racemate undergoes a transition between two rectangular centered phases, which differ by the tilt direction of the molecules. In the low-pressure region, the molecules are oriented in the NN direction, whereas at high pressures they are tilted toward the NNN direction. The NN to NNN tilt direction jump occurs at a transition pressure. The oblique to NNN transition in enantiomeric as well as in monolayer with a mixture of unequal amounts of enantiomers occurs continuously. At higher pressures both the racemic and enantiomeric monolayers exhibit the same NNN phase. The authors concluded that the influence of chiral center is suppressed at higher pressure.

Different GIXD studies of monolayers of amphiphiles without any asymmetric carbon atom revealed that oblique lattice structures indicating a chiral phase could be formed. For example, arachidic acid monolayers often used as a model show a chiral phase in which the molecular tilt is intermediate (I) and is between the NN and NNN directions.[108b] The intermediate tilt breaks the chiral symmetry. Similar to the results presented before for monostearoylglycerol monolayers, the I → NN transition is with a 60° change in the tilt direction, whereas the I → NNN transition is continuous.

Consequently, the GIXD studies in various amphiphilic systems indicate the presence of chirality at the lattice structure level. On the other hand, we observed chirality at the domain structural level, which is many times larger than the lattice dimension. Chirality-dependent interaction is operative in closed packed arrangement between successive neighbors, and the neighboring chirality-dependent interaction again prefers anisotropic molecular arrangements. Consequently, the manifestation of chirality at different length scales may be different, but the fundamental natures of the interactions seem to be alike. Further detailed studies are required in this direction.

5. Continuum Theories of Chiral Monolayers

In this section we discuss the continuum theories of monolayers. The microscopic features of the system present at the molecular length scale are neglected in this class of theories. In general, Frank free energy terms from liquid crystal theories[109] (splay, twist, and bend) are incorporated, and an additional term, which breaks the chiral symmetry, is incorporated. The symmetry breaking term is dependent on the dimensionality of the system. In addition, phenomenological terms are incorporated similar to those involved in Landau theories. In continuum theories a chiral order parameter is constructed that can incorporate the chiral features typical of the system. In these calculations, a vector is representing the average direction of the molecular tail directed away from the interface (called a "director"). Other than specifying the average direction of the tail, no other molecular features such as individual chemical structure are considered. Thus, it is not possible to differentiate one chiral molecule from the other in this representation.

Domain shapes observed in Langmuir monolayers are viewed as modulated phases.[110] Many different physicochemical systems such as magnetic garnet films, ferroelectric films, type I superconductor films, membranes and vesicles, convecting patterns, Turing patterns, and other systems exhibit similar modulated phases. These systems are stabilized by competing interactions such as dipolar repulsion and line tension at the domain boundary in the case of Langmuir monolayers. These phases are in general dependent on temperature and external fields and are characterized by one or more order parameters, which could be composition or density in the case of Langmuir monoalyers. A Ginzburg−Landau-type free energy functional with relevant order parameter can bring out several features of these systems.[110]

Attempts are made to explain the surface pressure induced chiral phase separation in monolayers of racemic amphiphiles at the air−water interface using the Braggs−Williams theory for binary mixtures. In these studies, the monolayer was mapped into a continuum-based curvature−elastic model of a bulk cholesteric liquid crystal.[111a−c] The monolayer is viewed as a film of cholesteric liquid crystal. The corresponding phenomenological free energy expression includes the usual splay, twist, and bend terms and a chiral order parameter, which is given by the local density fraction of the left- or right-handed enantiomer introduced to explain the chiral phase separation. It is shown that below a certain critical temperature compression can induce chiral phase separation with a stripe pattern from the racemic phase.[111a] In a more recent theoretical study, the compression-induced chiral phase separation in Langmuir films is considered using a similar approach with consideration of line tension at the chiral phase separation boundaries.[111b] The chiral phase separation boundaries are viewed as walls with finite line tension originated from chiral discrimination.

Structural changes in monolayers of the enantiomeric and racemic mixture of 1-hexadecylglycerol with temperature and surface pressure variations are investigated in the framework of the Landau theory.[112] Enantiomeric and racemic monolayers of 1-hexadecylglycerol show a change in tilt azimuth from NN to NNN direction on compression. However, the transition in the racemic is first order, whereas that

in the enantiomeric is continuous. A phenomenological free energy expression is used that relates the tilt azimuth, β, with the mean orientation to the neighbors, γ (the hexatic azimuth) as follows:

$$F = g \cos 6(\beta - \gamma) + g' \sin 6(\beta - \gamma)$$

In nonchiral monolayers, the sine term does not exist ($g' = 0$) due to symmetry. This requires that the free energy must be invariant corresponding to the change of the azimuths from β to $-\beta$ and from γ to $-\gamma$. In this case, the transition from NN ($\beta = \gamma$) to NNN ($\beta = \gamma + \pi/6$) occurs at a particular surface pressure (Π_0) corresponding to the change in the sign of g. The minimization of the free energy expression with respect to the azimuths gives the condition $\cot 6(\beta - \gamma) = g/g'$. Assuming g' to be constant, g is proportional to $\Pi_0 - \Pi$. With an increase in surface pressure, the tilt and the hexatic azimuths differ by angles ranging from 0 to $\pi/6$, corresponding to the observed transition, that is, NN to NNN.

Landau's theory for uniaxially distorted lattice is used to explain the chiral phase observed in the structure of the Langmuir monolayer of eicosanoic acid in which the molecular tilt is intermediate (denoted I) between the NN and NNN directions.[108] The free energy functional predicts a first-order phase transition from NN to I followed by an I to NNN transition. Later BAM is used to study the chiral I phase on an acidic subphase.[113]

The two-dimensional lattice gas theory [Blume−Emery−Griffiths (BEG) model] is used to study the chiral preference in Langmuir monolayers.[114] An effective antiferromagnetic coupling represents the heterochiral preference. An important result of this study is the proof of the heterochiral preference observed by Andelman based on the *tripodal* model using van der Waals interactions, which will be discussed in the next section. A cluster variation analysis of the BEG model was also presented. A heterochiral effective lattice gas model on the planar triangular lattice is considered. The choice of the lattice type is found to be important. However, the correlation between the lattice structure and the molecular interaction is yet to be investigated in detail.

Selinger and co-workers studied the chiral symmetry breaking in Langmuir monolayers and smectic films and resulting defect textures.[115] They used the following form of free energy functional:[115a]

$$F = \int \mathrm{d}^2 r[(^1/_2)\kappa(\nabla\psi)^2 + (^1/_2)t\psi^2 + (^1/_4)u\psi^4 + (^1/_2)K_1(\nabla\mathbf{c})^2 + (^1/_2)K_3(\nabla\mathbf{c})^2 - \lambda\psi\,(\nabla\mathbf{c})]$$

Here, the two-dimensional tilt director $\mathbf{c} = (\cos\varphi, \sin\varphi)$ is the normalized projection of the three-dimensional molecular director, $\mathbf{n}$, into the $x-y$ plane. $\psi(r)$ is a pseudoscalar-order parameter, which is coupled with the curl of the tilt director $\mathbf{c}$. The last term in the equation represents the coupling between the chiral order parameter and the tilt director. Numerical minimization of the free energy was carried out on one- and two-dimensional lattices. The generated phase diagram includes a uniform chiral phase along with other phases such as striped patterns and square lattices. It is pointed out that the chiral symmetry can be broken by several means in a Langmuir monolayer. In a tilted hexatic phase, if the tilt direction is locked at an angle between 0° and 30° from one of the local bond directions, the chiral symmetry is broken. It is also possible that molecules might pack in nonequivalent ways to give rise to symmetry breaking. Furthermore, racemic mixtures may separate into chiral domains. In a subsequent paper analytic calculation based on a similar free energy functional as well as Monte Carlo simulation are used to study the defect textures due to symmetry breaking.[115b] Two distinct length scales of symmetry breaking are argued. On the microscopic length scale, the nonchiral molecules can pack to form chiral textures. Also, on the longer length scale, the nonchiral stripes can form chiral spiral patterns. It is indicated that the former is observed experimentally in freely suspended smectic films and the latter type in Langmuir monolayers.

Fischer and co-workers used a Landau theory based model to study the morphology of Langmuir monolayers.[116] The model includes a chiral order parameter of the form $\langle \sin[6(\theta - \varphi)] \rangle$, where θ is the bond angle and φ is the tilt azimuth. The authors used this free energy functional to predict various chiral features in the textural motif and in particular the L phase, where the chiral symmetry is broken. A Landau free energy functional is also used to explain the chiral hedgehog textures in thin films.[117]

As mentioned before, despite the simplicity of the continuum models, it is difficult to follow the molecular origin of the chiral terms included in the free energy functionals used in such theories. As molecular features are neglected by the use of a featureless director, such theories fail to predict the wide variety of chiral features in Langmuir monolayers starting from first principles. To explain the various mesoscopic chiral morphologies arising from different molecular systems, molecular considerations are necessary, which is discussed in the following section.

6. Molecular Theories of Chiral Monolayers

The molecular theories are most promising to explain the chirality-induced features of chiral monolayers. Experimental results observed in chiral amphiphiles using isotherm studies, optical measurements, and diffraction techniques indicate that several features of the domain shape as well as the underlying molecular arrangement are crucially dependent on the molecular structure of the concerned amphiphile. However, a complete molecular theory or simulation is difficult to develop due to several factors such as the complete absence of symmetry of the molecule, the lack of detailed knowledge of the structural details of the LE/LC interface at the molecular level as well as the molecular arrangement in the underlying subphase, the heterogeneity of the system, and the large number of molecules present in a domain. However, despite these difficulties, several theoretical studies and simulations have taken this direction, as discussed below.

A detailed theoretical framework of shape transition of finite lipid monolayer domains has been developed in recent years.[23,77,118−131] The shape transition is governed by the competition between the shape-dependent dipolar energy (F_{el}) of the domains and the energy of the line tension between the domains (LC phase) and the surrounding fluid (LE) phase (F_λ).[23]

$$F = F_{el} + F_\lambda$$

It was assumed that both the LC and LE phases are isotropic fluids and sharp well-defined boundaries exist between the phases. F_{el} is expressed in terms of a double-line integral along the domain perimeter by an ingenious application of Green's theorem. The resulting equation is

$$F = 2\pi Rn[\mu^2 \ln(e^2 \delta/4R) + \lambda]$$

where R is the radius of a single circular domain of a total of n number of domains, μ is the difference in dipole density of the phase within the domain and the phase surrounding the domains (practically, μ equals the dipole moment density of the phase within the domain), δ is a distance of the order of magnitude of the separation of molecular dipoles, and λ is the line tension. The minimization of the free energy functional gives the shape of the domain. The circular shape of a domain can become unstable with respect to the symmetry-breaking shape transitions. Shape-dependent energies of various shapes such as ellipse and torus are calculated.[23,77,118−131]

The harmonic shapes of various orders are also calculated by using a slightly modified form of the equation.[132]

$$F = F_{el} + F_\lambda + F_s$$

F_s is the shape-dependent part of the free energy. The radius of the domain is assumed to be dependent on the orientation of the radial vector drawn from the center of the domain (θ). The domain shape of the regularly undulating domains is then characterized by

$$R(\theta) = \Lambda[1 + \epsilon \cos(m\theta)]$$

Λ is the mean radius, ϵ is the relative amplitude of the undulation, and m is the mode. The equilibrium shape and the corresponding shape transition are governed by the relative importance of the electrical interaction and the line tension.

An exact analysis of the stability in the shape fluctuations of the circular domain is also available recently.[133] A major difficulty in shape analysis is the handling of the problem of divergence at zero separation between the dipoles. A cutoff distance is employed to avoid this.[23,77,118−131] However, a direct attack on the area integral involved in the calculation of the dipolar energy yields the following expression of the free energy:[133]

$$F = F_0 + (2\pi/R)\sum_{n>0}\Omega_n |\zeta_n|^2$$

F_0 is the energy of an unperturbed circle. Ω_n is given by

$$\Omega_n = \lambda(n^2 - 1) - 2\mu^2[B_1(\alpha/R) - B_n(\alpha/R)]$$

and

$$B_n(\alpha/R) = 2^{-(3/2)} \int_0^\pi \cos(n\theta)\, d\theta/[(1 + (\alpha/R)^2/2) - \cos\theta]^{3/2}]$$

It is possible to incorporate various repulsive interactions such as Coulomb interaction and exponential interaction in this theoretical framework.

Recently a closed-form solution of the above problem was developed to avoid the use of integrals or recursion formula, as used in the previous equations.[134] The integral representation for the associated Legendre function of the second kind was employed to obtain a closed-form solution. Thus, theoretical works by McConnell and co-workers, Deutch and co-workers, and Miranda lead together to the exact solution of the shape transition problem in lipid monolayers in a closed form. It is expected that more complicated shape transitions can be treated under the framework of the above theoretical treatment. The theoretical studies mentioned above unambiguously established the fact that the major forces responsible for the shape transition of the domain are the line tension at the domain boundary, which tends to form a compact shape, and the electrostatic repulsion, which favors an elongated shape.

A limitation of the previous approach to direct application to chiral systems is that the characteristic features of a particular lipid molecule are entering into the theoretical calculation via parameters such as the dipole moment (μ), the line tension (λ), and the cutoff distance of the neighboring dipoles (α). The incorporation of the explicit molecular features in this theoretical framework to study the effect of chirality of a particular lipid is yet to be worked out.

The origin of chiral shapes in monolayers is discussed in the literature.[23,77] It is suggested that surrounding the chiral domain the line tension could be anisotropic, and, thus, the molecules at the solid/fluid interface are subjected to local forces causing them to twist. This twist may propagate in the bulk to give rise to the chiral shape. Another possibility is that an intrinsic twisting force may be present, which can develop an intermolecular orientation. This mutual orientation may propagate in bulk to give rise to the chiral shape. A simple model of spiral domain growth is considered to demonstrate the effect of chirality on the domain shape.[77] In this model the domain growth is assumed to take place by successive addition of square blocks to the existing initial structure (at the beginning it could be a thin rectangle when the electrostatic forces are large). The addition of a block could take place in two ways: (i) the molecular director within the added block has the same direction with its immediate predecessor (no bending) or (ii) the director of the block is rotated by 90° with respect to the previous one (bending occurs). The origin of such bending could be the anisotropic

line tension. In the second way of adding the blocks (bending allowed), the free energy is higher due to line tension anisotropy compared to the first way. Growth takes place in the direction of a minimum increase in the free energy.

The formation of chiral spirals from a dipalmitoylphosphatidic acid monolayer is considered in another theory.[90] It is pointed out that the domain growth in such spiral shapes starts from a logarithmic spiral with decreasing angles between directors present in the adjacent segments. The equation governing the shape of such spirals is $r(\varphi) = a \exp(b\varphi)$, where a and b are characteristic parameters of the spirals. At large distance the spiral shape becomes archimedic with nearly the same distance between the neighboring arms along the perimeter. The forces considered in calculating the energy of the domain are (i) the short-range van der Waals-type attractive force (given by $F_{ij} = a/r^7_{ij}$, where r_{ij} is the distance between the ith and jth segments and a is an adjustable parameter), (ii) an interdomain angle (ϵ) dependent force which is used to minimize the angle ϵ and which gives rise to a torque ($T_{i,i-1} = b/\epsilon^{1/n}_i$, where b is an adjustable parameter and n is an integer in the range of 3−4 for not too strong attractive force), and (iii) a repulsive force originating from electrostatic repulsion ($F_{ij}(dipolar) = cr^{-4}_{ij}$). Excellent agreement between the theoretically obtained shape and the experimentally obtained spirals suggested that three such forces could describe the essential features of spiral domain formation. It is also observed that van der Waals attraction dominates the interaction between nearest neighbors but is inferior to dipolar repulsion when next nearest neighbors are considered. Also, the repulsive force was found to decay rapidly in order to obtain the crossover between the logarithmic and archimedic spirals. However, the physical origin of the angular dependent forces is not discussed. The domain width is found to be strongly dependent on temperature, which could be due to an ordering process. The existence of noncompensating in-plane dipole moments is suggested to lead to an anisotropic attraction. This attraction is dependent on the orientation of the molecules and is, hence, temperature dependent. The attractive contribution may be included as an angle-dependent force in the theoretical scheme for the calculation of the shape of the spirals. The growth of newly crystallized domains from the center of another domain is also another interesting problem.[91] The interdomain repulsion[135−137] will increase with increasing domain size, and the radius of the curvature is expected to increase. In the case of spiral growth, one can observe the increasing distance between the spiral arms starting from the inner arm.

An important molecular model for orientation- and distance-dependent interaction due to the chiral structure of the molecule is the "*tripodal model*".[138a,b,139] In this model, the chiral molecule is assumed to be composed of a chiral carbon to which four groups are attached. The tail points toward the air, away from the air/water interface, and the other three groups form a tripod toward the interface (Figure 31).

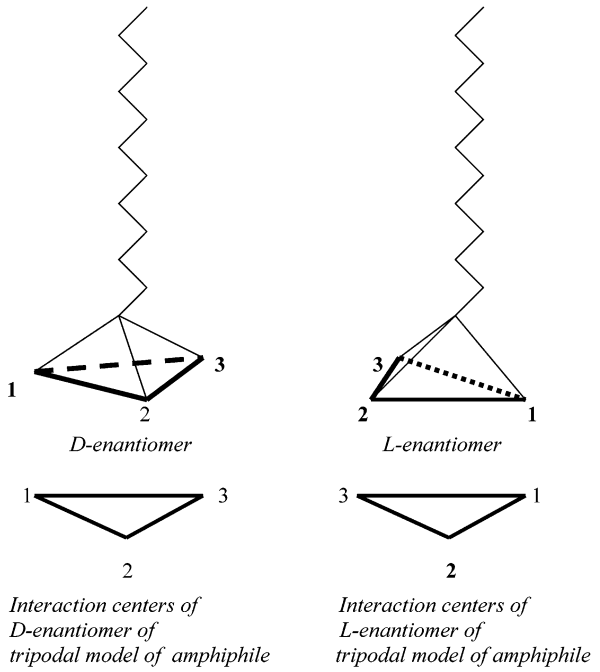

Figure 31. Schematic representation of the *tripodal* amphiphile model:[138a,b,139] (top) tetrahedral arrangements of the D- and L-enantiomers; (bottom) interaction centers of the tripodal model (projected on the water surface) for the two enantiomers.

The superiority of this *tripodal model* over the continuum representation (molecular director) is that it is far less abstract and the depiction of the molecular representation is close to real amphiphiles at the interfaces. The difference between the second virial coefficient of the pure enantiomeric monolayer and the same of the racemic monolayer is proposed as a chiral discrimination parameter.[138b] The calculation based on Boltzman weighted averaging of molecular interactions predicts a preferred heterochiral behavior for van der Waals interactions and homochiral behavior for electrostatic ones. Monte Carlo simulation was also carried out to study the chiral discrimination of D- and L-alanine. Homochiral preference was observed, which is suggested to arise from the short-range steric interactions. To reduce the calculational difficulty, rigid tetrahedrally shaped molecules are also considered as molecular model. The rigidity in shape reduces the number of degrees of freedom to 5. In this model, heterochiral preference is observed for the Lennard-Jones (LJ) potential. It is also observed that the chiral preference is dependent on the intermolecular separation. At short separations homochirality is favored, whereas at larger distances heterochirality is favored.

It may be noted that a major problem in calculating the chirality-dependent interaction is the computational time required for such calculations. Even for a simple molecule such as alanine, calculations of the pair potential using an all-atom method can take days of CPU time with a supercomputer.[138b] A micrometer-sized domain observed in the condensed phase contains millions of molecules, each of which contains many groups. Understandably, the detailed computation of interaction energies for amphiphilic molecules present within a domain is a formidable

task. However, model calculations are carried out for monolayers[138a,b] and bilayers[140a,b] where either the degrees of freedom of the molecule are restricted or an effective pair potential has been used to reduce the computational task.

The model calculations provided important molecular understanding of the chiral domain shape. The tripodal model is the first model to incorporate the molecular features of a monolayer in a detailed way. Another theory developed in recent years considers the *effective pair potential* (EPP) between the chiral molecules. The EPP is calculated from the consideration of the detailed molecular chiral structure. It is pointed out that the subtle stereogenicity at the chiral center of a molecule is the driving force for the chiral features (like specific curvature or handedness) in the shape of the aggregate composed of the molecules. The EPP-based theory was originally developed to explain the origin of the helical structure formed by chiral bilayers.[140a,b] Intermolecular twist is observed in dense amphiphilic bilayers due to chirality of the molecules. This twist propagates over the whole aggregate, and a helical structure is formed.[55] The EPP-based theory is successful in explaining the molecular origin of the intrinsic bending force in bilayers.[140a,b] It is natural to apply this concept to study the chirality-driven features in monolayers composed of chiral molecules (Figure 32). The wide variety of the domain shapes obtained from different amphiphilic molecules supports the view that molecular chirality drives the mesoscopic or macroscopic chiral shape. Thus, it seems possible to understand the structure of the domain from the effective interaction potential between the molecules in the condensed phase of monolayers.

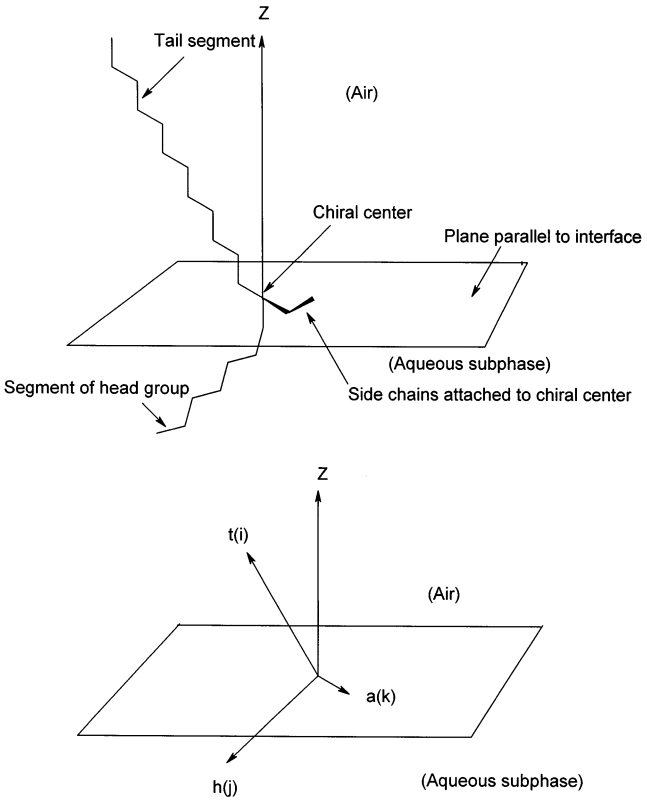

Figure 32. Schematic representation of the model of chiral amphiphilc molecule in the EPP model:[39,40,146] (top) molecular segments of the molecule, present in air and aqueous subphase; (bottom) a few vectors that show the orientations as well as the distances of molecular segments of the *i*th tail group [*t*(*i*)], the *j*th headgroup [*h*(*j*)], and the *k*th group of side chain attached to the chiral center [*a*(*k*)]. Interactions between all possible pairs of groups are considered.

The EPP minimally depends on the distance and orientation between the groups of the neighboring chiral molecules (Figure 33). Whereas the EPP includes the essential stereochemical features of the neighboring chiral molecules, it is necessarily a reduced interaction obtained after summing over many detailed interactions. By varying the distance and orientation between the groups, the minimal energy arrangement can be obtained from this EPP. As the molecules within the domains are in a closely packed state, both attractive and repulsive forces are important and a LJ 6−12-type interaction can be a suitable choice to represent the intermolecular potential. Reliable estimates of the LJ parameters for alkyl and other groups are available in the literature.[141−143]

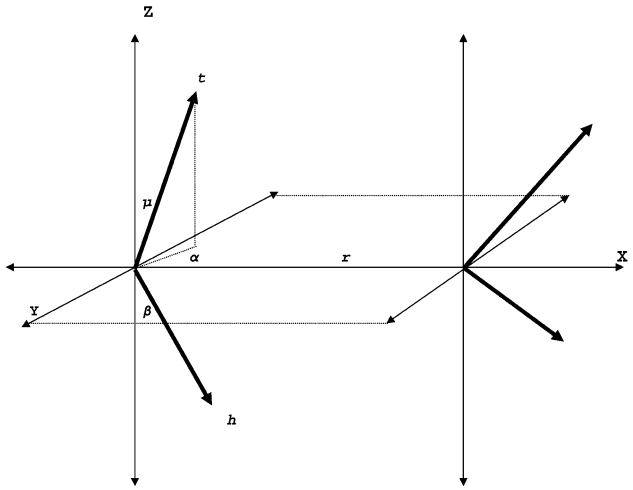

Figure 33. Schematic diagram showing examples of different vectors connecting the chiral center to the center of different groups. Different angles and distances necessary for calculation are indicated. In the figure, a tail group (*t*) and its azimuthal projection (α) as well as tilt from the normal (*μ*) are shown. A headgroup (*h*) and its orientation from normal (*β*) and the intermolecular separation *r* are also shown.

Although both the EPP-based theory and the tripodal model start from the chirality at the molecular level, the EPP-based theory is different from the tripodal model in several respects. For example, (i) the tripodal model ignores the individual features of the molecular orientation taken by a particular amphiphile (it considers the interaction between the centers obtained by projecting the groups on a triangle), whereas exact orientation-dependent distances between the groups are considered in the EPP-based model (the EPP-based theory utilizes the experimentally obtained molecular tilt and azimuthal projection in the calculation) and (ii) the tripodal model considers only the closest of the interactions and neglects the tail−tail interaction, whereas the EPP-based model considers interaction among all groups attached to two neighboring molecules.

The EPP theory is applied to chiral amphiphiles containing amino acid headgroups. The orientation-dependent EPP values of the pair of molecules of *N*-palmitoylaspartic acid and *N*-stearoylserine methyl ester are calculated.[39] The expressions for the orientation-dependent distances between several groups of a pair of amphiphiles are derived. The EPP was then calculated by varying the distance and the mutual azimuthal orientation between them. The molecule is approximated as composed of four different groups representative of the groups attached to the chiral centers (equivalent sphere assumption). The orientation-dependent pair potentials of *N*-palmitoylaspartic acid and *N*-stearoylserine methyl ester for pairs of the same type of enantiomers are shown in Figures 34 and 35, respectively.

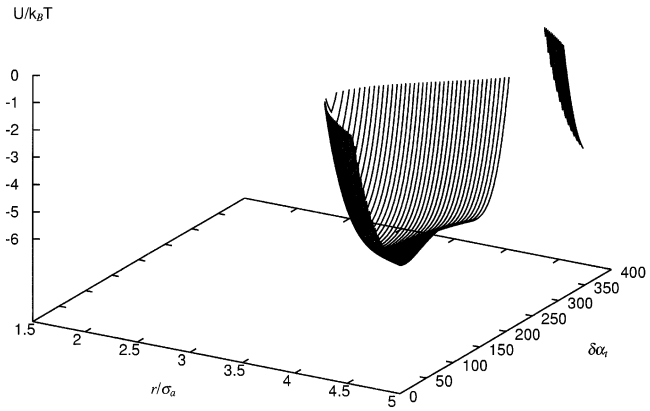

Figure 34. Plot of the intermolecular pair potential of the same type of enantiomers of *N*-palmitoylaspartic acid.[39] The calculation is based on the assumption that the groups attached to the chiral centers are represented by the corresponding equivalent hard spheres. The EPP is expressed in units of k_BT ($T = 293.15$ K). The intermolecular separation is scaled by the diameter of the smallest group attached to the chiral center (3.7 Å) and is expressed in dimensionless units. The mutual azimuthal orientation, $\delta\alpha_t$, is varied over 2π. The pairs of molecules are placed along the short axis of the lattice positions.

The plots show that the pair potential is dependent on the relative orientation between the azimuthal projection of the two molecules on the air/water interfacial plane as well as the distance between them. It is observed that the minimum of EPP corresponds to a mutual orientation between the pair of amphiphiles. However, BAM studies indicate that despite the curvature of the domain, there is no change in the azimuthal projection of the molecule within a domain but that the overall shape of the domain is curved. Thus, at the LC domain/fluid phase interface, the curvature is present which is due to the presence of mutual intermolecular orientation between successive neighbors. Consequently, the favored intermolecular mutual orientation is in competion with an interaction, which favors parallel arrangement between the molecules within the domain. This later interaction is expected to be weaker than the chirality-dependent interaction at the LC domain/fluid phase interface where the curvature develops.

The question arises as to how the molecules meet the energy requirement to achieve the parallel orientation between them, and specifically it is interesting to ask which interaction could favor parallel arrangement between the molecules. In amino acid amphiphiles, cycles of hydrogen bonding are present between the neighboring molecules, and these bonds are the strongest candidates for supplying the energy needed for parallel arrangement. It is well-known that hydrogen bonding is highly cooperative and directional in nature. The presence of twist between the neighboring molecules disturbs the symmetry of the molecular arrangement and is disfavored for a strong cycle of hydrogen bonding. The measured and calculated hydrogen-bonding energies of the polar groups of amino acids (in competition with solvent water) range between 8 and 22 kJ/mol. The energy per hydrogen bonding of the −NH−CO− unit of a peptide group is −5.86 kJ/mol, that of the $-COO^-$ unit of an aspartic acid group is −7.11 kJ/mol, and that of the −OH unit of a serine group is −4.6 kJ/mol.[144] Considering the number of hydrogen bonds per molecule, it is expected that the hydrogen-bonding cycle between the headgroups provides the energy to form the parallel molecular arrangement within the domain, which is observed in experimental studies. However, the theoretical proposition that the hydrogen-bonding pattern actually prevents the chiral tendency of having a mutual orientation between neighboring molecules is yet to be experimentally verified.

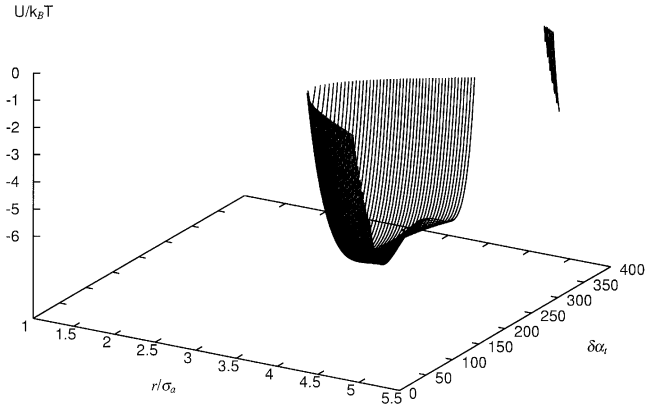

Figure 35. Plot of the intermolecular pair potential of same type of enantiomers of *N*-stearoylserine methyl ester.[39] The calculation is based on the assumption that the groups attached to the chiral centers are represented by the corresponding equivalent hard spheres. The EPP is expressed in units of k_BT ($T = 293.15$ K). The intermolecular separation is scaled by the diameter of the smallest group attached to the chiral center (2.71 Å) and is expressed in dimensionless units. The mutual azimuthal orientation, $\delta\alpha_t$, is varied over 2π. The pairs of molecules are placed along the short axis of the lattice positions.

The interaction energy of an external chiral molecule with all molecules in a domain is position and orientation dependent. The calculation of the interaction potential of an external molecule with all molecules present within a domain is found to be lowest at a certain orientation when measured with respect to a given external axis at the center of the domain.[39] The excess energy at the surface being large at these regions specified by the orientations mentioned above, the growth may happen preferentially in these directions according to Wulf's theorem.[145] This is the

consequence of the underlying pair potential, which favors a twisted state. This factor may act in concert with the underlying twisting tendency of the molecules to make the aggregate shape as anisotropic. This conclusion corroborates the conclusions of McConnell and co-workers about the chiral shapes.[77] This effect may have an influence on the curvature of the domains in addition to the intrinsic tendency of the molecules to twist.

A fascinating aspect of the domains composed of chiral molecules is that the handedness (or sense) of their curvature is highly specific about the chirality of the molecule concerned. If the D-enantiomer gives the right-handedness of the aggregate, the L-enantiomer will give left-handedness and vice versa. Continuum theories completely fail to predict this handedness. Consideration of the molecular interaction seems to have promising features in predicting the sense of amphiphilic aggregates.[140b] It is essential to know how the molecules are arranged in the aggregate as well as the orientation of the molecule with respect to a given external axis. Then the molecular arrangement (and the concomitant curvature of the aggregate) can be understood by using the customary rule that the handedness is observed as the curvature of the aggregate moves away from the observer.

However, there is no completely general way to define the handedness of a chiral object.[27] It depends on how the observer looks at the object. On the other hand, the conclusion that chirality drives the curvature amounts to saying that one should, in principle, correlate the mutual molecular orientation with the variation of the curvature of domains formed by molecules with respect to an observer. Once the criterion of how the observer looks at the domain is selected, there remains no ambiguity in defining the handedness. A simple way to define the handedness in the monolayer is to refer to the direction of the progress of the longer direction starting from a nucleus, and the direction of progress is always measured away from the observer. Thus, the handedness of the monolayer aggregate can be concluded from the growth kinetics. Static images of the domain can be useful for identifying that two handedness exists for two enantiomers and no more. For a general discussion about the handedness concerning dissymmetric molecules we refer to the standard literature.[1,3]

EPP theory is applied to monolayers of amino acid amphiphiles such as *N*-palmitoylaspartic acid, *N*-stearoylserine methyl ester, *N*-palmitoyl-*allo*-threonine methyl ester, and *N*-stearoyl-*allo*-threonine methyl ester to predict the domain handedness composed by these molecules.[40] The domain shapes of SSME are shown in Figure 9.

To predict the handedness, a reference molecule is placed in a corner of the unit cell. Experimental information about the average azimuthal projection and the tilt from the normal is obtained from GIXD studies. These data are used only for the reference molecule. Subsequently, other molecules in the remaining three corners are brought to their respective locations from an infinite separation (where interaction with the reference molecule is essentially absent). The intermolecular pair potential is calculated between the groups of neighboring amphiphiles using a LJ potential. The potential is dependent on the orientation-dependent distance between the groups of neighboring amphiphiles. All possible intermolecular pair interactions are considered and represent the short-range repulsion and long-range attraction over all nonbonded pairs of groups (g) of the ith and jth molecules.

$$U/k_{\mathrm{B}}T = \sum_{\substack{g(i)\\ g(j)}} (4/T)(\epsilon^{g(i)g(j)}/k_{\mathrm{B}})[(s^{g(i)g(j)}/\sigma^{g(i)g(j)})^{-12} - (s^{g(i)g(j)}/\sigma^{g(i)g(j)})^{-6}]$$

Here, $s^{g(i)g(j)}$ is the orientation-dependent distance between the $g(i)$ and $g(j)$ groups, $\sigma^{g(i)g(j)}$ is the average LJ diameter of the corresponding groups, and the energy parameter $\epsilon^{g(i)g(j)}$ is given by the Berthelot rule.

$$\epsilon^{g(i)g(j)} = (\epsilon^{g(i)}\epsilon^{g(j)})^{1/2}$$

The exact expression of the orientation-dependent distances between the groups is obtained by geometric relations.[39,40] Each molecule is oriented by 2π, relative to the reference molecule. The orientations of the three molecules with respect to the reference molecule are observed at the minimum of intermolecular pair potential. If the azimuthal projections of the other molecules do not coincide with that of the reference molecule and the change in azimuthal projection occurs in an anticlockwise fashion (with respect to the reference molecule), then the handedness of the aggregate would be anticlockwise (left). In all cases the reference molecule is placed away from the observer and the remaining molecules further away from the observer. The handedness of the curved domain is experimentally observed from the video images of the growth process of the curvature using BAM. The results of the theoretical prediction of the EPP-based theory and the experimentally observed handedness are in complete agreement with each other in the different monolayer systems considered.[40,146]

From a simulation, it has been recently concluded that the EPP of a pair of chiral molecules can better explain the curvature of domains in monolayers.[147] However, it remained inconclusive that the assumed presence of chiral EPP in the total free energy is due to the chiral structure of lipid (DPPC) or the chirality of the added substance (cholesterol). In other words, the origin of the spontaneous curvature was not quantitatively related to the molecular structure in DPPC monolayers. Consequently, the origin of the handedness of the domain curvature specific for a particular enantiomer could not be explained.

Orientation- and distance-dependent interaction due to the chiral structure of the molecules in DPPC monolayers[146] is calculated using the EPP theory. The morphology of DPPC monolayers has been extensively investigated experimentally, and the domain shape of enantiomeric monolayers is triskellion-shaped with arms curved in a specific direction. The domain curvature is specific for enantiomers, and no

curvature is observed for racemates. BAM studies suggested that the neighboring molecular directors are in a mutually oriented state along the width and length of the arms of the triskelions.[86−88] The recent EPP-based study on DPPC monolayers is based on a coarse-grained description of the molecular structure[146] (Figure 36).

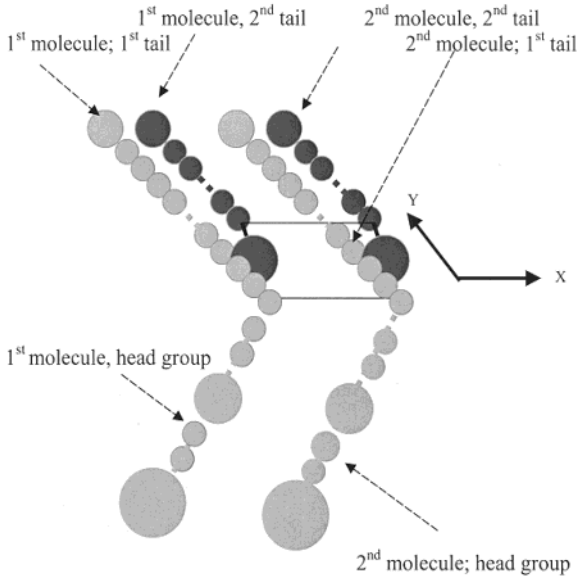

Figure 36. Coarse-grained representation of a pair of DPPC molecules placed on a lattice.

This description is more realistic and an improvement over the equivalent sphere description of the groups used in previous theoretical studies[39,40] and the simulation studies in which molecular structure was not considered.[147] As a result, the EPP profile obtained from the coarse-grained description is expected to depict the molecular interaction in a more detailed way than previous studies. As mentioned before, from the minima of the pair potential, the preferred orientation of a pair of aggregating molecules can be obtained. The mutual orientation between the pair of molecules provides information about the domain handedness of the aggregate in the condensed state where the molecules are aligned in a next-to-next order. It is important to note that in the condensed state of the domains, the molecules are in a close separation and chirality-dependent interactions are dominant. The effect of the orientational distribution of the headgroup in the aqueous subphase on the chiral shape of the aggregate is also investigated.

In the coarse-grained description, the tails and heads of the molecule are represented by an array of collinear spherical groups (CH_2, CH_3, CH, and COO groups, etc.). This is shown in Figure 36. Although atomistic details are neglected in the calculation, the average orientations of the groups with respect to the chiral center are considered over a reasonably small length scale. The molecular segments are placed at the lattice positions. Information about the orientation of the reference molecule with respect to the normal and azimuthal tilt direction of the tail (projected on the perpendicular plane to the normal) is obtained from the GIXD data.[148] The calculation uses no adjustable parameters. No information about the orientation of the headgroup is available from the GIXD studies. All possible orientations of the headgroup with respect to the interface normal and the corresponding possible azimuthal projections are considered to calculate the pair potential of a pair of headgroups of neighboring amphiphiles. The lowest value of all such minima is thus the most probable orientation of the headgroups in the aqueous subphase with respect to the interface. It is observed that the pair potential is favorable over a broad range of orientation but most favorable when they are oriented at an angle with respect to the air/water interface.

The EPP profiles of different molecular segments such as tails and headgroups are considered.[146] The results of the calculation show that, taking the orientation of a tail of any molecule as the same as that obtained from GIXD data, the orientation of the other tail of the same molecule as well as the orientation of the tails of an adjacent molecule is oriented in a right-handed way (Figure 37). If one

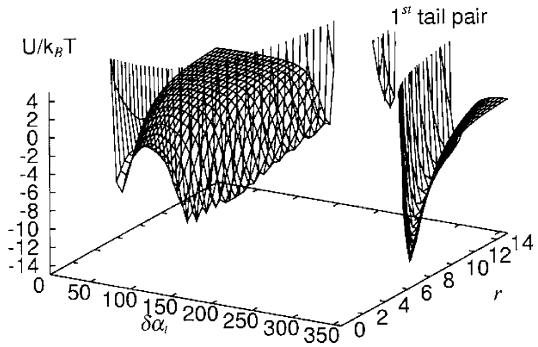

Figure 37. EPP plot expressed in k_BT (T = 293.15 K) for the first tails of neighboring DPPC molecules with variations in the mutual azimuthal orientation of the tails ($\delta\alpha_t$) and intermolecular separation (r).

tail of the reference molecule is located closest to the observer and the other tail of the neighboring molecule is located farthest from the observer, the progress of such an arrangement represents the growth process of the domain where the molecules are aligned in next-to-next fashion. Thus, the interaction between a pair of tails and a pair of heads indicates that all pairs of molecular segments have a large favorable pair potential (measured pairwise with the reference) when the mutual azimuthal projection (counted anticlockwise) is between ∼350° and ∼235°.

This indicates that the molecule segments have a large favorable energy when they all are oriented in a right-handed way with respect to the tail, which is closest to the observer in aggregates composed of D-enantiomer. This mutual orientation is cooperative in the sense that all segments favor the tendency to have a right-handed turn with respect to the reference at the minima of the pair potential. A high-energy barrier in all cases separates the minimum of the EPP, which favors the opposite handedness (left-handedness). The favorable mutual azimuthal orientation gradually moves to parallel arrangement with increase in molecular separation. Also, the EPP becomes increasingly shallow with an increase in

temperature. These facts corroborate well with the wisdom that an increase in molecular separation (by lowering pressure) or an increase in temperature destroys the effect of chirality.

A favorable broad range of orientation of a molecular segment is also expected to diminish the effect of chirality due to effective sphericalization. The present calculation shows that the headgroup pair potential remained favorable over a broad range of mutual orientations of headgroups of the neighboring amphiphiles. The headgroup of the second molecule is found to be oriented in a right-handed way, keeping the reference molecule closest to the observer. This indicates that the effect of chirality is not destroyed even if a distribution of orientation of headgroups exists in the aqueous subphase.[146]

Recently, the chiral discrimination energies in domains composed of chiral amphiphilic monolayers were theoretically studied.[149] Initially, calculations on simpler model systems were carried out, which showed that the depth of the effective pair potential is greatly dependent on the extent of coarse graining of the molecular structure used in theoretical calculation. However, by systematic coarse-graining of model systems, it is shown that the consistent use of a set of parameters (necessary for calculation) can correctly predict the chiral preference (homo- or heterochirality). The model calculation further suggests that with a gradual loss of chirality of the model molecule, the chirality-dependent interaction is diminished. Calculations of the chiral discriminating pair potential of three chiral compounds, *N*-stearoylserine methyl ester, *N*-palmitoylaspartic acid, and *N*-tetradecyl-γ,δ-dihydroxypentanoic acid amide, indicate homochiral preference. The preference is observed both in the packing of a pair of molecules and in the pair potential energy profile. The enantiomeric pairs are closely packed and have a lower minimum pair potential compared to the racemic pairs. The homochiral preference corroborates well with the domain features observed by BAM. The growth in both directions observed in racemic domains is suggestive of local chiral symmetry breaking, which is possible in the case of homochirally preferred interactions. Although the basic conclusions of this EPP-based calculation and the tripodal model agree, the EPP model reveals nontrivial distance and orientation dependence of the discrimination energy. The results are shown to be insensitive to the choice of parameters.

Recently, the concept of a "quantitative chirality measure" developed by Zabrodsky et al. was used to study the LC phase domains of DPPC.[150a,b,151a−c] The study attempts to quantify the chirality of the mesoscopic domain shape. However, a quantitative correlation of the chiral structure of the molecule and the corresponding domain shape based on this approach is yet to be done.

As mentioned before, several questions are to be addressed relating to chirality effects in two dimensions, which can be answered only from a molecular consideration. It is worth investigating why the mutual intermolecular orientation is present between a pair of molecules of a particular amphiphile in the condensed phase and for other amphiphiles such a mutual orientation is absent. Furthermore, the role of hydrogen bonding in the shape formation is also important to investigate, because an extensive hydrogen bond network is present in several amphiphilic aggregates. Hydrogen bonds are also sensitive about the orientation of the donor and acceptor groups. Whether the hydrogen bonding interaction is acting in concert with orientation- and distance-dependent interaction due to the chiral structure of the molecules is yet to be investigated in detail. With the advent of experimental techniques such as GIXD and BAM, detailed structural features are revealed and theoretical methods exploited the information to obtain a better understanding of the monolayer systems. Due to the wide variety of molecular structures of chiral amphiphiles, more theoretical studies based on molecular approaches are necessary to provide a clear understanding of the diverse chirality effects observed in monolayers. The development of density functional theories could be useful in explaining the chirality effects. Also, theories that can combine the explicit molecular structure, electrostatic interaction, and line tension are expected to provide the simplest picture of the shape variations. As indicated before, these studies are expected to be helpful in the understanding of other relevant biological systems such as membranes.

7. Chiral Discrimination Effects in Chiral Monolayers

Chiral discrimination is apparent in differences in the morphology or the physical behavior of a monolayer system as a function of its enantiomeric content. It is expected that the discrimination effect will be observed in the condensed phase where the orientation- and distance-dependent interaction due to the chiral structure of the molecules becomes significant. We have already noted examples of the manifestations of chiral discrimination in previous sections. The discriminating behavior can be concluded from different experimental techniques such as $\pi-A$ isotherm measurements or optical techniques such as BAM as well as from lattice structural information based on GIXD studies. The discrimination is manifested in various ways, such as the shape and characteristic features of the isotherm, the shapes of the domains formed in the condensed phase, or the differences in lattice structures of the enantiomer (or its mirror image) and racemic mixture.

However, the underlying mechanism of the discriminating effect is important. From the viewpoint of the interaction at the molecular level, two types of interactions can take place. If D−D or L−L interaction is favored over the D−L interaction, it is called "homochiral interaction". On the other hand, if interaction of the two different enantiomers (D−L) is more favored compared to the interaction between a pair of the same type of enantiomers (D−D or L−L), it is called "heterochiral interaction". If the homochiral interaction is sufficiently strong, then it is possible that D- rich or L-rich domains would separate out from a racemic mixture. Such phase separation is an example of "chiral symmetry breaking". As

indicated in the Introduction, chiral symmetry breaking is related to the origin of the homochiral evolution. However, in many cases the conclusions about the preferred chirality-dependent interaction (homo- or hetero-) from experimental studies using different techniques are at variance. Furthermore, isotherm measurements and BAM or isotherm measurements and GIXD often show different sensitivities to the chiral preferences, as discussed in the present section. Experimental techniques such as isotherm measurements measure the thermodynamic quantities, which are macroscopic properties such as surface pressure. On the other hand, GIXD probes the characteristics of the monolayer system such as the lattice dimensions in the range of molecular length scale. The underlying interactions have different relative weightiness in two experiments because of the different ranges of the interactions. Thus, it is not surprising that two different methods predict two different chiral sensitivities.

The direct observations of the chiral segregation in bidimensional films are made only in recent years based on optical methods and GIXD studies. BAM studies indicating preferential chirality-dependent interaction have been reviewed previously[24b,152] and will be discussed further in this section. Recently, X-ray crystallographic studies on the separation of racemic mixtures into two-dimensional crystals are reviewed.[26] However, early conclusions on chiral segregation based only on the behavior of the $\pi-A$ isotherm of racemates should be judged with caution as numerous other phenomena can affect the surface tension.

In section 6 it was pointed out that heterochiral interaction is preferred on the basis of van der Waals interaction, whereas homochiral interaction was suggested to be dominant when electrostatic interaction predominates on the basis of the tripodal model. It is important to note that both hetero- and homochirality are observed experimentally, and it is still unclear which interaction is dominant in which amphiphilic system. It might be noted that hydrogen-bonding interactions (which are of primarily electrostatic origin) are dominant in several amphiphilic monolayers (for example, amphiphiles containing amino acid or amide headgroups). Consequently, a competition between the homochiral (which could originate from van der Waals interaction) and heterochiral interaction (which could originate from hydrogen bonding or other electrostatic interactions such as those between the partial charges on the segments of headgroups) might take place in these monolayers. The chiral preference in these cases is still far from understood. We describe the experimental studies on the chiral discrimination in such systems as follows.

Early observations of chiral discrimination are based on isotherm studies, the results of which indicate instantaneous resolution.[28,153,154] The diastereomeric aldonamide monolayers are interesting two-dimensional systems for studying chiral discrimination effects on the morphology of the dendritic crystallization. The condensed phase dendrites of the enantiomeric monolayers of both diastereomers have low mechanical stability. Immediately after solidification, the brittle dendrites are frozen in their nonequilibrium state and remain metastable in this state as long as the monolayer state is unchanged. Thus, the low surface pressure state at the beginning of the compression is best suited to discriminate the chiral forms.

Measurements of the $\pi-A$ isotherm of the pure enantiomers of *N*-dodecyl-D- and -L-gluconamide and the corresponding racemic mixtures, performed at 10 °C and a quite high compression rate of 0.1 nm/molecule, indicate that the isotherm of the racemic mixture is shifted to lower molecular areas compared with that of the enantiomers. At $\pi = 20$ mN/m the racemic mixture has a molecular area of 20.1 Å^2, whereas the enantiomers have an area of 22.2 Å^2. The more compressed state of the racemic monolayer compared to that of the enantiomeric monolayer indicates preferred heterochiral interaction[56] (Figure 39). At higher temperatures (25 °C) the shape of the $\pi-A$ isotherm is already strongly affected by the transition of the two-dimensional monolayer into three-dimensional material. As orientation- and distance-dependent interaction due to the chiral structure of the molecules depends on spatial arrangements of amphphiles or its molecular segments, it is expected that the transformation from two- to three-dimensional structures affects the orientation- and distance-dependent interaction due to the chiral structure of the molecules during the process. The enantiomeric monolayers develop dendritic crystal growths, whereas an isotropic solidification happens in the racemic mixtures. As a result of the two-dimensional ↔ three-dimensional transition, the enantiomeric monolayer can form multilayered dendritic crystals and the racemic monolayers form isotropically distributed multilayerd structure.[56]

Strong relaxation effects are observed in the gluconamide amphiphiles, and discrimination effects are observed in the relaxation behavior.[56] Although the relaxation behaviors of both the enantiomers agree with each other within the limit of experimental error, the racemic form relaxes more rapidly. The absolute relaxation rate and also the differences in the relaxation of the enantiomeric and racemic forms increase considerably with temperature (Figure 38).

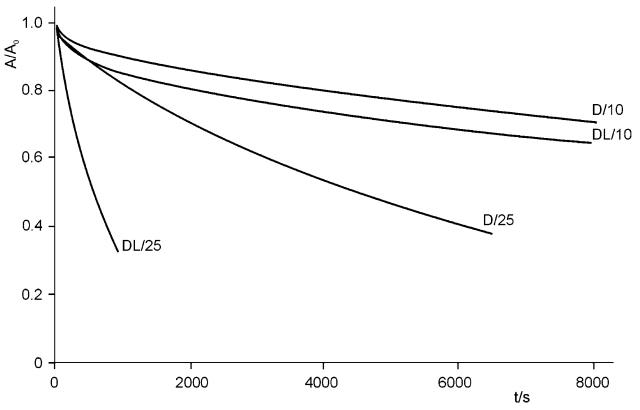

Figure 38. Constant surface pressure relaxation at $\pi =$ 10 mN/m observed for monolayers of the enantiomeric *N*-dodecyl-D- or -L-gluconamide and the racemic mixture (D:L = 1:1) at 10 and 25 °C.[56]

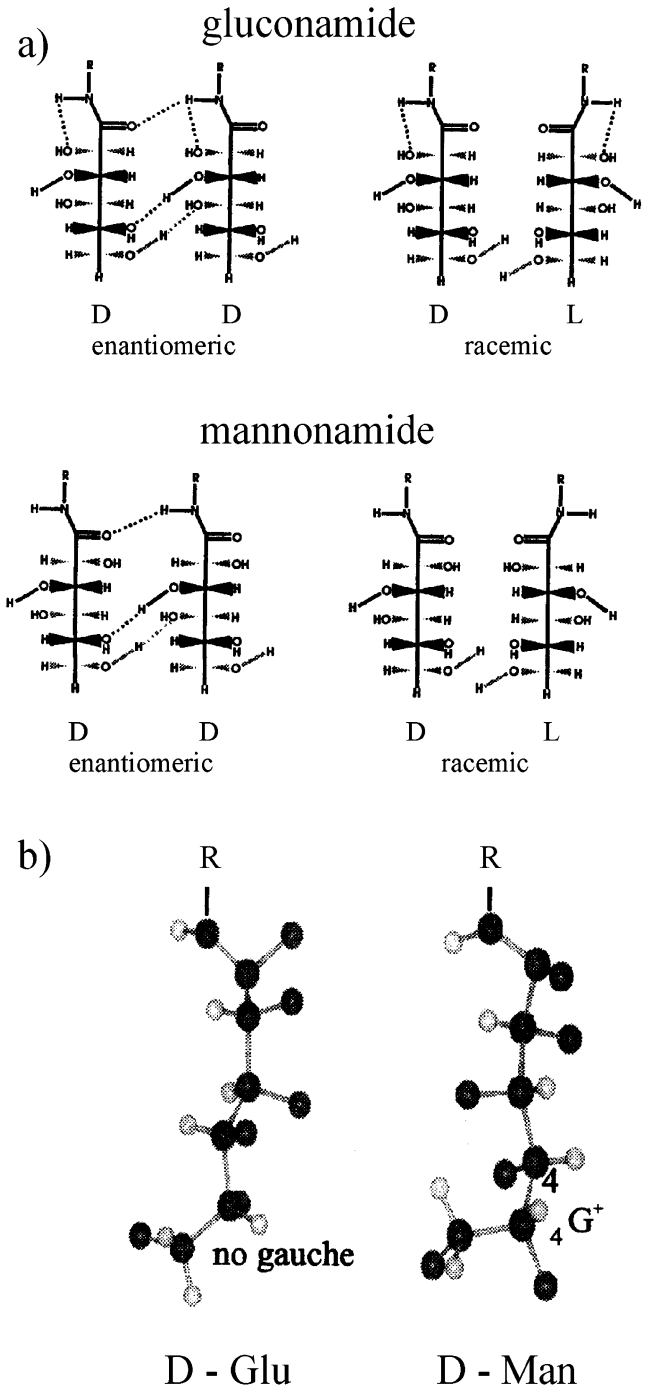

Figure 39. Proposed orientation and conformation of the headgroups of aggregated *N*-dodecylmannonamide monolayers: (a) hydrogen bond cycles are present in pure enantiomers, but not in racemates (hydrogen bonds are shown by dotted lines); (b) as found in 3D crystals of D-gluconamide, the chiral headgroup has a linear conformation, whereas in 3D crystallites of D-mannonamide a gauche bent at C4 is present. The *all-trans*-configured alkyl chains *R* are omitted for clarity.

The chiral discrimination effect is observed in the diasteareomeric mannonamide monolayer. The discriminating behavior is different from the behavior in the gluconamide monolayer. The studies are based on isotherm measurements, BAM studies, and relaxation measurements.[57] The $\pi-A$ measurements show that the molecules in the monolayer of the enantiomeric *N*-dodecylmannonamide amphiphile are more densely packed than in the racemic monolayer. This indicates clear homochiral discrimination in the condensed phase in contrast to the diastereomeric *N*-dodecylgluconamide monolayer. The time dependence of the constant surface pressure relaxation of the enantiomeric amphiphiles is faster compared to that in the racemic monolayers. This trend is also opposite that of the gluconamide monolayers. It is important to note that the only difference in the chemical structure of the two aldonamides (gluconamide and mannonamide) is the chirality of the C2 position of the open sugar chain. Obviously, the slight change in the configuration in the headgroup is responsible for the drastic difference between the two cases. *N*-Alkylaldonamides form cyclic networks of hydrogen bonds of the hydroxyl groups. The difference in the configuration of the headgroups of the mannonamide and gluconamide amphiphiles may lead to different hydrogen-bonding patterns in the two cases and to alteration of the chiral preference from one to the other.

BAM studies strongly support homochiral preference. Featherlike dendrites are observed in the enantiomeric monolayers using BAM.[57] Sidearms develop from these featherlike shapes preferentially in one direction along the main axis. The L-form develops arms oriented in the left-handed way, and the D-form develops arms oriented in the right-handed way. In the case of racemic monolayers, the sidearms are evolved in both directions. The specificity of handedness of the curvature of domains in enantiomeric monolayers strongly suggests that spontaneous chiral segregation might take place in the racemic monolayers, where the arms have curvatures in both directions. Theoretical studies on dendritic systems have shown that such growth is typical for anisotropic systems.[155−158] However, no theoretical description exists for the chirality-dependent anisotropic growth shapes with side branches developing preferentially in one direction along the main axes. As pointed out earlier, the predominant structural difference in the two diastereomeric amphiphiles is the conformation of the glucon- and mannonamides. The observed morphological differences of the diastereomeric monolayers of the two alkylaldonamides cannot be understood alone from first principles of theoretical models, and correlations must exist between the growth patterns of the dendritic structure and the structural features of the sugar headgroups.

The molecules in the *N*-alkyl-D-gluconamide crystals have a hydrogen bond network[159−161] and L-mannon- acid hydrazide also possesses similar patterns of hydrogen bonds.[162] The open-chain sugar is in *all-trans* conformation in both amphiphiles. However, the difference in hydrogen bond pattern in the two amphiphiles is that the interaction between the hydroxyl group at C2 and the amide carbonyl oxygen fixes a linear conformer of the open-chain sugar in the enantiomeric gluconamide monolayer and the same interaction is prevented in mannonamide monolayers because of the different configuration at C2. Besides, there are further conformational differences in the headgroup packing of both diastereomers.[57] The headgroup of gluconamide is present in an *all-*

trans conformation, whereas a gauche bent is observed at C4 of the mannonamide headgroup (Figure 39).

A chiral discrimination effect is also observed in the monolayers of the amphiphilic monoglycerols. The $\pi-A$ isotherms of the enantiomeric and racemic amphiphiles 1-stearylaminoglycerol monolayers are similar and show no discriminating behavior.[47] However, optical techniques and GIXD studies clearly revealed chiral discrimination. Although the domains composed of both enantiomers are filigree-shaped, the domains composed of individual enantiomers are curved in opposite directions, indicating chiral discrimination. The domains composed of *R*(+)-enantiomers are curved in a clockwise direction, whereas the domains composed of *S*(−)-enantiomers are curved in a counterclockwise direction. The domains composed of the racemic mixture have no specific sense of orientation and are fractal-like. The discriminating behavior is also observed in the lattice structure. The enantiomeric monolayers have an oblique lattice, where at compression the tilt direction changes continuously from angles nearly toward the NN direction to angles nearly toward the NNN direction. The condensed phase of the 1:1 racemic mixture gives rise to rectangular-centered lattices, indicating a phase transition accompanied by the change in the tilt direction from NN at 1 mN/m to NNN at 5 mN/m.

The chiral discriminating behavior exhibited by domains of monoglycerol ethers[45,80] is of a different kind, but the domains have the same sense of curvature as those found in the domain of 1-stearylaminoglycerol. In the monoglycerol ethers, the spiral shapes grow from initially compact domains at the end of the plateau region of the $\pi-A$ isotherm. In the case of enantiomeric monolayers they are curved in a chirality-dependent way having the same sense, but racemic monolayers develop spirals curved in both directions. Thus, the discriminating effect is dependent on the chiral structure of the molecules. In some cases the chirality-dependent interaction leads to the development of curvatures in opposite directions within a domain itself and in some cases leads to no net curvature or develops irregular shape. Theoretical studies, as discussed in the previous section, suggest that the different chiral structures of the amphiphilic molecules lead to different chiral intermolecular interaction profiles. Various chiral intermolecular potential profiles and their interplay with other interactions, such as line tension and electrostatic interaction, lead to various shapes. When the chirality-dependent interaction is strong to lead to the chiral phase separation, the segregated segments of the domains may result in the development of curvature in opposite direction.

The chiral discrimination behaviors of monoalkanoylglycerols at higher and lower temperatures are compared using BAM and GIXD.[100] Chiral discrimination is not observed in the monopalmitoylglycerol at 20 °C. However, the BAM studies of monostearoylglycerol at 5 °C indicate a chiral discrimination effect. In the racemic monolayer a change in the brightness of the areas within the domains is observed. The change in brightness corresponds to the change in orientation of the molecules, which is characteristic for a phase transition. For the pure enantiomer there is no indication of a change in the orientation of the condesed phase domains. The GIXD results clearly indicate the presence of an oblique lattice for the enantiomeric monolayer at all surface pressures investigated. The lattice structure of the racemic mixture is rectangular, and the lattice exhibits a transition between 6 and 12 mN/m in which the intermolecular orientation changes from NN to NNN. It was suggested that at high temperatures the thermal motion of the headgroups prevents specific chirality-dependent interaction. The detailed phase diagrams of the monostearoylglycerols corroborate the chiral discrimination of the enantiomeric and racemic forms. At lower temperatures, the molecular packing is dense compared to the packing at higher temperatures, which favors chirality-dependent interaction. This suggestion confirms the recent theoretical studies that the EPP of two chiral molecules is becoming less orientation-specific and the favorable potential is reducing with increasing temperature.[39,40,146] However, the temperature dependence of the chirality-dependent interaction in monolayers is yet to be understood in detail. For example, it is unclear why chiral discrimination appears in the monolayers of *N*-octadecanoylserine methyl ester at higher temperature (at 297 K) and such an effect is not observed at lower temperatures (293 K).[29,162]

Amino acid amiphiphiles are of special interest in studying chiral discrimination effects. Chiral discrimination is concluded in monolayers of amphiphilic amino acid derivatives in many early studies based on $\pi-A$ isotherm studies.[21,22] Monolayers of enantiomeric *N*-stearoylvaline are in a more compressed state compared to the corresponding racemic monolayer as observed in $\pi-A$ isotherm studies.[31] Similar observations are made for the *N*-palmitoylvaline monolayers. This is indicative of homochiral preference. The transition pressure (π_{tr}) (defined as the minimum π value after the overshoot on compression) shows a linear dependence on temperature for the enantiomeric and racemic stearoylvaline monolayer. The slopes of the $\pi_{tr}-T$ curves are, however, different for enantiomeric ($\pi_{tr} = 1.50 \pm 0.10$ dyn cm^{-1} K^{-1}) and racemic ($\pi_{tr} = 1.61 \pm 0.08$ dyn cm^{-1} K^{-1}) monolayers. The dependence of π_{tr} on the enantiomeric mole fraction is nonlinear. "Wishbone"-shaped twinned domains with right-handed or left-handed curvatures are observed in the fluorescence studies of racemic *N*-acylvaline monolayers. The observation of chiral domains (curved with a specific handedness) in a racemic monolayer is suggested to be due to the separation into domains of D- and L-isomers. The corresponding L-enantiomers exhibit dendritic structure formation. *N*-Palmitoylalanine does not show any curvature, and domains with irregular side branching were observed.[31] The differences between the domains composed of valine and alanine residues could possibly due to the larger size of the valine headgroup, which may favor the tilting of the alkyl chain. The uniform tilt order possibly promotes coherence in the crystalline orientation, and that results in a mesoscopic curvature of the domain

shape. Such crystalline order may be reduced in *N*-palmitoylalanine monolayers.

Homochiral preference is also observed in the condensed phase monolayers of *N*-octadecanoyl-L-alanine based on $\pi-A$ isotherm measurements.[35] An intermolecular distance of 5.4 Å was obtained from the area per molecule of 23 Å^2. This value is smaller than the intermolecular distance obtained from Monte Carlo simulation of the homochiral effect of alanine derivatives in Langmuir monolayers (6.5 Å). On the basis of the smaller intermolecular separation obtained in the isotherm measurements, a homochiral preference in monolayers is concluded. Fourier transform infrared (FTIR) spectroscopic studies of *N*-octadecanoyl-L-alanine indicated that below the transition temperature, the intensities of the N−H stretching vibration, the vibration for the carbonyl group in the carboxylic acid, and the amide I and amide II bands of the chiral headgroup attenuate progressively with temperature, and these bands tend to be absent or unresolved above the transition temperature.[33] It is possible that in the fluid-like phase the headgroups are in a fully disordered state and the enantiomeric homochiral interaction is likely to be absent.

Chiral discrimination effects are studied in *N*-stearoyltyrosine monolayers using $\pi-A$ isotherm and fluorescence measurements.[32] The isotherms of both racemic and enantiomeric monolayers show a transition kink corresponding to the transition from the fluid phase to the condensed phase at 33 °C. The plot of the transition pressure exhibits a smooth but nonlinear dependence with a minimum at the racemic composition. Contrary to the homochiral preference of most other *N*-alkanoyl amino acid monolayers, this behavior suggests a heterochiral preference. The morphology of the domains composed of enantiomeric and racemic monolayers indicates chirality-induced discriminating features. The shapes of the enantiomeric domains are elongated and similar over the range of temperature reported (14−33 °C). With increasing temperature, the shapes of the racemic domains are compact, and they evolve to shapes similar to those of the enantiomeric domains. At higher pH, however, for example, at pH 7, both the enantiomeric and racemic monolayers are expanded and are virtually identical at 22 °C so that no transition to the condensed phase takes place and the chiral discrimination disappears. The ionization of the carboxyl group results obviously in Coulombic repulsion between the headgroups and suppresses the formation of a condensed phase. In contrast, the isotherms of *N*-stearoyltyrosine methyl ester measured at pH 7.0 using a phosphate buffer at 22 °C for the pure L and the racemic monolayer are not identical. The isotherms of the enantiomeric monolayer are more compressed than the racemic monolayer, which indicates homochiral preference. The difference in the chiral preference from the free *N*-stearoyltyrosine is attributed to the effect of the hydrogen bonds. The headgroup of the *N*-stearoyltyrosine methyl ester cannot form hydrogen bonds, whereas the *N*-stearoyltyrosine molecules can evolve into a strong hydrogen-bonded system.

The temperature dependence of the chiral discrimination effect is also studied in *N*-hexadecanoylalanine monolayers on a pure aqueous subphase as well as in the presence of 1 mM solutions of $CaCl_2$ and $ZnCl_2$, respectively, at various temperatures in the range of 293−308 K using $\pi-A$ isotherm measurements and infrared reflection absorption spectroscopy (IRRAS).[33] Within a relatively small temperature range, such as 5 K, a change from homo- to heterochirally preferred interaction is observed in the monolayer on an aqueous subphase containing 1 mM $ZnCl_2$. Such a chiral preference is not observed in the isotherm measurements. It is argued that different interactions, such as electrostatic interactions, hydrogen-bonding interaction, or complex formation by counterions could be operative over different length scales. This could give rise to such varying behavior. Also, a significant effect of cations such as Ca^{2+} or Zn^{2+} in the aqueous subphase on the chiral recognition process is observed. These ions should exert strong expanding effects on the *N*-hexadecanoylalanine monolayer. While the homochiral interaction is largely weakened by the presence of ions at the macroscopic level, at the molecular level a change from homo- to heterochiral interaction occurs as the temperature rises. Earlier studies also emphasized the role of ions in the chiral discrimination.[163−166]

Homochiral interaction is observed in the $\pi-A$ isotherm measurement of enantiomeric and racemic *N*-stearoylglutamic acid monolayers at 20 °C [34] on an aqueous subphase at pH 2 and also in the presence of $CdCl_2$. The isotherm of the L-enantiomer exhibits features of a more condensed state than the racemic monolayer at area/molecule of $\leq$40 Å^2 on an aqueous subphase in acidified water. More condensation in the enantiomeric as well as racemic monolayers results from the $\pi-A$ isotherms measured on an aqueous $CdCl_2$ subphase; that is, the homochiral preference is more pronounced in the monolayers on an aqueous $CdCl_2$ subphase.

Heterochiral preference is observed in the $\pi-A$ isotherm measurements of the monolayers of stereoisomers of hexadecylthiophospho-2-phenylglycinol[59] and *N*-stearoyltyrosine.[167] Similar studies of the $\pi-A$ isotherms of tyrosine derivatives also suggest heterochiral preference.[168]

The chiral discrimination effect is also studied in TDHPA monolayers.[42a,b] It is again interesting to note that although the isotherm measurement does not reveal significant chiral discrimination, BAM studies clearly indicated such effects on the shape of the condensed phase domains. The dendritic main growth axes of the *R*- and *S*-enantiomeric domains have a mirror relationship. Such minor axes with specific growth directions are unobserved in racemic monolayers. It is suggested that the directed interactions in the enantiomer monolayers lead to the preferred growth direction, whereas such symmetry effects are canceled in the racemic mixture and result in two main dendritic growth directions, although the shape differences are insignificant. The GIXD studies indicate that at all surface pressures the lattice constants and the unit cell areas of the racemates are slightly smaller than those of the enantiomers (Fig-

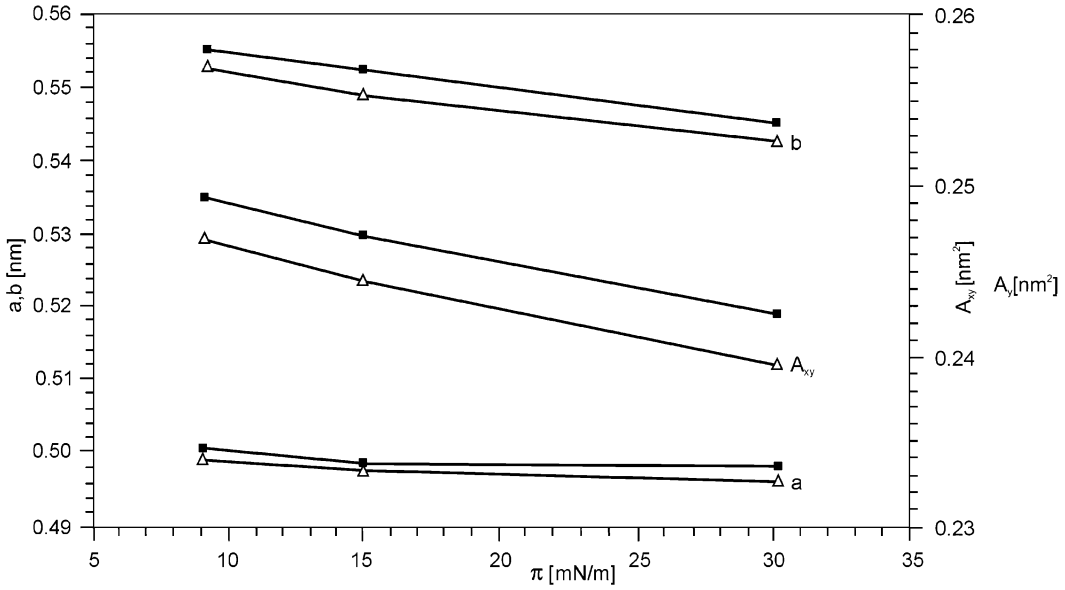

Figure 40. Comparison of lattice constants (*a*, *b*) and unit cell area (A_{xy}) of the *R*-enantiomer (■) and racemate (△) at different surface pressures.

ure 40). This indicates a slightly denser arrangement in the racemic monolayer and suggests weak heterochiral interactions.

A study of the acid−base interactions between MA and PEA demonstrates spontaneous chiral segregation of these two chiral molecules from the racemic mixture.[106] Diastereomeric interactions between the two different chiral molecules are used to study the spontaneous chiral segregation. Using GIXD analysis, it was observed that the chiral disorder is less in the amine component than in the acid component. Three different mixtures are considered [(*R*-MA, *R*-PEA), (*R*-MA, *S*-PEA), and (*R*,*S*-MA, *R*,*S*-PEA)]. The GIXD studies show that each unit cell area contains two long-chain molecular units corresponding to one acid and one amine molecule and they are symmetry independent. The integrated intensities and positions of the Bragg peaks and the shapes of the corresponding Bragg rods are different for *R*,*R*′ and *R*,*S*′ mixtures. Those characteristics of *R*,*S*,*R*′,*S*′ are almost identical with the same characteristics of *R*,*R*′. Considering the highly crystalline state of the monolayer, it is possible that the *R*,*S*,*R*′,*S*′ mixture separates into domains of *R*,*R*′- and *S*,*S*′-enantiomers. It was pointed out that the molecular crystal structure analysis combined with the lattice energy calculations could provide conclusive evidence on whether chiral segregation is taking place or not. It is pointed out that it is difficult to obtain conclusive evidence of chiral segregation in two-dimensional films.[106] The racemic mixtures of the chiral compounds have a lower tendency to separate into enantiomeric-rich domains because the hydrocarbon chains can pack into a herringbone motif where *R* and *S* molecules are related by glide symmetry.[107] Also, an objection is raised about the assumption that the presence of an oblique lattice is evidence of a chiral phase separation. Such an assumption is usually made to conclude that chiral segregation has taken place.[38,105,169,170] In the presence of translation symmetry, an oblique lattice structure of the unit cell in the aggregate strongly suggests that phase separation has taken place. However, the presence of translation symmetry is valid in crystalline aggregates but invalid in mesophases because of the presence of the molecular disorder in the later. It is possible that the oblique lattice is formed by the hydrocarbon chains whereas the underlying *R* and *S* chiral headgroups are randomly distributed.

In some cases, the segregation does not take place at all. For example, the racemic monolayer of dipalmitoylphosphatidylethanolamine (DPPE) remains in the state of racemic compound as evidenced by the rectangular cell observed in GIXD studies.[105] The enantiomeric and racemic monolayers of 1-monopalmitoylglycerol monolayers exhibit also identical domain shape as well as lattice structure. Thus, the effect of chirality is expected to be too weak to have any effect on the monolayer morphology.[82,99] The question arises as to which factors are responsible for triggering the chiral phase separation in a monolayer. More molecular studies are necessary to resolve this question.

Techniques other than described above, such as Maxwell displacement current (MDC) measurements, are carried out to study the chiral phase separation. The generation of the MDC is related with the presence of a dipole moment in the molecule. It is argued that the molecular dipole is not directed along the long axis but oriented on a cylindrical surface assuming the molecule as a cylinder. MDC measurements have been carried out in enantiomeric and racemic DPPC monolayers.[171] It was observed that at the plateau region of the isotherm, some critical MDC peaks are generated with varying amplitude and sign depending on the chirality of the molecule concerned. It is indicated that these peaks are related with the molecular conformational changes.

A very interesting problem but yet under discussion is the chiral segregation. In a previous study it was concluded that racemic myristoylalanine monolayers should be subjected to chiral segregation over

Table 3. Chiral Amphiphile and the Preference for Chirality-Dependent Interaction (Homochirality or Heterochirality) As Observed by Various Experimental Techniques

amphiphile	chiral preference	method of observation
N-tetradecyl-γ,δ-dihydroxypentanoic acid	heterochiral—weak	GIXD
N-dodecylmannonamide	homochiral	BAM, $\pi-A$[57]
N-dodecylgluconamide	heterochiral	BAM, $\pi-A$[56,57]
N-stearoylvaline	homochiral	$\pi-A$[31]
N-octadecanoylalanine	homochiral	$\pi-A$[35]
N-myristoylalanine	homochiral	$\pi-A$, fluorescence, GIXD[38]
N-myristoylalanine	homochiral	$\pi-A$[76]
N-stearoylserine methyl ester	homochiral	$\pi-A$[163]
hexadecylthiophospho-2-phenylglycinol	heterochiral	$\pi-A$[59]
N-stearoylglutamic acid	homochiral	$\pi-A$[34]

a long time at a time interval which could be up to 1 h.[38] In this study, a surface pressure relaxation experiment combined with fluorescence microscopy and GIXD measurements is carried out. However, recent combined studies of surface pressure relaxation, GIXD, and BAM have unequivocally shown that according to the homochiral preference of this monolayer instantaneous segregation takes place at molecular and microscopic levels.[172] Homochiral preference, concluded from the differences in the $\pi-A$ compression isotherms of the racemic and enantiomeric monolayers, means that interaction between the same enantiomers is preferred; that is, in the compression isotherm the first-order phase transition to the condensed phase is shifted to larger area values. However, the decompression isotherms starting at high surface pressures of the enantiomeric and racemic mixtures are nearly identical. BAM studies provide less specific textures of the condensed phase domains not suitable for discrimination between enantiomeric and racemic forms.

On the other hand, the GIXD measurements provided exactly the same oblique lattice for both the enantiomeric monolayer and the racemic mixture without any indication of structural changes with time. This is clear evidence that the condensed monolayer phase is subjected to instantaneous chiral segregation. This indicates also the agreement between the decompression isotherms of the racemic and enantiomeric monolayers. Here, under the starting conditions the chiral forms are already segregated in the racemic monolayer. On the other hand, in the case of monolayer compression an ideal mixing of both enantiomeric forms exists in the fluid (LE) phase. The mixture with the opposite enantiomeric form facilitates the formation of a supersaturated state. Consequently, the surface pressure relaxation expresses the reduction of the supersaturation with fluid phase. This means that at monolayer compression an ideal mixing is produced in the fluid phase, followed by chiral segregation after transition in the consensed phase (LC). Consequently, in all cases of homochirality spontaneous molecular chiral segregation should be expected at transition to the condensed monolayer state obviously accompanied by different microscopic ordering in the system. Examples of discrimination effects exhibited by various amphiphiles are given in Table 3. The chiral amphiphile and the preference for chiral interaction (homochirality or heterochirality) as observed by various experimental techniques are summarized in the table. Recent theoretical studies on chiral discrimination[149] show that the nature of discrimination (homo- or hetero-) is dependent on the molecular structure as well as the lattice arrangement, which is determined by the interaction of the amphiphilic molecules with each other as well as due to the presence of the interface. More studies are required in this direction to completely understand the discrimination effect, which has significance in the evolution process.

8. Concluding Remarks

In this review we discussed the present status of knowledge gained from experimental and theoretical studies in Langmuir monolayers composed of chiral molecules. The purpose of these studies has been primarily to understand the chirality-dependent interaction in monolayers, which is expected to serve as a biomimetic system that is easy to handle. The chiral amphiphilic molecules include a variety of chemical compositions such as amino acid amphiphiles, lipids, amphiphilic monoglycerols, acid and acid amide amphiphiles, and other tailored amphiphiles. A variety of techniques are used to probe the monolayer morphology from mesoscopic length scale to microscopic length scale. BAM and fluorescence microscopy studies revealed that different molecular structures lead to widely different chiral patterns. The experimental techniques clearly demonstrate that the monolayer morphology could express chirality at both length scales. Whereas at the molecular length scale the molecules are chiral, the lattice composed of such molecules as well as the domains formed by millions of such enantiomeric molecules lacks symmetry in many cases. The specific handedness of the domains formed by enantiomeric amphiphiles indicates the influence of the chirality on the domain morphology in such monolayers. However, it is now clearly demonstrated that the information gained from thermodynamic measurements such as isotherm studies must be carefully considered in order to draw conclusions about the underlying molecular interaction. In many cases, the isotherm studies do not reveal significant chiral discrimination effects, which in turn are revealed in optical studies.

On the other hand, the bewildering variety of domain shapes obtained from different molecules, which are observed in optical studies, poses challenges to drawing some general conclusions about the relationship of domain shape as well as the inner texture with the molecular structure. It seems that

each morphology has to be considered on a casewise basis. Only subtle changes in the molecular structure could bring about a very different domain shape or orientation of molecules within a domain. This in turn points out the decisive influence of molecular chiral structure on the domain morphology.

Theoretical studies attempted to correlate the chirality of the molecule with the mesoscopic chirality. The curved shape of the domain expresses the chirality in the later length scale. The relationship between microscopic chirality and chirality at the mesoscopic as well as macroscopic level of the monolayer structure is yet to be understood in detail. This understanding will be particularly helpful in explaining the similar relationship in other biomimetic systems such as bilayers and membranes. However, the experimental results and initial theoretical as well as simulation studies strongly indicate that the chirality on the microscopic level is manifested in the chirality of the macroscopic structure. The theories developed on the basis of molecular models and effective interactions seem promising in this case. However, these theories must include all possible factors such as hydrogen bonding, line tension, and electrostatic interactions that may act in concert or opposition with the nonbonded interaction dependent on chiral structure.

In addition to chirality, several other factors are important in determining the domain morphology. For example, the roles of line tension and electrostatic interaction (in the form of charge and dipolar interaction) are subjects of intensive study. Hydrogen bonding has electrostatic origin and has tremendous importance in biological structure formation. The importance of hydrogen bonding in domain morphology is also emphasized in the literature.[173] Theoretical studies, as discussed in section 6, indicate that hydrogen bondings may compete with chirality-dependent interactions within a domain.[39,40] More quantitative studies are required for a better understanding of the interplay between hydrogen-bonding systems and orientation- and distance-dependent interaction due to the chiral structure of the molecules. Understanding such correlations is of biological significance because hydrogen bonding is omnipresent in biological structures. The importance of the hydrogen bonding also leads to another principal question about the role of solvent for the monolayer structure with particular emphasis on orientation-dependent interactions. The interaction of substrate (water in case of Langmir monolayers) with the amphiphile is important in understanding the amphiphile monolayer structure, as shown in a series of studies by Rice and co-workers using analytical theory and simulation as well as experiment.[174a−r] However, a detailed density functional theory, which includes the microscopic structure of water as well as molecular dissymmetry of the amphiphile, has yet to be developed. Recent detailed studies on the effect of solvent on the crystal growth of alkylgluconamide, asparagine monohydrate, and rhamnose monohydrate show that solvent has an important influence on the morphology of three-dimensional systems.[175,176] Considering the success of the two-dimensional Hartman−Perdok analysis in explaining the surface properties of crystalline systems, a similar development in chiral amphiphilic systems may prove to be useful.[177]

As indicated in the Introduction, it is important to understand why nature has so much preference for chirality. It is indeed surprising in how many ways the chirality is manifested in biomolecular systems in its structural hierarchy. Both geometrical and topological chirality are observed in biomolecules such as proteins. It is pointed out that lower order chiral features of proteins, for example, the L-enantiomeric form of amino acid molecule units, possibly trigger the chirality at a higher level, for example, the specific handedness observed in extended polypeptide chains.[18] The related question of homochiral evolution in biosystems is still an open problem. Recent studies on chiral synthesis of oligopeptides in two-dimensional cryatlline domains on water indicate that ordered self-assembled clusters may have an important role in this process.[178] Theoretical studies on the influence of the protein secondary level chirality (namely, helical structure) on the ligand interaction indicate that the presence of chirality at all levels of hierarchy of complex systems such as proteins has functional significance.[179] Recent theoretical study on chiral recognition of odorant molecules by lipids shows that chirality may have important influence on biologically important recognition precesses.[180] Recent theoretical studies revealed the importance of cooperative effects in chiral symmetry breaking.[181,182] Theories related to pattern formation in magnetic systems in Hele−Shaw cells are applied to study the formation and shape of domains in amphiphiles.[183] More studies are required to understand how molecular cooperativity is leading to the chiral order at various molecular structural hierarchies. A related problem is the understanding of the structure−function correlation. A detailed understanding of the correlation of the chiral structure with the function might be useful for understanding the protein folding process or understanding the building up principle of tertiary structure from primary structure. Study of the interaction of chiral lipid and chiral odorant indicates that chirality plays a role in biological processes such as odor perception.[179] Further experimental and theoretical studies are required to understand the effect of chirality in biomolecules. Studies of chirality in monolayer systems seem promising to serve as model studies aimed at this goal. Such understanding is expected to unravel some fundamental principles of nature.

9. Symbols and Abbreviations

A = area per amphiphilic molecule
AFM = atomic force microscopy
BAM = Brewster angle microscopy
BEG = Blume−Emery−Griffiths (model)
DPPC = dipalmitoylphosphatidylcholine
DPPE = dipalmitoylphosphatidylethanolamine
DPP(Me)E = dipalmitoyl phosphatidyl-*N*-monomethylethanolamine
$DPP(Me)_2E$ = dipalmitoylphosphatidyl-*N*-dimethylethanolamine

DMPA = dimyristoylphosphatidic acid
DMPE = dimyristoylphosphatidylethanolamine
EPP = effective pair potential
E-Gl = enantiomeric 3-stearoyl-*sn*-glycerol
FFM = friction force microscopy
GIXD = grazing incidence X-ray diffraction
HOBD = 4-hexadecyloxybutane-1,2-diol
IRRAS = infrared reflection absorption spectroscopy
LE = liquid expanded (phase of monolayer)
LC = liquid condensed (phase of monolayer)
MA = *p*-pentadecylmandelic acid
MDC = Maxwell displacement current
NN = nearest neighbor
NNN = next nearest neighbor
π = surface pressure
π_t = transition pressure
PEA = *p*-tetradecylphenylethylamine
POPC = 1-palmitoyl-2-oleoylphosphatidylcholine
Rac = racemic
R-Gl = racemic 1-stearoyl-*rac*-glycerol
SSME = stearoylserine methyl ester
TDHPA = *N*-tetradecyl-γ,δ-dihydroxypentanoic acid amide

10. Acknowledgments

We thank Dr. S. Siegel for help with cover artwork. This work is partially supported by the Alexander von Humboldt foundation.

11. References

(1) Testa, B. *Principles of Organic Stereochemistry*; Dekker: New York, 1979.
(2) Flapan, E. *When Topology Meets Chemistry*: *A Topological Look at Molecular Chirality*; Cambridge University Press: Cambridge, U.K., 2000.
(3) Eliel, E. L.; Wilen, S. H.; Mander, L. N. *Stereochemistry of Organic Compounds*; Wiley: New York, 1994.
(4) van't Hoff, J. H. *Die Lagerung der Atome im Raume*; Vieweg: Braunschweig, Germany, 1894.
(5) van't Hoff, J. H. *Arch. Neerl. Sci. Exactes Nat.* **1874**, *9*, 455.
(6) Le Bel, J. A. *Bull. Soc. Chim. Fr.* **1874**, *22*, 337.
(7) Pasteur, L. *Ann. Chim. Phys.* **1848**, *24*, 442.
(8) Stinson, S. *Chem. Eng. News* **2001**, *79* (20), 45; *Chem. Eng. News* **2001**, *79* (40), 79.
(9) Stinson, S. *Chem. Eng. News* **1999**, *77* (47), 57.
(10) Stinson, S. *Chem. Eng. News* **1999**, *77* (41), 101.
(11) Borman, S. *Chem. Eng. News* **2001**, *79* (35), 9.
(12) Jacques, J.; Collet, A.; Wilen, S. H. *Enantiomers, Racemates and Resolutions*; Wiley: New York, 1981.
(13) Kuhn, H.; Kuhn, C. *Angew. Chem., Int. Ed.* **2003**, *42*, 262.
(14) (a) Mason, S. F. *Nature* **1984**, *311*, 19. (b) Mason, S. F. *Int. Rev. Phys. Chem.* **1983**, *3*, 217.
(15) Miller, S. W.; Orgel, L. E. *The Origin of Life on Earth*; Prentice Hall: Englewood Cliffs, NJ, 1974.
(16) Fox, S. W.; Dose, K. *Molecular Evolution and Origin of Life*; Dekker: New York, 1977.
(17) Kondepudi, D. K.; Nelson, G. W. *Nature* **1985**, *314*, 438.
(18) Maggiora, G. M.; Mao, B.; Chou, K. *New Developments in Molecular Chirality*; Mezey, G. P., Ed.; Kluwer Academic Publishers: Dordrecht, The Netherlands, 1991; p 9.
(19) Möhwald, H. *Annu. Rev. Phys. Chem.* **1990**, *41*, 441.
(20) Knobler, C. M. *Adv. Chem. Phys.* **1990**, *77*, 397.
(21) Arnett, E. M.; Harvey, N. G.; Rose, P. L. *Acc. Chem. Res.* **1989**, *22*, 131.
(22) Heath, J. G.; Arnett, E. M. *J. Am. Chem. Soc.* **1992**, *114*, 4500.
(23) McConnell, H. M. *Annu. Rev. Phys. Chem.* **1991**, *42*, 171.
(24) (a) Vollhardt, D. *Adv. Colloid Interface Sci.* **1996**, *64*, 143. (b) Vollhardt, D. In *Encyclopedia of Surface and Colloid Science*; Hubbard, A., Ed.; Dekker: New York, 2002; p 3585.
(25) Kaganer, V. M.; Möhwald, H.; Dutta, P. *Rev. Mod. Phys.* **1999**, *71*, 779.
(26) Kuzmenko, I.; Rapaport, H.; Kjaer, K.; Als-Nielsen, J.; Weissbuch, I.; Lahav, M.; Leiserowitz, L. *Chem. Rev.* **2001**, *101*, 1659.
(27) Harris, A. B.; Kamien, R. D.; Lubensky, T. C. *Rev. Mod. Phys.* **1999**, *71*, 1745.
(28) (a) Lundquist, M. *Ark. Kemi.* **1961**, *17*, 183. (b) Lundquist, M. *Ark. Kemi.* **1963**, *21*, 395. (c) Lundquist, M. *Ark. Kemi.* **1965**, *23*, 299. (d) Lundquist, M. *Prog. Chem. Fats Other Lipids* **1978**, *16*, 101.
(29) Stine, K. J.; Uang, J. Y.-J.; Dingman, S. D. *Langmuir* **1993**, *9*, 2112.
(30) Rietz, R.; Rettig, W.; Brezesinski, G.; Möhwald, H. *Pharmazie* **1997**, *52*, 701.
(31) Parazak, D. P.; Uang, J. Y.-J.; Turner, B.; Stine, K. J. *Langmuir* **1994**, *10*, 3787.
(32) Stine, K. J.; Whitt, S. A.; Uang, J. Y.-J. *Chem. Phys. Lipids* **1994**, *69*, 41.
(33) Hoffman, F.; Hühnerfuss, H.; Stine, K. J. *Langmuir* **1998**, *14*, 4525.
(34) Zhang, Y. J.; Song, Y.; Zhao, Y.; Li, T. J.; Jiang, L.; Zhu, D. *Langmuir* **2001**, *17*, 1317.
(35) Du, X.; Shi, B.; Liang, Y. *Langmuir* **1998**, *14*, 3631.
(36) Du, X.; Liang, Y. *Langmuir* **2000**, *16*, 3422.
(37) Du, X.; Liang, Y. *J. Phys. Chem. B* **2000**, *104*, 10047.
(38) Nassoy, P.; Goldmann, M.; Bouloussa, O.; Rondelez, F. *Phys. Rev. Lett.* **1995**, *75*, 457.
(39) Nandi, N.; Vollhardt, D. *Colloid Surf. A* **2001**, *183*−*185*, 67.
(40) Nandi, N.; Vollhardt, D. *Colloid Surf. A* **2002**, *198*−*200* (SI), 207.
(41) Jeffrey, G. A.; Saenger, W. *Hydrogen Bonding in Biological Structures*; Springer-Verlag: Berlin, Germany, 1991.
(42) (a) Melzer, V.; Weidemann, G.; Vollhardt, D. *Annual Report II, Hamburger Synchrotronstrahlungslabor* (*HASYLAB*) *am Deutschen Elektronen-Synchrotron (DESY)*; 1995; p 205. (b) Melzer, V.; Weidemann, G.; Vollhardt, D.; Brezesinski, G.; Wagner, R.; Struth, B.; Möhwald, H. *J. Phys. Chem. B* **1997**, *101*, 4752.
(43) Vollhardt, D.; Gehlert, U.; Siegel, S. *Colloid Surf. A* **1993**, *76*, 187.
(44) Fainerman, V. B.; Vollhardt, D.; Melzer, V. *J. Phys. Chem.* **1996**, *100*, 15482.
(45) Gehlert, U.; Vollhardt, D. *Prog. Colloid Polym. Sci.* **1994**, *97*, 302.
(46) Gehlert, U.; Vollhardt, D. *Langmuir* **1997**, *13*, 277.
(47) Vollhardt, D.; Gehlert, U. *J. Phys. Chem. B* **2002**, *106*, 4419.
(48) Bringezu, F.; Brezesinski, G.; Nuhn, P.; Möhwald, H. *Biophys. J.* **1996**, *70*, 1789.
(49) Dietrich, A.; Brezesinski, G.; Möhwald, H.; Dobner, B.; Nuhn, P. *Nuovo Cimento* **1994**, *16*, 1537.
(50) Dietrich, A.; Möhwald, H.; Rettig, W.; Brezesinski, G. *Langmuir* **1991**, *7*, 539.
(51) Brezesinski, G.; Böhm, C.; Dietrich, A.; Möhwald, H. *Physuca B (Amsterdam)* **1994**, *198*, 146.
(52) Brezesinski, G.; Dietrich, A.; Dobner, B.; Möhwald, H. *Prog. Colloid Polym. Sci.* **1995**, *98*, 255.
(53) Fuhrhop, J.-H.; Schnieder, P.; Rosenberg, J.; Boekema, E. *J. Am. Chem. Soc.* **1987**, *109*, 3387.
(54) Fuhrhop, J.-H.; Boettcher, C. *J. Am. Chem. Soc.* **1990**, *112*, 1768.
(55) Fuhrhop, J.-H.; Helfrich, W. *Chem. Rev.* **1993**, *93*, 1565.
(56) Vollhardt, D.; Gutberlet, T.; Emrich, G.; Fuhrhop, J.-H. *Langmuir* **1995**, *11*, 2661.
(57) Vollhardt, D.; Emrich, G.; Gutberlet, T.; Fuhrhop, J.-H. *Langmuir* **1996**, *12*, 5659.
(58) van Esch, J. H.; Nolte, R. J. M.; Ringsdorf, H.; Wildburg, G. *Langmuir* **1994**, *10*, 1955.
(59) Dvolaitzky, M.; Guedeau-Boudeville, M.-A. *Langmuir* **1989**, *5*, 1200.
(60) Gruniger, H.; Mobius, D.; Meyer, H. *J. Chem. Phys.* **1983**, *79*, 3701.
(61) Orrit, M.; Möbius, D.; Lehmann, U.; Meyer, H. *J. Chem. Phys.* **1986**, *85*, 4966.
(62) Loschek, R.; Möbius, D. *Chem. Phys. Lett.* **1988**, *151*, 176.
(63) Lehmann, U. *Thin Solid Films* **1988**, *160*, 257.
(64) Hönig. D.; Möbius, D. *J. Phys. Chem.* **1991**, *95*, 4590.
(65) Hönig. D.; Möbius, D. *Thin Solid Films* **1992**, *210*, 64.
(66) Henon, S.; Meunier, J. *Rev. Sci. Instrum.* **1991**, *62*, 936.
(67) Henon, S.; Meunier, J. *J. Chem. Phys.* **1993**, *98*, 9148.
(68) Melzer, V.; Weidemann, G.; Vollhardt, D. *Annual Report II, Hamburger Synchrotronstrahlungslabor* (*HASYLAB*) *am Deutschen Elektronen-Synchrotron (DESY)*; 1995; p 207.
(69) Melzer, V.; Vollhardt, D.; Weidemann, G.; Brezesinski, G.; Wagner, R.; Möhwald, H. *Phys. Rev. E* **1998**, *57*, 901.
(70) Akamatsu, S.; Bouloussa, O.; To, K.; Rondelez, F. *Phys. Rev. A* **1992**, *46*, R4504.
(71) Ben Amar, M.; Pomeau, Y. *Europhys. Lett.* **1986**, *2*, 307.
(72) Ivantsov, G. P. *Dokl. Akad. Nauk. U.S.S.R.* **1947**, *58*, 567.
(73) Ben Jacob, E.; Goldenfeld, N. D.; Langer, J. S.; Schön, G. *Phys. Rev. A* **1984**, *29*, 330.
(74) Langer, J. S. In *Lectures in the Theory of Pattern Formation in Chance and Matter*; Les Houches Summer School, Session XLVI, 1986; Souletie, J., Stora, R., Vannimenus, J., Eds.; Elsevier: New York, 1987.
(75) Kessler, D. A.; Koplik, J.; Levine, H. *Adv. Phys.* **1988**, *38*, 3043.

(76) Bouloussa, O.; Dupeyrat, M. *Biochim. Biophys. Acta* **1988**, *938*, 395.
(77) McConnell, H. M.; Moy, V. T. *J. Phys. Chem.* **1988**, *92*, 4520.
(78) Vollhardt, D.; Siegel, S. *Annual Report, Hamburger Synchrotronstrahlungslabor* (*HASYLAB*) *am Deutschen Elektronen-Synchrotron (DESY)*; 2001; p 627.
(79) Vollhardt, D. Unpublished results.
(80) Vollhardt, D.; Gehlert, U. *Tenside, Surfactants, Deterg.* **1996**, *33*, 196.
(81) Gehlert, U.; Weidemann, G.; Vollhardt, D. *J. Colloid Interface Sci.* **1995**, *174*, 392.
(82) Weidemann, G.; Gehlert, U.; Vollhardt, D. *Langmuir* **1995**, *11*, 864.
(83) (a) Kleber, W. *An Introduction to Crystallography*, 1st ed.; Verlag Technik: Berlin, Germany, 1970; p 102. (b) Kleber, W. *Einfuhrung in die Kristallographie*, 16th ed.; Verlag Technik: Berlin, Germany, 1985; p 74.
(84) Meine, K.; Vollhardt, D.; Weidemann, G. *Langmuir* **1998**, *14*, 1815.
(85) Rietz, R.; Rettig, W.; Brezesinski, G.; Bouwman, W. G.; Kjaer, K.; Möhwald, H. *Thin Solid Films* **1996**, *284*, 211.
(86) Weidemann, G.; Vollhardt, D. *Colloid Surf. A* **1995**, *100*, 187.
(87) Weidemann, G.; Vollhardt, D. *Thin Solid Films* **1995**, *264*, 94.
(88) Weidemann, G.; Vollhardt, D. *Biophys. J.* **1996**, *70*, 2758.
(89) Weis, R. M.; McConnell, H. M. *Nature* **1984**, *310*, 47.
(90) Heckl, W. M.; Möhwald, *Ber. Bunsen-Ges. Phys. Chem.* **1986**, *90*, 1159.
(91) Heckl, W. M.; Lösche, M.; Cadenhead, D. A.; Möhwald, H. *Eur. Biophys. J.* **1986**, *14*, 11.
(92) Worthman, L.-A. D.; Nag, K.; Davis, P. J.; Keough, K. M. W. *Biophys. J.* **1997**, *72*, 2569.
(93) Als-Nielsen, J.; Möhwald, H. In *Hand Book of Synchrotron Radiation*; Ebashi, S., Koch, M., Rubenstein, E., Eds.; Elsevier Science: Amsterdam, The Netherlands, 1991; Vol. 4, p 1.
(94) Als-Nielsen, J.; Jacquemain, D.; Kjaer, K.; Lahav, M.; Leveiller, F.; Leiserowitz, L. *Phys. Rep.* **1994**, *246*, 251.
(95) Als-Nielsen, J.; Kjaer, K. *Phase Transition in Soft Condensed Matter*; Riste, T., Sherrington, D., Eds.; Plenum Press, New York, 1989; p 113.
(96) Penfold, J.; Thomas, R. K. *J. Phys. Condensed Matter* **1990**, *2*, 1369.
(97) Berge, B.; Lenne, P. F.; Renault, A. *Curr. Opin. Colloid Interface Sci.* **1998**, *3*, 321.
(98) Rietz, R.; Brezesinski, G.; Möhwald, H. *Ber. Bunsen-Ges. Phys. Chem.* **1993**, *97*, 1394.
(99) Brezesinski, G.; Scalas, E.; Struth, B.; Möhwald, H.; Bringezu, F.; Gehlert, U.; Weidemann, G.; Vollhardt, D. *J. Phys. Chem.* **1995**, *99*, 8758.
(100) Gehlert, U.; Vollhardt, D.; Brezesinski, G.; Möhwald, H. *Langmuir* **1996**, *12*, 4892.
(101) Gehlert, U.; Vollhardt, D. *Langmuir* **2002**, *18*, 688.
(102) Scalas, E.; Brezesinkski, G.; Möhwald, H.; Kaganer, V. M.; Bouwman, W. G.; Kjaer, K. *Thin Solid Films* **1996**, *284*−*285*, 56.
(103) Brezesinski, G.; Dietrich, A.; Struth, C.; Böhm, C.; Bowman, G.; Kjaer, K.; Möhwald, H. *Chem. Phys. Lipids* **1995**, *76*, 145.
(104) Böhm, C.; Möhwald, H.; Leiserowitz, L.; Als-Nielsen, J.; Kjaer, K. *Biophys. J.* **1993**, *64*, 553.
(105) Weissbuch, I.; Berfeld, M.; Bouwman, W.; Kjaer, K.; Als-Nielsen, J.; Lahav, M.; Leiserowitz, L. *J. Am. Chem. Soc.* **1997**, *119*, 933.
(106) Kuzmenko, I.; Weissbuch, I.; Gurovich, E.; Leiserowitz, L.; Lahav, M. *Chirality* **1998**, *10*, 415.
(107) Kuzmenko, I.; Kjaer, K.; Als-Nielsen, J.; Lahav, M.; Leiserowitz, L. *J. Am. Chem. Soc.* **1999**, *121*, *2657*.
(108) (a) Datta, A.; Kmetko, J.; Yu, C.-J.; Richter, A. G.; Chung, K.-S.; Bai, J.-M.; Dutta, P. *J. Phys. Chem. B* **2000**, *104*, 5797. (b) Durbin, M. K.; Malik, A.; Richter, A. G.; Ghaskadvi, R.; Gog, T.; Dutta, P. *J. Chem. Phys.* **1997**, *106*, 8216.
(109) de Gennes, P. G.; Prost, J. *The Physics of Liquid Crystals*; Clarendon: Oxford, U.K., 1993.
(110) Seul, M.; Andelman, D. *Science* **1995**, *267*, 476.
(111) (a) Iwamoto, M.; Wu, C. X.; Ou-Yang, Z. C. *Phys. Rev. E* **1996**, *59*, 586. (b) Zhao, W.; Wu, C. X.; Iwamoto, M. *Phys. Rev. E* **2000**, *61*, 6669. (c) Iwamoto, M.; Wu, C. X.; Ou-Yang, Z. C. *Chem. Phys. Lett.* **1998**, *285*, 306.
(112) Scalas, E.; Brezesinkski, G.; Kaganer, V. M.; Möhwald, H. *Phys. Rev. E* **1998**, *58* (2 part B), 2172.
(113) Lautz, C.; Fischer, T. M. *Eur. Phys. J. B* **1999**, *7*, 263.
(114) Pellizola, A.; Pretti, M.; Scalas, E. *J. Chem. Phys.* **2000**, *112*, 8126.
(115) (a) Selinger, J. V.; Wang, Z.-G.; Bruinsma, R. F.; Knobler, C. M. *Phys. Rev. Lett.* **1993**, *70*, 1139. (b) Selinger, J. V.; Selinger, R. L. B. *Phys. Rev. E* **1995**, *51*, R860.
(116) Fischer, T. M.; Bruinsma, R. F.; Knobler, C. M. *Phys. Rev. E* **1994**, *50*, 413.
(117) Loh, K.-K.; Kraus, I.; Meyer, R. B. *Phys. Rev. E* **2000**, *62* (part A), 5115.
(118) McConnell, H. M.; Tamm, L. K.; Weis, R. M. *Proc. Natl. Acad. Sci. U.S.A.* **1984**, *81*, 3249.
(119) Seul, M. S.; Subramaniam, S.; McConnell, H. M. *J. Phys. Chem.* **1985**, *89*, 3592.
(120) McConnell, H. M.; Keller, D.; Gaub, H. *J. Phys. Chem.* **1986**, *90*, 1717.
(121) Gaub, H. E.; Moy, V. T.; McConnell, H. M. *J. Phys. Chem.* **1986**, *90*, 1721.
(122) Keller, D. J.; McConnell, H. M.; Moy, V. T. *J. Phys. Chem.* **1986**, *90*, 2311.
(123) Gaub, H. E.; McConnell, H. M. *J. Phys. Chem.* **1986**, *90*, 6830.
(124) McConnell, H. M.; Keller, D. *Proc. Natl. Acad. Sci. U.S.A.* **1987**, *84*, 4706.
(125) Subramaniam, S.; McConnell, H. M. *J. Phys. Chem.* **1987**, *91*, 1715.
(126) Keller, D. J.; Korb, J. P.; McConnell, H. M. *J. Phys. Chem.* **1987**, *91*, 6417.
(127) Moy, V. T.; Keller, D. J.; McConnell, H. M. *J. Phys. Chem.* **1988**, *92*, 4520.
(128) McConnell, H. M. *Proc. Natl. Acad. Sci. U.S.A.* **1989**, *86*, 3452.
(129) Rice, P. A.; McConnell, H. M. *Proc. Natl. Acad. Sci. U.S.A.* **1989**, *86*, 6445.
(130) McConnell, H. M. *J. Phys. Chem.* **1990**, *94*, 4728.
(131) McConnell, H. M.; de Koker, R. *J. Phys. Chem.* **1992**, *96*, 7101.
(132) Vanderlick, T. K.; Möhwald, H. *J. Phys. Chem.* **1990**, *94*, 886.
(133) Deutch, J. M.; Low, F. E. *J. Phys. Chem.* **1992**, *96*, 7097.
(134) Miranda, J. A. *J. Phys. Chem. B* **1999**, *103*, 1303.
(135) Helm, C. A.; Laxhuber, L. A.; Lösche, M.; Möhwald, H. *J. Colloid Polym. Sci.* **198**, *264*, 46.
(136) Fischer, A.; Lösche, M.; Möhwald, H.; Sackmann, E. *J. Phys. Lett.* **1984**, *45*, L785.
(137) Lösche, M.; Helm, C. A.; Mattes, H. D.; Möhwald, H. *Thin Solid Films* **1985**, *132*−*134*, 1.
(138) (a) Andelman, D. *J. Am. Chem. Soc.* **1989**, *111*, 6536. (b) Andelman, D.; Orland, H. *J. Am. Chem. Soc.* **1993**, *115*, 12322.
(139) Andelman, D.; de Gennes, P.-G. *Compt. Rend. Acad. Sci. (Paris)* **1988**, *307* (II), 233.
(140) (a) Nandi, N.; Bagchi, B. *J. Am. Chem. Soc.* **1996**, *118*, 11208. (b) Nandi, N.; Bagchi, B. *J. Phys. Chem. A* **1997**, *101*, 1343.
(141) Ben Amotz, D.; Herschbach, D. R. *J. Phys. Chem.* **1990**, *94*, 1038.
(142) Bondi, A. *J. Phys. Chem.* **1964**, *68*, 441.
(143) Jorgensen, W.; Tirado-Rives, J. *J. Am. Chem. Soc.* **1988**, *110*, 1657.
(144) Table 2.5b in ref 41.
(145) Burton, W. K.; Cabrera, N.; Frank, F. C. *Proc. R. Soc. London A* **1951**, *243*, 299.
(146) (a) Nandi, N.; Vollhardt, D. *J. Phys. Chem. B* **2002**, *106*, 10144; *J. Phys. Chem. B.* **2003**, *107*, 1932 (erratum). (c) Nandi, N.; Roy, R. K.; Upadhaya, S.; Vollhardt, D. *J. Surf. Sci. Technol.* **2002**, *18*, 51.
(147) Krüger, P.; Lösche, M. *Phys. Rev. E* **2000**, *62*, 7031.
(148) (a) Dahmen-Levison, U.; Brezesinski, G.; Möhwald, H. *Thin Solid Films* **1998**, *327*, 616. (b) Brezesinski, G. Unpublished data recorded at 20 °C and 41 mN/m.
(149) Nandi, N.; Vollhardt, D. *J. Phys. Chem.* **2003**, *107*, 3464.
(150) (a) Kane, S. A. *Langmuir* **2002**, *18*, 9853. (b) Kane, S. A.; Compton, M.; Wilder, N. *Langmuir* **2000**, *16*, 8447.
(151) (a) Zabrodsky, H.; Peleg, S.; Avnir, D. *J. Am. Chem. Soc.* **1992**, *114*, 7843. (b) Zabrodsky, H.; Peleg, S.; Avnir, D. *J. Am. Chem. Soc.* **1993**, *115*, 8278. (c) Zabrodsky, H.; Avnir, D. *J. Am. Chem. Soc.* **1995**, *117*, 462.
(152) Vollhardt, D.; Emrich, G.; Melzer, V.; Weidemann, G.; Gehlert, U. *Short and Long Tails at Interfaces*; Proceedings of the XXXth Rencontres De Moriond; Daillant, J., Guenoun, P., Marques, C., Muller, P., Trân Thanh Vân, J., Eds.; Editions Frontiers: Gif-sur-Yvette, France, 1995; p 149.
(153) Arnett, E.; Thompson, O. *J. Am. Chem. Soc.* **1981**, *103*, 968.
(154) Stewart, M.; Arnett, E. *Top. Stereochem.* **1982**, *13*, 489.
(155) Nittman, J.; Stanley, H. E. *Nature* **1986**, *321*, 663.
(156) Langer, J. S. *Science* **1989**, *243*, 1150.
(157) Langer, J. S. *Rev. Mod. Phys.* **1980**, *52*, 1.
(158) Ben-Jacob, E.; Garik, P. *Nature* **1984**, *310*, 47.
(159) Zabel, V.; Muller-Fahrnow, A.; Hilgenfeld, R.; Saenger, B.; Pfannemuller, B.; Enkelmann, V.; Welte, W. *Chem. Phys. Lipids* **1986**, *39*, 313.
(160) Andre, C.; Luger, P.; Gutberlet, T.; Vollhardt, D.; Fuhrhop, J.-H. *Carbohydr. Res.* **1995**, *272*, 129.
(161) Andre, C.; Luger, P.; Rosengarten, B.; Fuhrhop, J.-H. *Acta Crystallogr.: Sect. B: Struct. Sci.* **1993**, *49*, 375.
(162) Harvey, N. G.; Mirajovsky, D.; Rose, P. L.; Verbiar, R.; Arnett, E. M. *J. Am. Chem. Soc.* **1989**, *111*, 1115.
(163) Neumann, V.; Gericke, A.; Hühnerfuss, H. *Langmuir* **1995**, *11*, 2206.
(164) Hühnerfuss, H.; Gericke, A.; Neumann, V.; Stine, K. J. *Thin Solid Films* **1996**, *284*−*285*, 694.
(165) Hühnerfuss, H.; Neumann, V.; Stine, K. J. *Langmuir* **1996**, *12*, 2561.
(166) Simon-Kutscher, J.; Gericke, A.; Hühnerfuss, H. *Langmuir* **1996**, *12*, 1027.
(167) Zeelen, F. J.; Havinga, E. *Recl. Trav. Chim. Pay-Bas* **1958**, *77*, 267.

(168) Marr-Leisy, D.; Neumann, R.; Ringsdorf, H. *Colloid Polym. Sci.* **1958**, *263*, 791.
(169) Eckhardt, C.; Peachey, N.; Swanson, D.; Takacs, J.; Khan, M.; Gong, X.; Kim, J.; Wang, J.; Uphaus, R. *Nature* **1993**, *362*, 614.
(170) Stevens, F.; Dyer, D.; Walba, D. *Angew. Chem., Int. Ed. Engl.* **1996**, *35*, 900.
(171) Iwamoto, M.; Wu, C. X. *Mol. Cryst. Liq. Cryst.* **2000**, *349*, 141.
(172) Brezesinski, G.; Vollhardt, D. In preparation.
(173) Stine, K. J.; Leventhal, A. R.; Parazak, D. P.; Uang, J. Y.-J. *Enantiomer* **1996**, *1*, 41.
(174) (a) Popielawski, J.; Rice, S. A. *J. Chem. Phys.* **1988**, *88*, 1279. (b) Wang, Z-. G.; Rice, S. A. *J. Chem. Phys.* **1988**, *88*, 1290. (c) Harris, J.; Rice, S. A. *J. Chem. Phys.* **1988**, *88*, 1298. (d) Harris, J.; Rice, S. A. *J. Chem. Phys.* **1988**, *89*, 5898. (e) Lin, B.; Peng, J. B.; Ketterson, J. B.; Dutta, P.; Thomas, B. N.; Buontempo, J.; Rice, S. A. *J. Chem. Phys.* **1989**, *90*, 2393. (f) Cai, Z.; Rice, S. A. *Faraday Disscuss. Chem. Soc.* **1990**, *89*, 211. (g) Cai, Z.; Rice, S. A. *J. Chem. Phys.* **1989**, *90*, 6716. (h) Shin, S.; Wang, Z.-G.; Rice, S. A. *J. Chem. Phys.* **1990**, *92*, 1427. (i) Shin, S.; Rice, S. A. *J. Chem. Phys.* **1990**, *93*, 5247. (j) Barton, S. W.; Goudot, A.; Bouloussa, O.; Rondelez, F.; Lin, B.; Novak, F.; Acero, A.; Rice, S. A. *J. Chem. Phys.* **1992**, *96*, 1343. (k) Shin, S.; Collazo, N.; Rice, S. A. *J. Chem. Phys.* **1992**, *96*, 1352. (l) Bell, K.; Rice, S. A. *J. Chem. Phys.* **1993**, *99*, 4160. (m) Buontempo, J. T.; Rice, S. A. *J. Chem. Phys.* **1993**, *99*, 7030. (n) Acero, A. A.; Li, M.; Lin, B.; Rice, S. A.; Doldman, M.; Azouz, I. B.; Goudot, A.; Rondelez, F. *J. Chem. Phys.* **1993**, *99*, 7214. (o) Gao, J.; Rice, S. A. *J. Chem. Phys.* **1993**, *99*, 7020. (p) Shin, S.; Rice, S. A. *J. Chem. Phys.* **1994**, *101*, 2508. (q) Schofield, J.; Rice, S. A. *J. Chem. Phys.* **1995**, *103*, 5792. (r) Bell, K.; Rice, S. A. *J. Chem. Phys.* **1996**, *104*, 1684.
(175) Shimon, L. J. W.; Vaida, M.; Addadi, L.; Lahav, M.; Leiserowitz, L. *J. Am. Chem. Soc.* **1990**, *112*, 6215.
(176) Wang, J.; Leiserowitz, L.; Lahav, M. *J. Phys. Chem.* **1992**, *96*, 15.
(177) (a) Hartman, P.; Perdok, W. *Acta Crystallogr.* **1955**, *8*, 49. (b) Hartman, P.; Perdok, W. *Acta Crystallogr.* **1955**, *8*, 521. (c) Hartman, P.; Perdok, W. *Acta Crystallogr.* **1955**, *8*, 525. (d) Benneman, P.; van der Eerden, J. In *Morphology of Crystals*; Sunagawa, I., Ed.; Terra Scientific: Tokyo, Japan, 1987; p 1. (e) Benneman, P. In *Handbook of Crystal Growth*; Elsevier: Amsterdam, The Netherlands, 1993; p 477. (f) Hollander, F. F. A.; Plomp, M.; van de Streek, J.; van Enckevort, W. J. P. *Surface Sci.* **2001**, *471*, 101.
(178) (a) Zepik, H.; Shavit, E.; Tang, M.; Jensen, T. R.; Kjaer, K.; Bolbach, G.; Leiserowitz, L.; Weissbuch, I.; Lahav, M. *Science* **2002**, *295*, 1266. (b) Weissbuch, I.; Bolbach, G.; Zepik, H.; Shavit, E.; Tang, M.; Frey, J.; Jensen, T. R.; Kjaer, K.; Leiserowitz, L.; Lahav, M. *J. Am. Chem. Soc.* **2002**, *124*, 9093. (c) Nery, J. G.; Bolbach, G.; Weissbuch, I.; Lahav, M. *Angew. Chem., Int. Ed.* **2003**, *42*, 2157. (d) Weissbuch, I.; Zepik, H.; Bolbach, G.; Shavit, E.; Tang, M.; Jensen, T. R.; Kjaer, K.; Leiserowitz, L.; Lahav, M. *Chem. Eur. J.* **2003**, *9*, 1782.
(179) Nandi, N. *J. Phys. Chem.* **2003**, submitted for publication.
(180) Nandi, N. *J. Phys. Chem. A* **2003**, *107*, 4588 (Letter).
(181) Bersuker, G. *J. Chem. Phys.* **1999**, *110*, 10907.
(182) Bersuker, G.; Pekker, M. *J. Chem. Phys.* **1999**, *110*, 10923.
(183) Cēbers, A.; Janmey, P. A. *J. Phys. Chem. B* **2002**, *106*, 12351.

CR0006674